Three-nucleon force in chiral effective field theory with explicit Δ(1232) degrees of freedom: Longest-range contributions at fourth order

H. Krebs,[1,*] A. M. Gasparyan,[1,2,†] and E. Epelbaum[1,‡]

[1]*Institut für Theoretische Physik II, Ruhr-Universität Bochum, D-44780 Bochum, Germany*

[2]*Institute for Theoretical and Experimental Physics, B. Cheremushkinskaya 25, 117218 Moscow, Russia*

(Received 23 April 2018; published 30 July 2018)

We analyze the longest-range two-pion exchange contributions to the three-nucleon force at leading-loop order in the framework of heavy-baryon chiral effective field theory with explicit Δ(1232) degrees of freedom. All relevant low-energy constants which appear in the calculation are determined from pion-nucleon scattering. Comparing our results with the ones obtained in the Δ-less theory at next-to-next-to-next-to-next-to leading order (N^4LO), we find effects of the Δ isobar for this particular topology to be rather well represented in terms of resonance saturation of various low-energy constants in the Δ-less approach.

DOI: 10.1103/PhysRevC.98.014003

I. INTRODUCTION

Three-nucleon forces ($3N$F) and their impact on nuclear structure and reactions have become an important frontier in nuclear physics; see Refs. [1–25] for a selection of recent studies along these lines and Refs. [26,27] for review articles. Chiral effective field theory (EFT) provides a model-independent and systematically improvable theoretical framework to describe nuclear forces and low-energy nuclear structure and dynamics in harmony with the symmetries of QCD [28,29]. Nucleon-nucleon (NN) scattering has been extensively studied in chiral EFT in the past two decades following the pioneering work by Weinberg [30] and Ordonez *et al.* [31]. In particular, NN potentials at next-to-next-to-next-to-leading order (N^3LO) in the chiral expansion have been available for about 15 years [32,33] and served as a basis for numerous *ab initio* calculations of nuclear structure and reactions. Recently, accurate and precise chiral EFT potentials up to fifth order in the chiral expansion, i.e., N^4LO, have been developed [34–37]. In particular, the semilocal N^4LO^+ potentials of Ref. [37] provide a description of the 2013 Granada database of neutron-proton and proton-proton scattering data below $E_{\rm lab} = 300$ MeV, which is comparable to or even better than that based on the available high-precision phenomenological potentials.

The chiral expansion of the $3N$F at one-loop level, i.e., up to and including next-to-next-to-next-to-next-to-leading-order (N^4LO) contributions, can be described in terms of six topologies depicted in Fig. 1. The first nonvanishing contributions emerge at next-to-next-to leading order (N^2LO) from tree-level diagrams of types shown in Figs. 1(a), 1(d) and 1(f) [38,39]. The resulting $3N$F at N^2LO has been intensively explored in three- and four-nucleon scattering calculations as well as in nuclear structure calculations; see Refs. [1–11,13,17–24] for some recent examples and the review articles [26,27] and references therein. The first corrections to the $3N$F emerge at N^3LO from all possible one-loop diagrams of types shown in Figs. 1(a)–1(e) constructed from the lowest-order vertices. The resulting parameter-free expressions have been worked out in Refs. [40,41]; see also Ref. [42]. An interesting feature of the N^3LO $3N$F contributions is their rather rich isospin-spin-momentum structure emerging primarily from the ring topology [Fig. 1(c)]. This is in contrast with the quite restricted operator structure of the N^2LO $3N$F. Numerical implementation of the N^3LO $3N$F corrections requires their partial wave decomposition [15,43] and a consistent implementation of the regulator. This work is currently in progress; see Refs. [4,12,14,44] for some preliminary results. We further emphasize that four-nucleon forces also start to contribute at N^3LO and have been worked out in Refs. [45,46]. Pioneering applications of the chiral four-nucleon forces to the α-particle binding energy [47,48] and neutron matter [11,22,49] indicate that their effects in these systems are fairly small.

While the impact of the first corrections to the chiral $3N$F on few- and many-nucleon observables is yet to be investigated, one may ask whether the chiral expansion of the $3N$F at subleading order, i.e., at N^3LO, provides a reasonable approximation to the converged result. To clarify this issue, we have worked out the next-to-next-to-next-to-next-to-leading-order (N^4LO) contributions to the long-range [50] and intermediate-range [51] $3N$F corresponding to Fig. 1(a) on one hand and Figs. 1(b) and 1(c) on the other hand. The corresponding potentials at large distance emerge as parameter-free predictions as they are completely determined by the chiral symmetry of QCD and experimental information on pion-nucleon scattering needed to fix the relevant low-energy constants (LECs). More precisely, for the two-pion-exchange topology, the N^4LO $3N$F contributions depend on some of the LECs c_i, $\bar{d}_i$, and $\bar{e}_i$ from the order-Q^2, Q^3, and Q^4 effective pion-nucleon Lagrangians, which have been extracted from the available πN partial wave analyses. The resulting longest-range $3N$F was shown to

*hermann.krebs@rub.de

†ashotg@tp2.rub.de

‡evgeny.epelbaum@rub.de

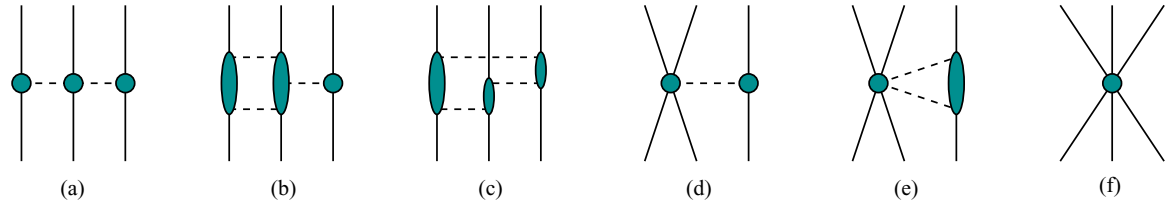

FIG. 1. Various topologies contributing to the $3NF$ up to and including N^{4}LO: two-pion (2π) exchange (a), two-pion–one-pion (2π-1π) exchange (b), ring (c), one-pion exchange contact (d), two-pion exchange contact (e) and purely contact (f) diagrams. Solid and dashed lines represent nucleons and pions, respectively. Shaded blobs represent the corresponding amplitudes.

converge reasonably fast [50]. The situation appears to be very different for the two-pion–one-pion (2π-1π) exchange and ring $3NF$ topologies corresponding to Figs. 1(b) and 1(c): The formally leading contributions emerging at N^{3}LO turn out to be rather small in magnitude while the first corrections at N^{4}LO are considerably larger [51]. The origin of such an unnatural convergence pattern can be understood if one assumes the intermediate $\Delta(1232)$ excitation as a dominant $3NF$ mechanism, which is well in line with various phenomenological studies [52–54]. In the standard formulation of chiral EFT based on pions and nucleons as the only explicit degrees of freedom and used, in particular, in Refs. [50,51], all effects of the Δ (and heavier resonances as well as heavy mesons) are taken into account implicitly through (some of the) LECs starting from the subleading effective Lagrangian, i.e., $c_i, \bar{d}_i, \bar{e}_i, \ldots$. In particular, the values of the LECs $c_{3,4}$, which contribute to the two-pion exchange $3NF$ at N^{2}LO, are known to receive large contributions from the Δ. Thus, for this longest-range $3NF$ topology, effects of the Δ are already, to a large extent, accounted for at the lowest order (N^{2}LO). The first corrections at N^{3}LO emerge from one-loop diagrams constructed from the leading-order pion-nucleon vertices, which are not affected by the Δ, and the corresponding potentials appear to be fairly small in magnitude. This explains the observed good convergence pattern of the chiral expansion for the two-pion exchange $3NF$. On the other hand, for the intermediate-range topologies, the expansion starts at N^{3}LO while the first effects of the Δ appear at N^{4}LO and lead to large corrections. Moreover, since the N^{4}LO contributions to the 2π-1π and ring $3NF$s are proportional to c_i, only effects due to single-Δ excitations are implicitly taken into account at that order. This raises the question of whether the double- and triple-Δ excitations, which in the standard Δ-less formulation of chiral EFT are taken into account at even higher orders, might lead to sizable $3NF$ contributions. While this question could, at least in principle, be clarified by extending the calculations to even higher orders in the chiral expansion, this would require calculation of two–loop diagrams and also dealing with a large number of new LECs, which makes this strategy hardly feasible. Instead, we follow a different approach and use chiral EFT with explicit Δ degrees of freedom, which offers a more efficient way to resum the contributions due to intermediate Δ excitations. To be specific, we employ a formulation in which the Δ-nucleon mass splitting is treated on the same footing as the pion mass, which is known as the small-scale expansion (SSE) [55]. Following the pioneering calculations in Refs. [56,57], we have already worked out the contributions of the Δ to the two- and three-nucleon forces up to N^{2}LO in the SSE [58,59] and also looked at isospin-breaking corrections to the NN potential [60]. These calculations confirmed a better convergence of the Δ-full EFT formulation compared to its standard, Δ-less version. Interestingly, for the $3NF$, the only nonvanishing Δ contribution up to N^{2}LO is the two-pion exchange diagram with an intermediate Δ resonance, commonly called the Fujita-Miyazawa force. This term is shifted in the Δ-full theory to next-to leading order (NLO).

In this paper, for the first time, we extend the SSE for the nuclear forces to N^{3}LO and concentrate on the longest-range contribution to the $3NF$ corresponding to Fig. 1(a). This topology is particularly challenging due to (i) the need to carry out a nontrivial renormalization program as will be explained later and (ii) the need to reconsider pion-nucleon scattering in order to determine the relevant LECs; see Ref. [50] where this program was carried out in the standard, Δ-less version of chiral EFT. We will also discuss in detail renormalization within the Δ-full framework and work out the Δ contributions to the relevant low-energy constants in the effective Lagrangian. Although we do not expect to see large benefits from the explicit treatment of the Δ for the 2π-exchange $3NF$, where the standard chiral expansion already shows a good convergence [40,50], this calculation is a necessary prerequisite for analyzing the Δ contributions to the more problematic intermediate-range diagrams. This work is in progress and will be reported in a separate publication.

Our paper is organized as follows. In Sec. II, we describe the framework and specify all terms in the effective Lagrangian that are needed in the calculation. Renormalization of the lowest-order effective Lagrangian to leading loop order is carried out in Sec. III. In Sec. IV, we provide analytic expressions for the contribution of the Δ to the relevant LECs c_i, $\bar{d}_i$, and $\bar{e}_i$ and determine the numerical values of these LECs from pion-nucleon scattering. Δ contributions to the 2π-exchange $3NF$ at N^{3}LO are worked out in Sec. V. In particular, we provide here parameter-free expressions both in momentum and coordinate spaces. A comparison of our findings with the ones of Refs. [40,50] is given in Sec. VI. Finally, the main results of our work are briefly summarized in Sec. VII. The appendices contain the unitary transformations of the nuclear Hamiltonian and the Δ contributions up to N^{3}LO to the πN invariant amplitudes.

II. THE FRAMEWORK

In the following, we briefly describe the formalism we employ in our analysis, namely the heavy-baryon formulation of chiral EFT with explicit $\Delta(1232)$ degrees of freedom [55]. In this framework, the soft scales are given by small external momenta Q, pion mass M_π, and the Δ-nucleon mass splitting $\Delta := m_\Delta - m_N$. The resulting expansion in powers of the small parameter ϵ defined as

$$\epsilon \in \left\{ \frac{Q}{\Lambda_\chi}, \frac{M_\pi}{\Lambda_\chi}, \frac{\Delta}{\Lambda_\chi} \right\}, \tag{2.1}$$

with $\Lambda_\chi \sim 1\,\text{GeV}$ denoting the chiral symmetry breaking scale, is known in the literature as the SSE.

We begin with specifying the effective chiral Lagrangian for pions, nucleons, and the Δ. It is well known that the free spin-3/2 Lagrangian is nonunique and can be written in the form

$$\begin{aligned}\mathcal{L}_\Delta^{\text{free}} = &-\bar\psi_\alpha^i O_A^{\alpha\mu}\big[(i\partial\!\!\!/ - m_\Delta)g_{\mu\nu} \\ &- \tfrac{1}{4}\gamma_\mu\gamma_\lambda(i\partial\!\!\!/ - m_\Delta)\gamma^\lambda\gamma_\nu\big]\xi_{3/2}^{ij} O_A^{\nu\beta}\psi_\beta^j,\end{aligned} \tag{2.2}$$

where the tensor

$$O_A^{\mu\nu} = g^{\mu\nu} + \tfrac{1}{2}\,A\,\gamma^\mu\gamma^\nu \tag{2.3}$$

parametrizes nonuniqueness in the description of a spin-3/2 theory in terms of a parameter A, which can be chosen arbitrarily subject to the restriction $A \neq -1/2$. Further, the quantity $\xi_{3/2}^{ij}$ is the isospin-3/2 projection operator given by

$$\xi_{3/2}^{ij} = \delta^{ij} - \tfrac{1}{3}\tau^i\tau^j\,, \tag{2.4}$$

where τ_i denote the isospin Pauli matrices. Physical observables do not depend on the choice of the parameter A since the entire dependence on A can be absorbed into a field redefinition of the Δ field. In practical calculations, the choice of A is a matter of convenience. In the *covariant* approach, one usually chooses $A = -1$ (see, e.g., Refs. [61–65]), since in this case the free Lagrangian takes the particularly simple form

$$\mathcal{L}_\Delta^{\text{free}} = \bar\psi_i^\mu\,(i\gamma_{\mu\nu\alpha}\,\partial^\alpha - m_\Delta\gamma_{\mu\nu})\xi_{3/2}^{ij}\,\psi_j^\nu, \tag{2.5}$$

with

$$\gamma_{\mu\nu\alpha} = \tfrac{1}{4}\{[\gamma_\mu,\gamma_\nu],\gamma_\alpha\}, \quad \gamma_{\mu\nu} = \tfrac{1}{2}[\gamma_\mu,\gamma_\nu]. \tag{2.6}$$

This form of the Lagrangian leads to a fairly compact and convenient expression for the free propagator of the Δ field

$$\begin{aligned}S^{\mu\nu} = \frac{p\!\!\!/ + m_\Delta}{p^2 - m_\Delta^2}\Big(&-g^{\mu\nu} + \frac{1}{3}\gamma^\mu\gamma^\nu \\ &+ \frac{1}{3m_\Delta}(\gamma^\mu p^\nu - \gamma^\nu p^\mu) + \frac{2}{3m_\Delta^2}p^\mu p^\nu\Big).\end{aligned} \tag{2.7}$$

For every interaction in the Lagrangian, one generally has a freedom to introduce an off-shell parameter. As a consequence, interaction terms depend, in addition to the point-transformation parameter A, also on the off-shell parameters z_i via the tensor

$$\tilde O_{z_i}^{\mu\lambda} O_{A\lambda}^{\nu} = g^{\mu\nu} + \big[z_i + \tfrac{1}{2}(1+4z_i)A\big]\gamma^\mu\gamma^\nu. \tag{2.8}$$

All terms proportional to the off-shell parameters are redundant [66–68], meaning that their contributions to observables can be absorbed into a redefinition of the corresponding low-energy constants (LECs). A particular choice of the off-shell parameters in the calculations is therefore a matter of convention. For example, in the covariant calculation of Ref. [64], we have set $A^{\text{Relativistic}} = -1$ and all $z_i^{\text{Relativistic}} = 0$. In the present analysis, we employ the heavy-baryon $1/m$ expansion worked out by Hemmert *et al.* [55], where the choice $A^{\text{HB}} = 0$ without specifying a particular value for the off-shell parameter z_0^{HB} of the leading-order pion-nucleon-Δ coupling has been made. In order to be consistent with the convention used in the covariant calculation of Ref. [64], we have to set

$$\begin{aligned}&z_0^{\text{HB}} + \tfrac{1}{2}\big(1+4z_0^{\text{HB}}\big)A^{\text{HB}} \\ &\quad = z_0^{\text{Relativistic}} + \tfrac{1}{2}\big(1+4z_0^{\text{Relativistic}}\big)A^{\text{Relativistic}} \\ &\quad \Longrightarrow z_0^{\text{HB}} = -\tfrac{1}{2}.\end{aligned} \tag{2.9}$$

This choice will be used throughout this work.

The effective heavy-baryon Lagrangians which contribute to the nuclear forces up to N^{3}LO are given by

$$\begin{aligned}\mathcal{L}_{\text{SSE}} = &\mathcal{L}_{\pi\pi}^{(2)} + \mathcal{L}_{\pi\pi}^{(4)} + \mathcal{L}_{\pi N}^{(1)} + \mathcal{L}_{\pi N}^{(2)} + \mathcal{L}_{\pi N}^{(3)} + \mathcal{L}_{\pi N\Delta}^{(1)} + \mathcal{L}_{\pi N\Delta}^{(2)} \\ &+ \mathcal{L}_{\pi N\Delta}^{(3)} + \mathcal{L}_{\pi\Delta\Delta}^{(1)} + \mathcal{L}_{\pi\Delta\Delta}^{(2)} + \delta\mathcal{L}_{\pi N}^{(2)},\end{aligned} \tag{2.10}$$

where the subscripts refer to the small-scale dimension. Notice that the last term denotes the contribution to the pion-nucleon effective Lagrangian induced by the nonpropagating spin-1/2 components of the Rarita-Schwinger field for the Δ. The relevant terms in the pion Lagrangians have the form [69]

$$\begin{aligned}\mathcal{L}_{\pi\pi}^{(2)} = &\frac{1}{2}(\partial_\mu\mathring{\boldsymbol\pi}\cdot\partial^\mu\mathring{\boldsymbol\pi} - M^2\mathring{\boldsymbol\pi}\cdot\mathring{\boldsymbol\pi}) + \frac{M^2}{8F^2}(8\alpha-1)(\mathring{\boldsymbol\pi}\cdot\mathring{\boldsymbol\pi})^2 \\ &+ \frac{1}{2F^2}(1-4\alpha)(\mathring{\boldsymbol\pi}\cdot\partial_\mu\mathring{\boldsymbol\pi})(\mathring{\boldsymbol\pi}\cdot\partial^\mu\mathring{\boldsymbol\pi}) \\ &- \frac{\alpha}{F^2}\mathring{\boldsymbol\pi}\cdot\mathring{\boldsymbol\pi}\,\partial_\mu\mathring{\boldsymbol\pi}\cdot\partial^\mu\mathring{\boldsymbol\pi},\end{aligned} \tag{2.11}$$

$$\mathcal{L}_{\pi\pi}^{(4)} = -\frac{l_3}{F^2}M^4\mathring{\boldsymbol\pi}\cdot\mathring{\boldsymbol\pi} + \frac{l_4}{F^2}M^2(\partial_\mu\mathring{\boldsymbol\pi}\cdot\partial^\mu\mathring{\boldsymbol\pi} - M^2\mathring{\boldsymbol\pi}\cdot\mathring{\boldsymbol\pi}), \tag{2.12}$$

where $\mathring{\boldsymbol\pi}$, M, and F refer to the pion fields in the chiral limit, the pion mass to leading order in quark masses, and the pion decay coupling in the chiral limit, while l_i are further LECs. Here and in what follows, $\mathring{X}$ indicates that the quantity X is taken in the chiral limit. Further, the parameter α reflects the freedom in the choice of a particular parametrization for the pion field. All physical quantities are, of course, independent of this parameter. We do not give here explicitly $\mathcal{L}_{\pi N}^{(1)}, \mathcal{L}_{\pi N}^{(2)}, \mathcal{L}_{\pi N}^{(3)}$ as all relevant terms are listed in Ref. [50] where, in order to be consistent with our notation, the LECs c_i and d_i should be replaced by $\mathring{c}_i$ and $\mathring{d}_i$. The remaining Lagrangians in Eq. (2.10) are given by [55]

$$\mathcal{L}_{\pi N\Delta}^{(1)} = -\frac{\mathring{h}_A}{F}\mathring{N}_v^\dagger\mathring{T}_\mu^i\partial^\mu\mathring{\pi}^i + \text{H.c.}, \tag{2.13}$$

$$\begin{aligned}\mathcal{L}_{\pi N\Delta}^{(2)} = &\frac{i}{F}(b_3+b_6)\mathring{N}_v^\dagger\mathring{T}_\mu^i\partial^\mu\partial\cdot v\,\mathring{\pi}^i \\ &+ i\frac{\mathring{h}_A}{Fm}\mathring{N}_v^\dagger\partial^\mu\mathring{T}_\mu^i\partial\cdot v\,\pi^i + \text{H.c.},\end{aligned}$$

$$
\begin{aligned}
\mathcal{L}^{(3)}_{\pi N\Delta} &= \frac{2}{F}(2\,h_7 - h_8 - 2\,h_9 - 2\,h_{10})M^2 \mathring{N}_v^\dagger \mathring{T}^i_\mu \partial^\mu \mathring{\pi}^i \\
&\quad - \frac{1}{F}(h_{12}+h_{13})\mathring{N}_v^\dagger \mathring{T}^i_\mu (\partial\cdot v)^2 \partial^\mu \mathring{\pi}^i + \text{H.c.}, \\
\mathcal{L}^{(1)}_{\pi\Delta\Delta} &= -\mathring{T}^{i\dagger}_\mu \left[i\,\partial\cdot v - \mathring{\Delta} - \frac{\mathring{g}_1}{F}\boldsymbol{\tau}\cdot(\partial_\alpha \mathring{\boldsymbol{\pi}})S^\alpha \right] \mathring{T}^j_\nu g^{\mu\nu}\delta_{ij}, \\
\mathcal{L}^{(2)}_{\pi\Delta\Delta} &= -4M^2 c_1^\Delta \mathring{T}^{i\dagger}_\mu \mathring{T}^j_\nu g^{\mu\nu}\delta_{ij} \\
&\quad + \frac{1}{2m}\mathring{T}^{i\dagger}_\mu [\partial^2 - (\partial\cdot v)^2] \mathring{T}^j_\nu g^{\mu\nu}\delta_{ij}, \\
\delta\mathcal{L}^{(2)}_{\pi N} &= \frac{\mathring{h}_A^2}{18F^2 m}\mathring{N}_v^\dagger [i\boldsymbol{\tau}\cdot(\partial_\mu\mathring{\boldsymbol{\pi}}\times\partial_\nu\mathring{\boldsymbol{\pi}}) - 2\,\partial_\mu\mathring{\boldsymbol{\pi}}\cdot\partial_\nu\mathring{\boldsymbol{\pi}}] \\
&\quad \times \left\{ 4\left[1 + 8\,z_0^{\rm HB} + 12\left(z_0^{\rm HB}\right)^2\right] S^\mu S^\nu \right. \\
&\quad \left. + \left[5 - 8\,z_0^{\rm HB} - 4\left(z_0^{\rm HB}\right)^2\right] v^\mu v^\nu \right\} \mathring{N}_v,
\end{aligned}
\tag{2.14}
$$

where N_v and T^i_μ denote the large components of the nucleon and Δ field, respectively, v is the four-velocity, and m is the nucleon mass in the chiral limit. For the sake of compactness, we do not show the velocity index explicitly in the case of the Δ fields T^i_μ. The quantity h_A denotes the $\pi N\Delta$ axial coupling; b_i, h_i, and c_i^Δ are further LECs; and the covariant spin operator is defined via

$$
S_\mu = \frac{1}{2} i\gamma_5\sigma_{\mu\nu}v^\nu, \quad \sigma_{\mu\nu} = \frac{i}{2}[\gamma_\mu,\,\gamma_\nu]. \tag{2.15}
$$

Last but not least, we emphasize that we adopt in the present work the convention for the pion-nucleon LECs which maintains an explicit decoupling of the Δ. To be specific, the results for a given amplitude or nuclear potential $\mathcal{M}$ have the form

$$
\mathcal{M} = \mathcal{M}_{\not\Delta} + \mathcal{M}_\Delta, \tag{2.16}
$$

where $\mathcal{M}_\Delta$ denotes the contribution associated with the Δ degrees of freedom while $\mathcal{M}_{\not\Delta}$ is the purely nucleonic part. As guaranteed by the decoupling theorem [70], all effects of the Δ isobar at low energy can be accounted for in an implicit way, i.e., through its contributions to the effective pion-nucleon Lagrangian. Expanding the Δ contribution $\mathcal{M}_\Delta$ around $\Delta\to\infty$, one generally finds terms with both positive and negative powers of the Δ. While the latter ones can be identified with the Δ-resonance saturation of the pion-nucleon LECs (see Sec. IV for more details), terms with positive powers of the Δ-nucleon mass splitting can, as a matter of convention, be eliminated by an appropriate redefinition of the pion-nucleon LECs. This is the convention we adopt in our analysis. It guarantees that no positive powers of the Δ appear in the finite expressions for all physical quantities and the $\Delta(1232)$ contributions decouple (vanish) in the large-Δ limit. Stated differently, this convention ensures that our results actually correspond to a partial resummation of the Δ-resonance contributions to the pion-nucleon LECs within the Δ-less formulation.

FIG. 2. Feynman diagrams which contribute to the nucleon self-energy up to order ϵ^3. Only nonvanishing diagrams are shown. Solid, dashed, and double lines represent nucleons, pions, and the Δ, respectively. Solid dots (filled circles) denote leading-order (subleading and higher order) vertices from the effective Lagrangian.

III. RENORMALIZATION OF THE EFFECTIVE LAGRANGIAN TO LEADING LOOP ORDER

We now discuss in detail renormalization of the lowest-order effective chiral Lagrangian at the one-loop level which is achieved by expressing all quantities in terms of renormalized parameters rather than their chiral limit values. We do not consider here renormalization in the pionic sector as it is extensively discussed in the literature and concentrate entirely on the nucleon and Δ sectors. We begin with introducing the renormalized fields and coupling constants via the relations

$$
\begin{aligned}
&\mathring{N}_v = \sqrt{Z_N}N_v, \quad \mathring{T}^i_\mu = \sqrt{Z_\Delta}T^i_\mu, \quad \mathring{\pi}^i = \sqrt{Z_\pi}\pi^i, \\
&M = M_\pi + \delta M, \quad m = m_N + \delta m, \quad \mathring{\Delta} = \Delta + \delta\Delta, \\
&Z_\pi = 1 + \delta Z_\pi, \quad Z_N = 1 + \delta Z_N, \quad Z_\Delta = 1 + \delta Z_\Delta, \\
&F = F_\pi + \delta F, \quad \mathring{g}_A = g_A + \delta g_A, \\
&\mathring{h}_A = h_A + \delta h_A, \quad \mathring{g}_1 = g_1 + \delta g_1.
\end{aligned}
\tag{3.1}
$$

and determine the shifts δX with $X\in\{M,F,m,\Delta,Z_N,Z_\Delta,g_A,h_A,g_1\}$ order by order in the small-scale expansion. Notice that in this formulation, the heavy baryon expansion corresponds to a $1/m_N$ expansion, where m_N is now the physical nucleon mass and *not* the nucleon mass in the chiral limit; see Ref. [71] for more details. We further emphasize that $\mathring{T}^i_\mu$ does not correspond to an interpolating field of an asymptotic state so that its renormalization prescription is conventional. Even if Z_Δ is a complex number, the replacement $\mathring{T}^i_\mu = \sqrt{Z_\Delta}T^i_\mu$ in the Lagrangian does not lead to a violation of unitarity in the kinematical region we are interested in simply because there are no *external* Δ lines. Indeed, the complex renormalization factor Z_Δ, which shows up in the Δ propagator, is compensated by vertices to which this Δ propagator is attached so the amplitude does not depend on Z_Δ. This argument does not rely on whether the renormalization factor is a real or complex number. The main motivation for us to make the replacement $\mathring{T}^i_\mu = \sqrt{Z_\Delta}T^i_\mu$ is to ensure that we can treat Δ fields in the same manner as stable particles. This procedure is a matter of convention and does not affect the final result for the amplitudes. In the following, we discuss in detail renormalization of the various quantities in Eq. (3.1).

A. Nucleon mass and field renormalization

To study nucleon-mass and field renormalization up to order ϵ^3, one needs to calculate the self-energy diagrams shown in Fig. 2. The full nucleon propagator in the rest frame of the

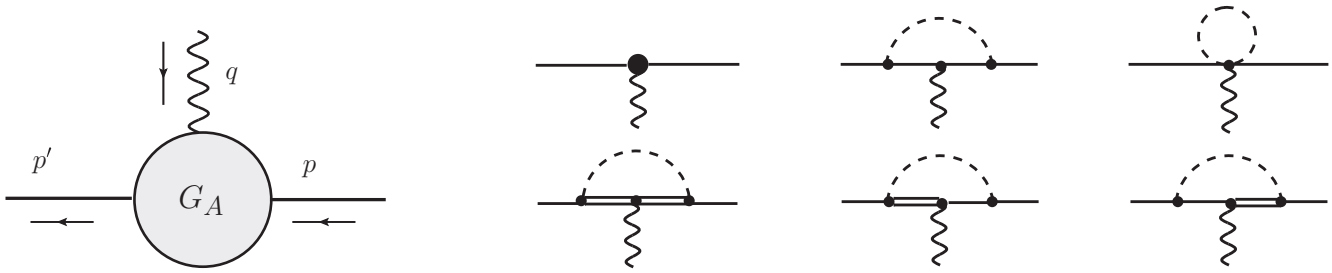

FIG. 3. Left panel: generic one-particle irreducible contribution to the axial-vector nucleon form factor. Right panel: Nonvanishing Feynman diagrams which contribute to $G_A(0)$ up to order ϵ^3. Wavy lines represent external axial sources. For the remaining notation, see Fig. 2.

nucleon can be parametrized via

$$D_N(p\cdot v)=\frac{1}{p\cdot v-\Sigma_N(p\cdot v)+i\epsilon}, \tag{3.2}$$

where $\Sigma_N(p\cdot v)$ denotes the nucleon self-energy. In the vicinity of $p\cdot v=0$, the propagator of the renormalized physical nucleon fields has a simpler form

$$D_N(p\cdot v)=\frac{1}{p\cdot v+i\epsilon}+\mathcal{O}[(p\cdot v)^0]. \tag{3.3}$$

Making the Taylor expansion

$$\begin{aligned}&p\cdot v-\Sigma_N(p\cdot v)\\&\quad=-\Sigma_N(0)+[1-\Sigma_N'(0)]p\cdot v+\mathcal{O}[(p\cdot v)^2],\end{aligned} \tag{3.4}$$

we obtain renormalization conditions for the nucleon mass and the Z-factor Z_N:

$$\Sigma_N(0)=0 \quad \text{and} \quad \Sigma_N'(0)=0. \tag{3.5}$$

The contribution of the first diagram in Fig. 2 to the nucleon self-energy is given by

$$\Sigma_N^{\text{tree}}(p\cdot v)=\delta m-4c_1M_\pi^2-\delta Z_N\,p\cdot v. \tag{3.6}$$

The contribution of the nucleonic one-loop diagram, see second graph in Fig. 2, to the self-energy at the order we are working is given by

$$\begin{aligned}\Sigma_N^{\text{loop},\pi N}(p\cdot v)=&\frac{3g_A^2}{4F_\pi^2}p\cdot vI(d:0)+\frac{3g_A^2}{4F_\pi^2}\big[M_\pi^2-(p\cdot v)^2\big]\\&\times I(d:0;(p,0)),\end{aligned} \tag{3.7}$$

while the Δ-loop contribution emerging from the last diagram in Fig. 2 is given by

$$\begin{aligned}\Sigma_N^{\text{loop},\pi\Delta}(p\cdot v)=&-\frac{2(d-2)h_A^2}{(d-1)F_\pi^2}(\Delta-p\cdot v)I(d:0)\\&+\frac{2(d-2)h_A^2}{(d-1)F_\pi^2}\big[M_\pi^2-\Delta^2+2\Delta p\cdot v\\&-(p\cdot v)^2\big]I(d:0;(p,\Delta)).\end{aligned} \tag{3.8}$$

Here, scalar master integrals in d dimensions are defined according to

$$\begin{aligned}I(d:p_1,\ldots,p_n)&=\frac{1}{i}\mu^{4-d}\int\frac{d^dl}{(2\pi)^d}\frac{1}{(l+p_1)^2-M_\pi^2+i\epsilon}\cdots\frac{1}{(l+p_n)^2-M_\pi^2+i\epsilon},\\I(d:p_1,\ldots,p_n;(p,\delta))&=\mu^{4-d}\frac{1}{i}\int\frac{d^dl}{(2\pi)^d}\frac{1}{(l+p_1)^2-M_\pi^2+i\epsilon}\cdots\frac{1}{(l+p_n)^2-M_\pi^2+i\epsilon}\frac{1}{(l+p)\cdot v-\delta+i\epsilon}.\end{aligned} \tag{3.9}$$

Using the renormalization conditions in Eq. (3.5), we obtain the following expressions at order ϵ^3 in four dimensions:

$$\begin{aligned}\delta m&=4c_1M_\pi^2+\frac{3g_A^2M_\pi^3}{32\pi F_\pi^2}+\frac{h_A^2\Delta}{36\pi^2F_\pi^2}\big(2\Delta^2-3M_\pi^2\big)+\frac{8h_A^2\Delta}{3F_\pi^2}\big(2\Delta^2-3M_\pi^2\big)\lambda_\pi+\frac{4h_A^2}{3F_\pi^2}\big(\Delta^2-M_\pi^2\big)\bar J_0(-\Delta),\\\delta Z_N&=-\frac{3g_A^2M_\pi^2}{32\pi^2F_\pi^2}+\frac{h_A^2}{4\pi^2F_\pi^2}\big(2\Delta^2-M_\pi^2\big)+\frac{1}{2F_\pi^2}\big[16h_A^2\big(2\Delta^2-M_\pi^2\big)-9g_A^2M_\pi^2\big]\lambda_\pi+\frac{4h_A^2\Delta}{F_\pi^2}\bar J_0(-\Delta),\end{aligned} \tag{3.10}$$

where the quantities λ_π and $\bar J_0$ are defined in Appendix B.

B. Renormalization of the nucleon axial coupling

To renormalize the axial-vector coupling constant $\mathring{g}_A$, we consider the axial-vector form factor of the nucleon as shown in Fig. 3. In the Breit frame ($q_0=0$), the matrix element can be parametrized via [72]

$$\mathcal{M}(p',p,q)=-\tau^j\vec\epsilon_A^{\,j}\cdot\vec\sigma\,\frac{E}{2m_N}G_A(q^2)+\cdots, \tag{3.11}$$

where the ellipses refer to terms which are of no relevance for renormalization of $\mathring{g}_A$. In the above expression, E denotes the

FIG. 4. Nonvanishing diagrams which contribute to Δ self-energy up to order ϵ^3. For the remaining notation, see Fig. 2.

energy of the incoming nucleon (which in the Breit frame is also equal to the energy of the outgoing nucleon) while $\vec{\epsilon}_A^{\,j}$ is the polarization vector of the jth component of an isotriplet external axial field. The physical value of the nucleon axial coupling g_A is defined as

$$g_A = G_A(0). \tag{3.12}$$

Up to order ϵ^3, the contributions to the axial form factor $G_A(0)$ emerge from the tree-level diagrams

$$G_A^{\rm tree}(0) = g_A + \delta g_A + g_A \delta Z_N + 4 d_{16} M_\pi^2, \tag{3.13}$$

one-loop diagrams without Δ excitations

$$G_A^{{\rm loop},\pi N}(0) = -\frac{g_A}{4F_\pi^2}\big(g_A^2(d-3)-4\big) I(d:0), \tag{3.14}$$

and one-loop diagrams with intermediate Δ excitations (see the second row of the right panel of Fig. 3)

$$\begin{aligned} G_A^{{\rm loop},\pi N\Delta}(0) = &-\frac{2(d-2)h_A^2}{9(d-1)^2F_\pi^2}[24g_A + 5(d^2-2d-3)g_1] I(d:0) - \frac{16(d-2)g_A h_A^2 M_\pi^2}{3(d-1)^2F_\pi^2\Delta} I[d:0;(0,0)] \\ &+ \frac{2(d-2)h_A^2}{9(d-1)^2F_\pi^2\Delta}\big[24g_A\big(M_\pi^2-\Delta^2\big) - 5(d^2-2d-3)g_1\Delta^2\big] I[d:0;(0,\Delta)]. \end{aligned} \tag{3.15}$$

Using the renormalization condition in Eq. (3.12), we obtain in four dimensions

$$\begin{aligned} \delta g_A = &-\delta Z_N g_A - 4 d_{16} M_\pi^2 - \frac{M_\pi^2}{7776\pi^2F_\pi^2}\big(243g_A^3 - 576 g_A h_A^2 + 1240 h_A^2 g_1\big) - \frac{h_A^2\Delta^2}{486\pi^2F_\pi^2}(24g_A - 155 g_1) - \frac{4g_A h_A^2 M_\pi^3}{27\pi F_\pi^2\Delta} \\ &+ \left[\frac{16h_A^2\Delta^2}{81F_\pi^2}(24g_A+25g_1) - \frac{M_\pi^2}{162F_\pi^2}\big(81g_A^3 + 36g_A\big(32h_A^2-9\big) + 400 h_A^2 g_1\big)\right]\lambda_\pi \\ &+ \left[\frac{4h_A^2\Delta}{81F_\pi^2}(24g_A+25g_1) - \frac{32 g_A h_A^2 M_\pi^2}{27F_\pi^2\Delta}\right]\bar{J}_0(-\Delta). \end{aligned} \tag{3.16}$$

C. Δ mass and field renormalization

To study the Δ mass and field renormalization, one needs to calculate the corresponding nonvanishing self-energy diagrams shown in Fig. 4. In general, the self-energy of the Δ resonance in the rest frame can be parametrized via

$$\Sigma_\Delta(p\cdot v)^{ij}_{\mu\nu} = P^{3/2}_{\mu\nu}\xi^{ij}_{I=3/2}\Sigma_\Delta(p\cdot v), \tag{3.17}$$

where the spin- and isospin-3/2 projector operators are defined by

$$P^{3/2}_{\mu\nu} = g_{\mu\nu} - v_\mu v_\nu + \tfrac{4}{3}S_\mu S_\nu \quad \text{and} \quad \xi^{ij}_{I=3/2} = \delta^{ij} - \tfrac{1}{3}\tau^i\tau^j, \tag{3.18}$$

respectively. The contribution of the tree-level diagram, see the first graph in Fig 4, to the Δ self-energy is given by

$$\Sigma_\Delta^{\rm tree}(p\cdot v) = -4c_1^\Delta M^2. \tag{3.19}$$

The contributions of the two one-loop diagrams with the πN and $\pi\Delta$ cuts in d space-time dimensions have the form

$$\begin{aligned} \Sigma_\Delta^{{\rm loop},\pi N}(p\cdot v) = &\frac{h_A^2}{(d-1)F_\pi^2}\big\{p\cdot v\, I(d:0) \\ &+ \big[M_\pi^2 - (p\cdot v)^2\big] I[d:0;(p,0)]\big\}, \\ \Sigma_\Delta^{{\rm loop},\pi\Delta}(p\cdot v) = &\frac{5(d^2-2d-3)g_1^2}{12(d-1)^2F_\pi^2}\big\{(p\cdot v-\Delta) I(d:0) \\ &+ \big[M_\pi^2 - (p\cdot v-\Delta)^2\big] I[d:0;(p,\Delta)]\big\}. \end{aligned} \tag{3.20}$$

The full Δ propagator in the rest frame of the Δ resonance can be written as

$$\begin{aligned} D_\Delta(p\cdot v)^{ij}_{\mu\nu} &= -D_\Delta(p\cdot v) P^{3/2}_{\mu\nu}\xi^{ij}_{I=3/2}, \quad \text{with} \\ D_\Delta(p\cdot v) &= \frac{i}{p\cdot v - \mathring{\Delta} - \Sigma_\Delta(p\cdot v)}. \end{aligned} \tag{3.21}$$

In the vicinity of the pole, the full Δ propagator has a simpler structure, namely

$$D_\Delta(p\cdot v) \simeq \frac{i}{p\cdot v - \Delta + i\Gamma_\Delta/2}. \tag{3.22}$$

Here, Δ and Γ_Δ denote the (pole-position) mass and width of the Δ resonance, respectively. Expanding the full propagator around the pole, one extracts the mass, width, and the complex Z_Δ factor:

$$\begin{aligned} &p\cdot v - \mathring{\Delta} - \Sigma_\Delta(p\cdot v) \\ &= \Delta - i\frac{\Gamma_\Delta}{2} - \mathring{\Delta} - \Sigma_\Delta\left(\Delta - i\frac{\Gamma_\Delta}{2}\right) \\ &\quad + \left[1 - \Sigma_\Delta'\left(\Delta - i\frac{\Gamma_\Delta}{2}\right)\right]\left(p\cdot v - \Delta + i\frac{\Gamma_\Delta}{2}\right) \\ &\quad + \mathcal{O}\left[\left(p\cdot v - \Delta + i\frac{\Gamma_\Delta}{2}\right)^2\right]. \end{aligned} \tag{3.23}$$

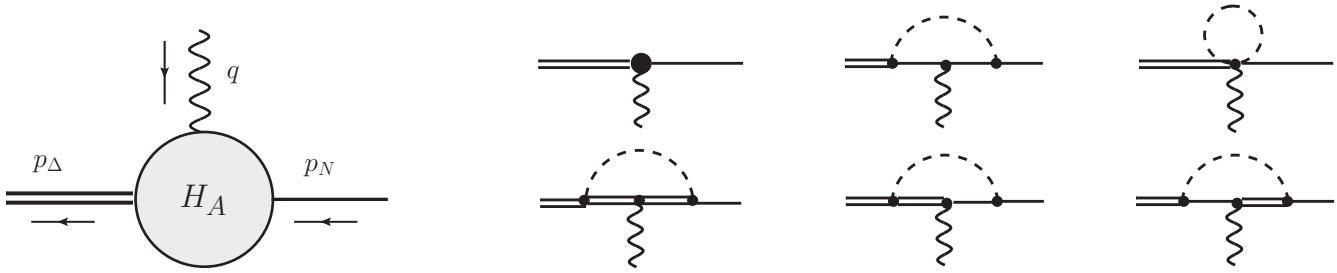

FIG. 5. Left panel: generic one-particle irreducible contribution to the axial-vector nucleon-δ transition form factor. Right panel: Nonvanishing Feynman diagrams which contribute to $H_A(\Delta,\Delta^2,0)$ up to order ϵ^3. Wavy lines represent external axial sources. For the remaining notation, see Fig. 2.

Renormalization of the Δ mass and width is determined from the condition

$$\Delta - i\frac{\Gamma_\Delta}{2} - \mathring{\Delta} - \Sigma_\Delta\left(\Delta - i\frac{\Gamma_\Delta}{2}\right) = 0. \tag{3.24}$$

From the real part of this condition, we deduce the Δ-mass renormalization as

$$\Delta - \mathring{\Delta} - \mathrm{Re}\,\Sigma_\Delta\left(\Delta - i\frac{\Gamma_\Delta}{2}\right) = 0, \tag{3.25}$$

while the imaginary part of this condition yields the following result for the width:

$$\frac{\Gamma_\Delta}{2} + \mathrm{Im}\,\Sigma_\Delta\left(\Delta - i\frac{\Gamma_\Delta}{2}\right) = 0. \tag{3.26}$$

The complex-valued Z_Δ factor is determined by the relation

$$\Sigma'_\Delta\left(\Delta - i\frac{\Gamma_\Delta}{2}\right) = 0. \tag{3.27}$$

At the one-loop level, we can replace the relations (3.25)–(3.27) by

$$\begin{aligned}&\Delta - \mathring{\Delta} - \mathrm{Re}\,\Sigma_\Delta(\Delta) = 0,\\ &\frac{\Gamma_\Delta}{2} + \mathrm{Im}\,\Sigma_\Delta(\Delta) = 0, \quad \text{and} \quad \Sigma'_\Delta(\Delta) = 0,\end{aligned} \tag{3.28}$$

One immediately sees that the above relations coincide with the Breit-Wigner conditions. The pole conditions in Eqs. (3.25)–(3.27) and the Breit-Wigner conditions start to differ from each other at the two-loop level, which is beyond the order we are working at. From the conditions in Eq. (3.28), we finally obtain

$$\begin{aligned}\delta\Delta &= 4c_1^\Delta M_\pi^2 + \frac{2h_A^2\Delta}{3F_\pi^2}\left(3M_\pi^2 - 2\Delta^2\right)\lambda_\pi + \frac{25g_1^2M_\pi^3}{864\pi F_\pi^2}\\ &\quad + \frac{h_A^2\Delta\left(2\Delta^2 - 3M_\pi^2\right)}{72\pi^2F_\pi^2} - \frac{h_A^2}{3F_\pi^2}\left(M_\pi^2 - \Delta^2\right)\mathrm{Re}\bar{J}_0(\Delta),\\ \delta Z_\Delta &= -\frac{1}{18F_\pi^2}\left[36h_A^2\left(M_\pi^2 - 2\Delta^2\right) + 25g_1^2M_\pi^2\right]\lambda_\pi\\ &\quad - \frac{65g_1^2M_\pi^2}{864\pi^2F_\pi^2} - \frac{h_A^2\Delta}{F_\pi^2}\bar{J}_0(\Delta).\end{aligned} \tag{3.29}$$

D. Renormalization of the $\pi N\Delta$ axial coupling

To renormalize the LEC $\mathring{h}_A$, we consider the axial-vector nucleon-Δ transition form factor, see Fig. 5, in the rest frame of the Δ:

$$\begin{aligned}&\mathcal{M}(p_\Delta,p_N,q)^i_\mu\\ &\quad = P^{3/2}_{\mu\nu}\xi^{ij}_{I=3/2}\epsilon_A(q)^\nu_j H_A(p_\Delta\cdot v, q^2, p\cdot v) + \cdots,\end{aligned} \tag{3.30}$$

where the ellipses refer to other terms which are not relevant for renormalization of the $\pi N\Delta$ axial coupling constant. We analytically continue the form factor H_A and choose the renormalization point to be

$$h_A = \mathrm{Re}\,H_A\left[\Delta - i\frac{\Gamma_\Delta}{2}, \left(\Delta - i\frac{\Gamma_\Delta}{2}\right)^2, 0\right], \tag{3.31}$$

which, in the one-loop approximation, becomes

$$h_A = \mathrm{Re}\,H_A(\Delta,\,\Delta^2,\,0). \tag{3.32}$$

Up to order ϵ^3, the quantity $H_A(\Delta,\Delta^2,0)$ receives contributions from the tree-level diagram (first graph in the right panel of Fig. 5)

$$H_A^{\mathrm{tree}}(\Delta,\Delta^2,0) = h_A + \delta h_A - (b_2+b_7)\Delta + \frac{h_A}{2}(\delta Z_N + \delta Z_\Delta) + 2[h_8 + 2(h_9+h_{10})]M_\pi^2, \tag{3.33}$$

one-loop diagrams without Δ excitations (the remaining two diagrams in the upper raw of the right panel of Fig. 5)

$$H_A^{\mathrm{loop},\pi N}(\Delta,\Delta^2,0) = \frac{h_A\left(d-1-g_A^2\right)}{(d-1)F_\pi^2}I(d:0) + \frac{g_A^2h_AM_\pi^2}{(d-1)F_\pi^2\Delta}I[d:0;(0,0)] - \frac{g_A^2h_A\left(M_\pi^2-\Delta^2\right)}{(d-1)F_\pi^2\Delta}I[d:0;(\Delta,0)], \tag{3.34}$$

and one-loop graphs with pions, nucleons, and Δ degrees of freedom (diagrams in the second raw of the right panel of Fig. 5)

$$\begin{aligned} H_A^{\text{loop},\pi N\Delta}(\Delta,\Delta^2,0) = &-\frac{(d-3)h_A}{36(d-1)^3F_\pi^2}\{12(d-1)h_A^2+5(d+1)g_1[3(d-1)^2g_A+4g_1]\}I(d:0)\\ &-\frac{5(d^2-2d-3)h_Ag_1^2M_\pi^2}{9(d-1)^3F_\pi^2\Delta}I[d:0;(0,0)]-\frac{(d-3)h_A^3\left(M_\pi^2-\Delta^2\right)}{6(d-1)^2F_\pi^2\Delta}I[d:0;(\Delta,0)]\\ &+\frac{(d-3)h_A\left(M_\pi^2-\Delta^2\right)}{18(d-1)^3F_\pi^2\Delta}\left[10(d+1)g_1^2+3(d-1)h_A^2\right]I[d:0;(0,\Delta)]. \end{aligned} \tag{3.35}$$

Substituting these expressions into the renormalization condition given in Eq. (3.32), we obtain the following order-ϵ^3 expression for δh_A in four dimensions:

$$\begin{aligned} \delta h_A = &-\frac{h_A}{2}(\delta Z_N+\text{Re}\,\delta Z_\Delta)+\Delta(b_2+b_7)-2[h_8+2(h_9+h_{10})]M_\pi^2+\left(3h_A^2+5g_1^2-27g_A^2\right)\frac{h_A\Delta^2}{972\pi^2F_\pi^2}\\ &-\frac{h_AM_\pi^2}{2592\pi^2F_\pi^2}\left(12h_A^2-108g_A^2+20g_1^2+195g_Ag_1\right)+\left(81g_A^2-25g_1^2\right)\frac{h_AM_\pi^3}{1944\pi F_\pi^2\Delta}\\ &+\left[h_A\left(81g_A^2+9h_A^2+25g_1^2\right)\frac{4\Delta^2}{243F_\pi^2}-h_A\left\{100g_1^2+225g_Ag_1+36\left[h_A^2+9\left(g_A^2-1\right)\right]\right\}\frac{M_\pi^2}{162F_\pi^2}\right]\lambda_\pi\\ &-\left(9h_A^2+50g_1^2\right)\frac{h_A\left(M_\pi^2-\Delta^2\right)}{486F_\pi^2\Delta}\bar{J}_0(-\Delta)+\left(h_A^2+18g_A^2\right)\frac{h_A\left(M_\pi^2-\Delta^2\right)}{54F_\pi^2\Delta}\text{Re}\,\bar{J}_0(\Delta). \end{aligned} \tag{3.36}$$

IV. DETERMINATION OF THE LECS FROM πN SCATTERING

Given that the LECs in the effective Lagrangian with and without explicit Δ degrees of freedom have a different meaning, we cannot use the values of the various LECs from our earlier work [50] based on the Δ-less formulation and have to redo the analysis of the pion-nucleon system utilizing the small-scale expansion. Specifically, we need to calculate the πN scattering amplitude up to order ϵ^3.

Before discussing renormalization of the πN amplitude in the explicit decoupling scheme as explained in Sec. II, we first perform the following shifts in the LECs in order to get rid of redundant terms:

$$\begin{aligned} h_A &\to h_A-\Delta(b_2+b_3+b_6+b_7)+\Delta^2(h_{12}+h_{13})+4M_\pi^2h_7,\\ \mathring{c}_2 &\to \mathring{c}_2+\frac{4(d-2)}{3(d-1)}h_A(b_3+b_6)-\frac{2(d-2)}{3(d-1)}\Delta(b_3+b_6)^2-\frac{4(d-2)}{3(d-1)}\Delta h_A(h_{12}+h_{13}),\\ \mathring{c}_3 &\to \mathring{c}_3-\frac{4(d-2)}{3(d-1)}h_A(b_3+b_6)+\frac{2(d-2)}{3(d-1)}\Delta(b_3+b_6)^2+\frac{4(d-2)}{3(d-1)}\Delta h_A(h_{12}+h_{13}),\\ \mathring{c}_4 &\to \mathring{c}_4+\frac{4}{3(d-1)}h_A(b_3+b_6)-\frac{2}{3(d-1)}\Delta(b_3+b_6)^2-\frac{4}{3(d-1)}\Delta h_A(h_{12}+h_{13}),\\ \mathring{d}_1+\mathring{d}_2 &\to \mathring{d}_1+\mathring{d}_2+\frac{d-2}{6(d-1)}(b_3+b_6)^2-\frac{d-2}{3(d-1)}h_A(h_{12}+h_{13}),\\ \mathring{d}_3 &\to \mathring{d}_3-\frac{d-2}{6(d-1)}(b_3+b_6)^2+\frac{d-2}{3(d-1)}h_A(h_{12}+h_{13}),\\ \mathring{d}_{14}-\mathring{d}_{15} &\to \mathring{d}_{14}-\mathring{d}_{15}-\frac{2}{3(d-1)}(b_3+b_6)^2+\frac{4}{3(d-1)}h_A(h_{12}+h_{13}). \end{aligned} \tag{4.1}$$

Notice that these replacements are performed in the amplitude written in d dimensions. After this shift, the amplitude does not depend on the LECs $b_3+b_6, b_2+b_7, h_{12}+h_{13}$, and h_7 anymore.

Let us now discuss renormalization of the pion-nucleon amplitude. All divergencies which remain after expressing the amplitude in terms of physical quantities as discussed in the previous section are absorbed into redefinition of the LECs c_i and d_i entering the order-Q^2 and Q^3 effective pion-nucleon Lagrangians. While the LECs c_i are finite in the Δ-less framework provided one uses dimensional regularization with the $\overline{MS}$ scheme, this does not hold true anymore in the Δ-full theory due to the appearance of ultraviolet divergencies $\propto\Delta$ at ϵ^3 and higher powers of Δ at orders beyond ϵ^3. We parametrize

the bare LECs $\mathring{c}_i$ and $\mathring{d}_i$ via

$$\mathring{c}_i = c_i + \Delta\left[\frac{\beta_i^c}{F_\pi^2}\lambda_\pi + \frac{1}{(4\pi F_\pi)^2}c_i^\Delta\right],$$
$$\mathring{d}_i = \frac{\beta_i^{d,N} + \beta_i^{d,\Delta}}{F_\pi^2}\lambda_\pi + d_i + \frac{1}{(4\pi F_\pi)^2}d_i^\Delta, \qquad (4.2)$$

where the various β functions relevant for pion-nucleon scattering are given by

$$\beta_1^c = 2\,h_A^2,$$
$$\beta_2^c = -\frac{80}{2187}h_A^2(9\,g_A - 5\,g_1)^2,$$
$$\beta_3^c = \frac{16}{2187}h_A^2\left[729 + 5(9\,g_A - 5\,g_1)^2\right],$$
$$\beta_4^c = -\frac{2}{2187}h_A^2\big(972 + 2349\,g_A^2 + 1152\,h_A^2 - 2250\,g_A\,g_1 + 125\,g_1^2\big),$$
$$\beta_1^{d,N} = -\frac{1}{6}g_A^4,$$
$$\beta_2^{d,N} = -\frac{1}{12} - \frac{5}{12}g_A^2,$$
$$\beta_3^{d,N} = \frac{1}{2} + \frac{1}{6}g_A^4,$$
$$\beta_5^{d,N} = \frac{1}{24} + \frac{5}{24}g_A^2,$$
$$\beta_{14}^{d,N} = \frac{1}{3}g_A^4,$$
$$\beta_{15}^{d,N} = \beta_{18}^{d,N} = 0,$$
$$\beta_1^{d,\Delta} + \beta_2^{d,\Delta} + \beta_3^{d,\Delta} = \frac{10}{27}h_A^2,$$
$$\beta_3^{d,\Delta} = \frac{h_A^2}{2187}\big(125\,g_1^2 + 288\,h_A^2 - 243\,g_A^2 - 450\,g_A g_1\big),$$
$$\beta_5^{d,\Delta} = -\frac{5}{27}h_A^2,$$
$$\beta_{18}^{d,\Delta} = 0,$$
$$\beta_{14}^{d,\Delta} - \beta_{15}^{d,\Delta} = \frac{2\,h_A^2}{2187}\big(288\,h_A^2 - 243\,g_A^2 - 450\,g_A\,g_1 + 125\,g_1^2\big). \qquad (4.3)$$

This particular form of the β functions guarantees that the amplitude remains finite in the $d \to 4$ limit. We use here the notation in which the divergencies associated with loop diagrams without Δ excitations (with Δ excitations) are cancelled by terms $\propto\beta_i^{d,N}$ ($\propto\beta_i^{c,\Delta}$ and $\propto\beta_i^{d,\Delta}$). Furthermore, in order to maintain the explicit decoupling scheme, we have introduced additional finite dimensionless shifts c_i^Δ and d_i^Δ. The explicit decoupling scheme is defined by the requirement that all observables calculated in the SSE include only nucleonic contributions after taking the $\Delta \to \infty$ limit. In this limit, all contributions emerging from the intermediate Δ excitations have to vanish (in the explicit decoupling scheme) so that the Δ isobar explicitly decouples from the theory. In order to satisfy the explicit decoupling, the values of the LECs c_i^Δ and d_i^Δ have to be chosen as

$$c_1^\Delta = 2h_A^2\log\left(\frac{2\Delta}{\mu}\right),$$
$$c_2^\Delta = -\frac{2\,h_A^2}{6561}\big(6399\,g_A^2 - 8910\,g_A\,g_1 + 3575\,g_1^2\big) - \frac{80\,h_A^2}{2187}(9\,g_A - 5\,g_1)^2\log\left(\frac{2\Delta}{\mu}\right),$$
$$c_3^\Delta = \frac{2\,h_A^2}{6561}\big(6399\,g_A^2 - 8910\,g_A\,g_1 + 3575\,g_1^2\big) + \frac{16\,h_A^2}{2187}[729 + 5\,(9\,g_A - 5\,g_1)^2]\log\left(\frac{2\Delta}{\mu}\right),$$
$$c_4^\Delta = \frac{h_A^2}{6561}\big(4860 - 35559\,g_A^2 + 1728\,h_A^2 + 28350\,g_A\,g_1 - 4775\,g_1^2\big) - \frac{2\,h_A^2}{2187}\big(972 + 2349\,g_A^2 + 1152\,h_A^2 - 2250\,g_A\,g_1 + 125\,g_1^2\big)\log\left(\frac{2\Delta}{\mu}\right), \qquad (4.4)$$

and

$$d_1^\Delta + d_2^\Delta = -\frac{h_A^2}{6561}\big(-2106 + 5103\,g_A^2 + 216\,h_A^2 - 3870\,g_A\,g_1 + 925\,g_1^2\big) + \frac{h_A^2}{2187}\big(810 + 243\,g_A^2 - 288\,h_A^2 + 450\,g_A\,g_1 - 125\,g_1^2\big)\log\left(\frac{2\Delta}{\mu}\right),$$
$$d_3^\Delta = \frac{h_A^2}{6561}\big(5103\,g_A^2 + 216\,h_A^2 - 3870\,g_A\,g_1 + 925\,g_1^2\big) + \frac{h_A^2}{2187}\big(-243\,g_A^2 + 288\,h_A^2 - 450\,g_A\,g_1 + 125\,g_1^2\big)\log\left(\frac{2\Delta}{\mu}\right),$$
$$d_5^\Delta = -\frac{13\,h_A^2}{81} - \frac{5\,h_A^2}{27}\log\left(\frac{2\Delta}{\mu}\right),$$

$$d_{14}^{\Delta}-d_{15}^{\Delta}=\frac{h_A^2}{6561}\left(5589\,g_A^2+432\,h_A^2-9090\,g_A\,g_1+3425\,g_1^2\right)+\frac{2\,h_A^2}{2187}\left(-243\,g_A^2+288\,h_A^2-450\,g_A\,g_1+125\,g_1^2\right)\log\left(\frac{2\Delta}{\mu}\right), \tag{4.5}$$

respectively. Clearly, the above expressions are unique modulo terms that vanish in the $\Delta\to\infty$ limit. On top of the explicit decoupling scheme, we put a constraint on negative powers of Δ. Specifically, we require that the $1/\Delta$ expansion of the pion-nucleon amplitude is consistent with the resonance saturation. This means that the $1/\Delta$ expansion of the Δ-full pion-nucleon amplitude should be equal to the Δ-less amplitude with the LECs c_i and $\bar{d}_i$ being replaced by Eqs. (4.13) and (4.14), respectively. In order to achieve this also for relativistic corrections, we have to perform additional shifts of c_i and d_i-LECs, namely

$$\begin{aligned} c_2 &\to c_2+\frac{8h_A^2}{9m_N},\\ d_1+d_2 &\to d_1+d_2+\frac{h_A^2}{18m_N\Delta},\\ d_3 &\to d_3-\frac{2h_A^2}{9m_N\Delta},\\ d_5 &\to d_5+\frac{h_A^2}{12m_N\Delta},\\ d_{14}-d_{15} &\to d_{14}-d_{15}-\frac{2h_A^2}{9m_N\Delta}. \end{aligned} \tag{4.6}$$

We now turn to pion-nucleon scattering. In the center-of-mass (c.m.) system, the amplitude for the reaction $\pi^a(q_1)+N(p_1)\to\pi^b(q_2)+N(p_2)$, with $p_{1,2}$ and $q_{1,2}$ being the corresponding four-momenta and a,b referring to the pion isospin quantum numbers, takes the form

$$T_{\pi N}^{ba}=\frac{E+m}{2m}\left(\delta^{ba}\left[g^+(\omega,t)+i\vec{\sigma}\cdot\vec{q}_2\times\vec{q}_1\,h^+(\omega,t)\right]+i\epsilon^{bac}\tau^c\left[g^-(\omega,t)+i\vec{\sigma}\cdot\vec{q}_2\times\vec{q}_1\,h^-(\omega,t)\right]\right). \tag{4.7}$$

Here, $\omega=q_1^0=q_2^0$ is the pion c.m. system energy, $E_1=E_2\equiv E=(\vec{q}^{\,2}+m^2)^{1/2}$ is the nucleon energy, and $\vec{q}_1^{\,2}=\vec{q}_2^{\,2}\equiv\vec{q}^{\,2}=[(s-M_\pi^2-m^2)^2-4m^2M_\pi^2]/(4s)$. Further, $t=(q_1-q_2)^2$ is the invariant momentum transfer squared while s denotes the total c.m. system energy squared. The quantities $g^\pm(\omega,t)$ $[h^\pm(\omega,t)]$ refer to the isoscalar and isovector non-spin-flip (spin-flip) amplitudes and can be calculated in chiral perturbation theory. The contributions to the amplitudes which do not involve intermediate Δ excitations up to order Q^4 (i.e., subleading one-loop order) are given in Ref. [50]. In Appendix B, we give explicitly the Δ-isobar contributions up to order ϵ^3. In a complete analogy to the Δ-less calculation reported in Ref. [50], the phase shifts are obtained from the partial-wave amplitudes in the isospin basis $f_{l\pm}^I(s)$ by means of the following unitarization prescription

$$\delta_{l\pm}^I(s)=\arctan\left[|\vec{q}|\,\mathrm{Re}\,f_{l\pm}^I(s)\right]. \tag{4.8}$$

Determination of the LECs is carried out using exactly the same procedure as in our Δ-less calculations [50]. While the πN scattering amplitude is worked out here only to order ϵ^3, we decided to include also the order-Q^4 terms obtained within the Δ-less theory when fitting the phase shifts in order to facilitate a direct comparison with the results of Ref. [50]. This way we make sure that the differences between the values of the LECs obtained in the two analyses are solely due to the explicit treatment of the Δ degrees of freedom. The impact of the Q^4 terms on the $3N$F will be discussed in Sec. VI.

For the pion-nucleon contributions to the scattering amplitude, we proceed in exactly the same way as in Ref. [50]. We remind the reader that certain LECs $\bar{e}_i$ from $\mathcal{L}_{\pi N}^{(4)}$ enter the amplitude only in linear combinations with the LECs c_i and therefore cannot be determined from πN scattering data. Following Refs. [73] and [50], these e_i contributions are absorbed into redefinition of the c_i's by setting

$$\begin{aligned} e_{22}-4e_{38}-\frac{l_3c_1}{F_\pi^2}&=0,\\ e_{20}+e_{35}&=0,\\ 2e_{19}-e_{22}-e_{36}+2\frac{l_3c_1}{F_\pi^2}&=0,\\ 2e_{21}-e_{37}&=0, \end{aligned} \tag{4.9}$$

without loss of generality. The LEC d_{18} from $\mathcal{L}_{\pi N}^{(4)}$ can be fixed by means of the Goldberber-Treiman discrepancy

$$g_{\pi NN}=\frac{g_A\,m_N}{F_\pi}\left(1-\frac{2M_\pi^2\,d_{18}}{g_A}\right), \tag{4.10}$$

where for $g_{\pi NN}$ we adopt the value from Ref. [74] of $g_{\pi NN}^2/(4\pi)\simeq 13.54$, which also agrees with the determination in Ref. [75] based on the Goldberger-Miyazawa-Oehme sum rule and utilizing the most accurate available data on the pion-nucleon scattering lengths. We set $d_{18}=0$ and use the effective, larger value for g_A of

$$g_A=\frac{F_\pi\,g_{\pi NN}}{m_N}\simeq 1.285 \tag{4.11}$$

in all expressions. This is a legitimate procedure at the order we are working. This leaves us with 13 independent (linear combinations of the) low-energy constants in the nucleonic contributions to the scattering amplitude which have to be fixed from a fit to the data, namely $c_{1,2,3,4}$, $\bar{d}_1+\bar{d}_2$, $\bar{d}_3$, $\bar{d}_5$, $\bar{d}_{14}-\bar{d}_{15}$, and $\bar{e}_{14,15,16,17,18}$; see Ref. [50] for more details and explicit expressions. Here bars of LECs indicate that we used $\overline{\mathrm{MS}}$ renormalization scheme where $\mu=M_\pi$. We also use the same values for the pion mass and decay constant as in that reference, namely $M_\pi=138.03$ MeV and $F_\pi=92.4$ MeV.

The contributions to the amplitude associated with the Δ excitations and given in Appendix B involve further LECs,

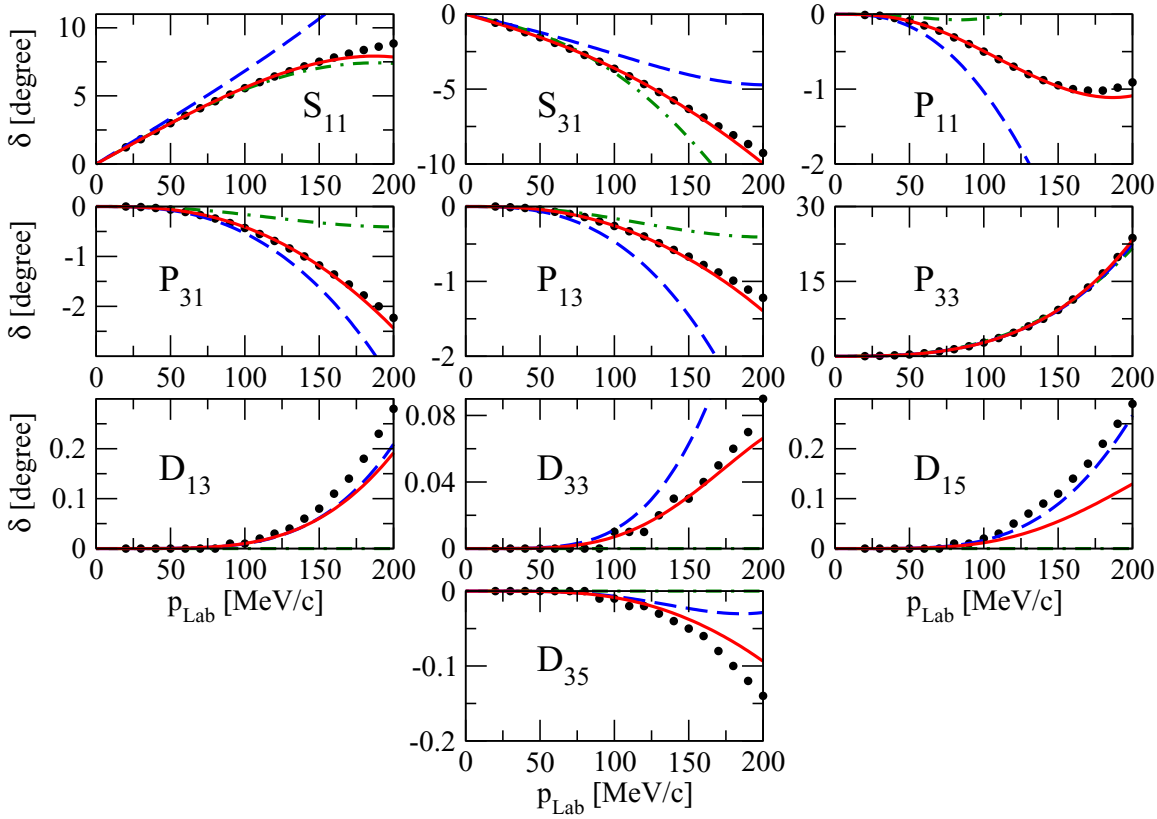

FIG. 6. Results of the fit for πN s-, p-, and d-wave phase shifts using the GW partial wave analysis of Ref. [79]. The solid curves correspond to the $\epsilon^3 + Q^4$ results, the dashed curves to the order-ϵ^3 results, and the dashed-dotted curves to the order-ϵ^2 calculation.

namely h_A and g_1. For the $\pi N\Delta$ axial vector constant, we adopt the value of $h_A = 1.34$ which is fixed from the width of the Δ resonance and also agrees well with the large-N_c prediction [76,77]. Notice that similarly to the convention adopted for g_A, the $\pi N\Delta$ Goldberger-Treiman discrepancy is implicitly taken into account by using the above value of the LEC h_A.[1] Our fits to πN data turn out to be fairly insensitive to a particular value of g_1. For this reason, we decided to fix it to its large-N_c value $g_1 = 9/5\, g_A \approx 2.31$ [76–78]. We, therefore, have to finally fix exactly the same combinations of the low-energy constants as in the Δ-less theory.

As in Ref. [50], we performed a combined fit for all s, p, and d waves. We remind the reader that it is crucial to include d waves in the fit as they impose severe constraints on some of the e_i constants, especially on $\bar{e}_{14}$ and $\bar{e}_{17}$, which also enter the N^{4}LO expressions for the three-body force. The results of the fits using the partial wave analysis (PWA) by the George-Washington University group (GW) [79] and the Karlsruhe-Helsinki group (KH) [80] are presented in Figs. 6 and 7, respectively. In these figures, we show the full, i.e., order-$\epsilon^3 + Q^4$ results (solid curves) as well as the phase shifts calculated up to order ϵ^3 without Q^4 terms (dashed curves) and ϵ^2 (dash-dotted curves) using the same parameters (from the order-$\epsilon^3 + Q^4$ fit) in all curves. We fit the data points from threshold up to $p_{\rm Lab} = 150\,{\rm MeV/c}$, and obtain a description of the phase shifts similar to the Δ-less case. Naturally, the description of the P_{33} partial wave (Δ s-channel) is significantly improved.

Notice that more sophisticated studies of pion-nucleon scattering employing a covariant formulation of baryon chiral effective field theory with and without explicit $\Delta(1232)$ degrees of freedom have been carried out recently; see Refs. [78,81–84]. Also, more reliable ways to extract the low-energy constants from the πN reaction and to estimate their uncertainties have been explored as compared to the ones employed in our analysis. Those include, in particular, analytic extrapolations of the scattering amplitude into the subthreshold region using the solutions to the Roy-Steiner equation and a direct determination of the LECs from the available πN scattering data in the physical region instead of using partial-wave analyses; see Refs. [78,82,83,85–87]. Future studies of nuclear forces and few-nucleon systems should, obviously, employ the most reliable available values of the πN LECs, such as the ones from Refs. [78,84,85]. In this paper, however, we focus mainly on the Δ contributions to the $3N$F. To facilitate a comparison between the Δ-full and Δ-less calculation of Refs. [50,51] and to allow for an unambiguous interpretation of our results in terms of resonance saturation, we follow here the same procedure for the determination of various LECs as adopted in Ref. [50].

[1]The results for the $3N$F are expected to be much less sensitive to the precise value of h_A than to the value of g_A. This is because the changes in h_A can, to some extent, be compensated by the changes in the LECs from the subleading and higher-order effective Lagrangian.

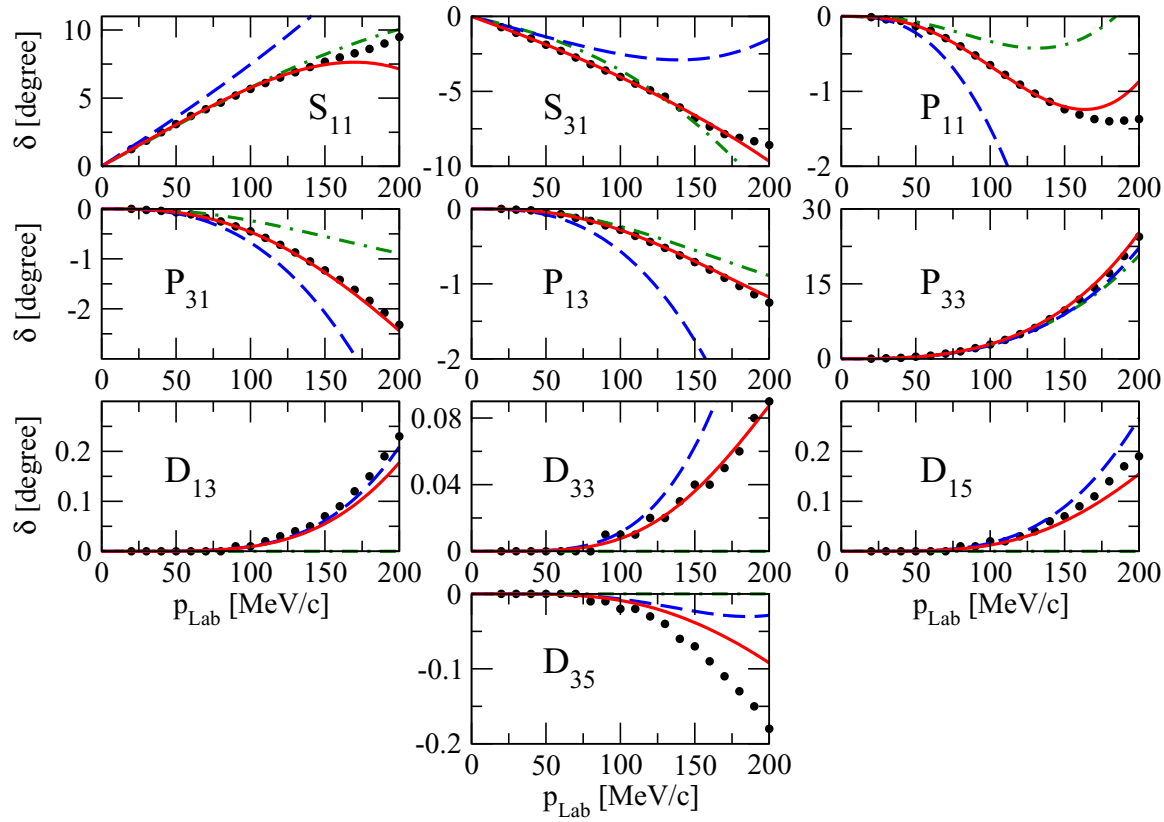

FIG. 7. Results of the fit for πN s-, p-, and d-wave phase shifts using the KH partial wave analysis of Ref. [80]. The solid curves correspond to the full $\epsilon^3 + Q^4$ results, the dashed curves to the order-ϵ^3 results, and the dashed-dotted curves to the order-ϵ^2 calculation.

We finally turn to the discussion of the extracted parameters. The obtained values of the low-energy constants are collected in Table I. We also looked at the statistical errors of the fitted parameters in order to see qualitatively which low-energy constants (or their linear combinations) are well constrained by the data and which of them are poorly determined. Similarly to the strategy utilized in Ref. [88], we assigned the same relative error to each data point from the partial-wave analyses equal to 5%. This ansatz is somewhat arbitrary but seems reasonable for an estimate of the relative uncertainties of different low-energy constants. Notice further that the statistical errors are calculated in the linearized approximation; i.e., the covariance matrix is taken to be the inverse of the Hessian matrix of the χ^2 function at its minimum. Such an approximation is sufficient for the qualitative analysis that we are going to perform. The resulting statistical uncertainties for all low-energy constants are listed in Table I and appear to be almost the same for both the KH and GW analyses. Moreover, they change very little when the fit is performed in the Δ-less case as in Ref. [50]. One can see that the low-energy constants c_2, $\bar{e}_{15}$, and $\bar{e}_{16}$ have the largest errors (0.8–5.1) in the corresponding natural units (GeV^{-1}, GeV^{-2}, and GeV^{-3} for the c_i, $\bar{d}_i$, and $\bar{e}_i$, respectively), indicating that these parameters are not well determined in the fit. On the other hand, $\bar{e}_{17}$, $\bar{e}_{14}$, which are the only LECs $\bar{e}_i$ contributing to the $3NF$ at order Q^5, and the LEC c_4 are strongly constrained by the data.

Another important quantity is a correlation between pairs of parameters. The largest in magnitude values for the correlation coefficients are obtained for the pairs $c_1 - c_2$ (0.99), $c_1 - \bar{e}_{16}$ (-0.98), $c_2 - \bar{e}_{16}$ (-0.99), and $[(\bar{d}_1 + \bar{d}_2) - (\bar{d}_{14} - \bar{d}_{15})]$ (-0.97). In order to get more detailed information on the correlation among various parameters, we have computed eigenvalues of the covariance matrix. The square roots of their numerical values in natural units are 5.41,0.59, 0.45,0.35,0.29,0.12,0.05,0.03,0.03,0.02,0.02,0.01,0.01 for the

TABLE I. Low-energy constants obtained from a fit to the empirical s-, p-, and d-wave pion-nucleon phase shifts using partial-wave analysis of Refs. [79,80]. Values of the LECs are given in GeV^{-1}, GeV^{-2}, and GeV^{-3} for the c_i, $\bar{d}_i$, and $\bar{e}_i$, respectively.

	c_1	c_2	c_3	c_4	$\bar{d}_1+\bar{d}_2$	$\bar{d}_3$	$\bar{d}_5$	$\bar{d}_{14}-\bar{d}_{15}$	$\bar{e}_{14}$	$\bar{e}_{15}$	$\bar{e}_{16}$	$\bar{e}_{17}$	$\bar{e}_{18}$
Fit to the GW PWA [79]	−1.32	0.39	−2.68	1.86	1.46	−1.01	−0.10	−2.16	0.06	−2.47	−0.05	−0.56	0.54
Statistical error	0.45	1.34	0.16	0.07	0.17	0.31	0.19	0.33	0.03	0.07	0.80	0.38	4.66
Fit to the KH PWA [80]	−0.85	0.45	−1.91	1.49	2.07	−2.45	0.66	−3.86	−0.12	−7.05	3.39	−0.38	2.85
Statistical error	0.50	1.47	0.18	0.10	0.19	0.33	0.20	0.36	0.03	0.08	0.90	0.48	5.12

TABLE II. Low-energy constants obtained from a fit to the empirical s-, p-, and d-wave pion-nucleon phase shifts up to $p_{\rm Lab} = 200\,{\rm MeV/c}$ using partial-wave analysis of Refs. [79,80]. Values of the LECs are given in $\rm GeV^{-1}$, $\rm GeV^{-2}$, and $\rm GeV^{-3}$ for the c_i, $\bar{d}_i$, and $\bar{e}_i$, respectively.

	c_1	c_2	c_3	c_4	$\bar{d}_1+\bar{d}_2$	$\bar{d}_3$	$\bar{d}_5$	$\bar{d}_{14}-\bar{d}_{15}$	$\bar{e}_{14}$	$\bar{e}_{15}$	$\bar{e}_{16}$	$\bar{e}_{17}$	$\bar{e}_{18}$
Fit to the GW PWA [79]	−1.31	0.11	−2.54	1.85	1.43	−0.90	−0.16	−2.09	0.07	−3.44	1.65	−0.46	0.47
Statistical error	0.19	0.48	0.08	0.04	0.14	0.19	0.11	0.28	0.02	0.04	0.33	0.17	1.48
Fit to the KH PWA [80]	−1.35	−0.89	−2.19	1.63	2.08	−2.13	0.45	−3.69	−0.05	−6.59	7.22	−0.35	1.88
Statistical error	0.21	0.51	0.08	0.05	0.15	0.20	0.11	0.29	0.02	0.04	0.37	0.22	1.57

KH analysis and 4.92,0.51,0.37,0.32,0.27,0.11,0.04,0.03,0.02, 0.02,0.01,0.01,0.01 for the GW analysis. One can see that the first eigenvalue is at least two orders of magnitude larger than any of the other eigenvalues. This indicates that fixing certain linear combination of parameters results in very slow changes in the χ^2 even if the individual values of the LECs entering this linear combination change significantly. This combination is the corresponding eigenvector and is approximately equal to $-0.1c_1 - 0.3c_2 - 0.1\bar{e}_{15} + 0.9\bar{e}_{16}$ (the other constants enter with much smaller coefficients). The coefficients are given in natural units. We indeed observe that these four parameters are strongly correlated and one can obtain fits comparable with the best one with those parameters being significantly shifted. The appearance of such a strong correlation among the parameters reflects the fact that one cannot fully resolve the energy dependence of the amplitude with a good accuracy in the low-energy regime. This interpretation is confirmed by performing a fit to higher energy, namely $p_{\rm Lab} = 200\,{\rm MeV/c}$; see Table II. In this case, both the statistical errors and the correlations (including the ones among c_1, c_2, $\bar{e}_{15}$, and $\bar{e}_{16}$) do become significantly smaller. Unfortunately, the purely perturbative approach cannot be expected to be applicable at such energies as the phase shifts become quite large.

Finally, it is interesting to compare the values of the LECs with the ones obtained in the Δ-less approach. As already pointed out before, one expects to find more natural values of the LECs in the Δ-full theory. This is indeed the case, as one can see from Table III, where such a comparison is carried out for the KH fits. The situation for the GW fits is similar; see Table I of Ref. [50]. Comparing the second and the third rows of this table, one observes a sizable reduction in magnitude for most of the LECs when the Δ is included as an explicit degree of freedom. This raises the question of whether these differences can be understood analytically. In the following, we address this question by isolating the contributions of the Δ to the various LECs. To this aim, we make a $1/\Delta$ expansion of the Δ-resonance contributions to the πN amplitude and match the expanded expressions to the amplitude obtained in the Δ-less theory up to order Q^4. We decompose the various renormalized LECs into Δ-less ($\not\Delta$) and Δ contributions (Δ) via

$$\begin{aligned} c_i &= c_i(\not\Delta) + c_i(\Delta), \\ d_i &= d_i(\not\Delta) + d_i(\Delta), \\ e_i &= e_i(\not\Delta) + e_i(\Delta). \end{aligned} \tag{4.12}$$

Expanding the ϵ^1 result up to order $1/\Delta$, we recover the well-known results for the c_i's [89]

$$\begin{aligned} &c_1(\Delta) = 0, \quad c_2(\Delta) = \frac{4\,h_A^2}{9\,\Delta}, \\ &c_3(\Delta) = -\frac{4\,h_A^2}{9\,\Delta}, \quad c_4(\Delta) = \frac{2\,h_A^2}{9\,\Delta}. \end{aligned} \tag{4.13}$$

From the $1/\Delta^2$ terms of the order-ϵ^1 πN amplitude, we obtain the Δ contributions to the LECs $\bar{d}_i$ given by

$$\begin{aligned} d_1(\Delta) + d_2(\Delta) &= \frac{h_A^2}{9\,\Delta^2}, \\ d_3(\Delta) &= -\frac{h_A^2}{9\,\Delta^2}, \\ d_{14}(\Delta) - d_{15}(\Delta) &= -\frac{2\,h_A^2}{9\,\Delta^2}. \end{aligned} \tag{4.14}$$

In principle, one could also expect $1/\Delta$ contributions from the order-ϵ^2 πN amplitude. However, all such terms turn out to contribute to renormalization of h_A and do not lead to resonance saturation of d_i. One observes from Table I that the Δ contributions explain at least a half of the size of the LECs $d_1 + d_2$,d_3, and $d_{14} - d_{15}$, which appear to be unnaturally large in the Δ-less approach; see also Ref. [78] for similar conclusions.

To explore Δ-resonance saturation of the LECs e_i from $\mathcal{L}^{(4)}_{\pi N}$ which enter the order-Q^4 pion-nucleon amplitude, we need to analyze the following terms:

(1) $1/\Delta^3$ contributions from ϵ^1 amplitude,
(2) $1/\Delta^2$ contributions from ϵ^2 amplitude (these terms vanish after renormalization of h_A), and
(3) $1/\Delta$ contributions from ϵ^3 amplitude.

TABLE III. Low-energy constants obtained from a fit to the empirical s-, p-, and d-wave pion-nucleon phase shifts using the partial wave analysis of Ref. [80] and the corresponding Δ-resonance contributions given in Eqs. (4.13)–(4.15). Values of the LECs are given in $\rm GeV^{-1}$, $\rm GeV^{-2}$, and $\rm GeV^{-3}$ for the c_i, $\bar{d}_i$, and $\bar{e}_i$, respectively.

	c_1	c_2	c_3	c_4	$\bar{d}_1+\bar{d}_2$	$\bar{d}_3$	$\bar{d}_5$	$\bar{d}_{14}-\bar{d}_{15}$	$\bar{e}_{14}$	$\bar{e}_{15}$	$\bar{e}_{16}$	$\bar{e}_{17}$	$\bar{e}_{18}$
Q^4, KH PWA [80]	−0.75	3.49	−4.77	3.34	6.21	−6.83	0.78	−12.02	1.52	−10.41	6.08	−0.37	3.26
$\epsilon^3 + Q^4$, KH PWA [80]	−0.85	0.45	−1.91	1.49	2.07	−2.45	0.66	−3.86	−0.12	−7.05	3.39	−0.38	2.85
Δ contribution	0	2.81	−2.81	1.40	2.39	−2.39	0	−4.77	1.87	−4.15	4.15	−0.17	1.32

The complete contribution of the Δ to these LECs is given by a sum of these terms and has the form

$$\begin{aligned}
\bar{e}_{14}(\Delta) &= \frac{h_A^2}{864\,F_\pi^2\,\pi^2\,\Delta}\left[7+10\,\log\left(\frac{2\,\Delta}{M_\pi}\right)\right],\\
\bar{e}_{15}(\Delta) &= -\frac{h_A^2}{18\,\Delta^3}-\frac{h_A^2}{839808\,F_\pi^2\,\pi^2\,\Delta}\left(3969\,g_A^2-4050\,g_A\,g_1+1225\,g_1^2\right),\\
\bar{e}_{16}(\Delta) &= \frac{h_A^2}{18\,\Delta^3}+\frac{h_A^2}{839808\,F_\pi^2\,\pi^2\,\Delta}\left(3969\,g_A^2-4050\,g_A\,g_1+1225\,g_1^2\right),\\
\bar{e}_{17}(\Delta) &= -\frac{h_A^2}{1728\,F_\pi^2\,\pi^2\,\Delta}\left[1+2\log\left(\frac{2\,\Delta}{M_\pi}\right)\right],\\
\bar{e}_{18}(\Delta) &= \frac{h_A^2}{36\,\Delta^3}+\frac{h_A^2}{839808\,F_\pi^2\,\pi^2\,\Delta}\left(2025\,g_A^2+3456\,h_A^2-450\,g_A\,g_1+425\,g_1^2\right)\\
&\quad-\frac{h_A^2\,g_A^2}{108\,F_\pi^2\,\pi^2\,\Delta}\log\left(\frac{2\,\Delta}{M_\pi}\right),\\
\bar{e}_{19}(\Delta)-\frac{1}{2}\bar{e}_{36}(\Delta)-2\bar{e}_{38}(\Delta) &= -\frac{h_A^2}{93312\,F_\pi^2\,\pi^2\,\Delta}\left(351+1296\,g_A^2+400\,g_1^2\right)\\
&\quad+\frac{h_A^2}{5184\,F_\pi^2\,\pi^2\,\Delta}\left(-33+81\,g_A^2-50\,g_A\,g_1+25\,g_1^2\right)\log\left(\frac{2\,\Delta}{M_\pi}\right),\\
\bar{e}_{20}(\Delta)+\bar{e}_{35}(\Delta) &= \frac{h_A^2}{5832\,F_\pi^2\,\pi^2\,\Delta}\left(81\,g_A^2+25\,g_1^2\right)-\frac{h_A^2}{5184\,F_\pi^2\,\pi^2\,\Delta}\left(81\,g_A^2-50\,g_A\,g_1+25\,g_1^2\right)\log\left(\frac{2\,\Delta}{M_\pi}\right),\\
\bar{e}_{21}(\Delta)-\frac{1}{2}\bar{e}_{37}(\Delta) &= -\frac{h_A^2}{62208\,F_\pi^2\,\pi^2\,\Delta}\left(72-999\,g_A^2+384\,h_A^2+750\,g_A\,g_1-175\,g_1^2\right)\\
&\quad+\frac{h_A^2}{10368\,F_\pi^2\,\pi^2\,\Delta}\left(-24+135\,g_A^2+50\,g_A\,g_1-25\,g_1^2\right)\log\left(\frac{2\,\Delta}{M_\pi}\right),\\
\bar{e}_{22}(\Delta)-4\,\bar{e}_{38}(\Delta) &= -\frac{h_A^2}{72\,F_\pi^2\,\pi^2\,\Delta}\left[1+\log\left(\frac{2\,\Delta}{M_\pi}\right)\right].
\end{aligned}\tag{4.15}$$

The appearance of logarithms of the physical pion mass in the above expressions is due to our choice of the renormalization scale $\mu = M_\pi$ in the definitions of c_i, $\bar{d}_i$, and $\bar{e}_i$. The LECs $\bar{e}_{15}(\Delta)$,$\bar{e}_{16}(\Delta)$, and $\bar{e}_{18}(\Delta)$ receive $1/\Delta^3$ contributions from the order-ϵ^1 πN amplitude. Numerically, these terms dominate over the loop contributions (as one would expect from naive dimensional analysis) and explain a half of the size of the LECs $\bar{e}_{15}$,$\bar{e}_{16}$, and $\bar{e}_{18}$, which appear to be unnaturally large in the Δ-less theory; see Table III. It is comforting to see that the Δ contributions to the LECs c_i, $\bar{d}_i$, and $\bar{e}_i$ given in the above expressions, whose numerical values are listed in Table III, are in a very good agreement with the differences between the Δ-less and Δ-full fits. Clearly, one should not expect this agreement to be perfect since the Δ contributions to the amplitude involve terms beyond the order-Q^4 Δ-less result. Our findings, however, indicate that these resummed contributions are likely to be small and the most important terms are well represented by the Δ-resonance contributions to the LECs c_i, $\bar{d}_i$, and $\bar{e}_i$.

Last but not least, we emphasize that the (linear combinations of the) LECs $\bar{e}_{19,20,21,22,35,36,37,38}$ and c_1 absorbed into redefinition of c_i's [see Eq. (4.9)] do receive contributions due to the Δ resonance [see Eq. (4.15)]. Assuming that these LECs are saturated by the Δ, we may estimate the shifts in the c_i induced by absorbing these order-Q^4 contributions via

$$\begin{aligned}
c_1 &\to c_1+2\,M_\pi^2\left(\bar{e}_{22}-4\,\bar{e}_{38}+\frac{l_3\,c_1}{F_\pi^2}\right),\\
c_2 &\to c_2-8\,M_\pi^2(\bar{e}_{20}+\bar{e}_{35}),\\
c_3 &\to c_3-4\,M_\pi^2(2\,\bar{e}_{19}-\bar{e}_{22}-\bar{e}_{36}),\\
c_4 &\to c_4-4\,M_\pi^2(2\,\bar{e}_{21}-\bar{e}_{37}).
\end{aligned}\tag{4.16}$$

Since the Δ-resonance contributions to the induced shifts of c_i's start with the loop corrections and do not have any $1/\Delta^3$ contribution from the order-ϵ^1 terms, the induced shifts appear to be rather small:

$$\begin{aligned}
2\,M_\pi^2\left[\bar{e}_{22}(\Delta)-4\,\bar{e}_{38}(\Delta)+\frac{\bar{l}_3\,c_1(\Delta)}{F_\pi^2}\right] &= -0.10\,\mathrm{GeV}^{-1},\\
-8\,M_\pi^2[\bar{e}_{20}(\Delta)+\bar{e}_{35}(\Delta)] &= -0.14\,\mathrm{GeV}^{-1},\\
-4\,M_\pi^2[2\,\bar{e}_{19}(\Delta)-\bar{e}_{22}(\Delta)-\bar{e}_{36}(\Delta)] &= 0.10\,\mathrm{GeV}^{-1},\\
-4\,M_\pi^2[2\,\bar{e}_{21}(\Delta)-\bar{e}_{37}(\Delta)] &= -0.26\,\mathrm{GeV}^{-1}.
\end{aligned}\tag{4.17}$$

V. Δ(1232) CONTRIBUTIONS TO THE TWO-PION EXCHANGE 3*N*F

After these preparations, we are now in the position to discuss the contributions to the two-pion exchange 3*N*F emerging from the intermediate Δ excitations up to the leading one-loop order (i.e., N^{3}LO).

In the isospin and static limits, the general structure of the two-pion exchange 3*N*F in momentum space has the following form (modulo terms of a shorter range; see Ref. [50] for more details):

$$V_{2\pi} = \frac{\vec{\sigma}_1 \cdot \vec{q}_1 \, \vec{\sigma}_3 \cdot \vec{q}_3}{\left[q_1^2 + M_\pi^2\right]\left[q_3^2 + M_\pi^2\right]} [\boldsymbol{\tau}_1 \cdot \boldsymbol{\tau}_3 \, \mathcal{A}(q_2) + \boldsymbol{\tau}_1 \boldsymbol{\tau}_3 \cdot \boldsymbol{\tau}_2 \, \vec{q}_1 \times \vec{q}_3 \cdot \vec{\sigma}_2 \, \mathcal{B}(q_2)], \tag{5.1}$$

where $\vec{\sigma}_i$ ($\boldsymbol{\tau}_i$) denote the Pauli spin (isospin) matrices for the nucleon i while $\vec{q}_i$ is the momentum transfer, $\vec{q}_i = \vec{p}\,'_i - \vec{p}_i$, with $\vec{p}\,'_i$ and $\vec{p}_i$ being the final and initial momenta of the nucleon i. Here and in what follows, we use the notation $q_i \equiv |\vec{q}_i|$. Unless stated otherwise, the expressions for the 3*N*F are given for a particular choice of the nucleon labels. The complete result can then be obtained by taking into account all possible permutations of the nucleons,

$$V_{3\mathrm{N}}^{\mathrm{full}} = V_{3\mathrm{N}} + 5 \text{ permutations}. \tag{5.2}$$

The quantities $\mathcal{A}(q_2)$ and $\mathcal{B}(q_2)$ in Eq. (5.1) are scalar functions of the momentum transfer q_2 of the second nucleon whose explicit form is derived within the chiral expansion. In the Δ-less framework, this expansion starts at N^{2}LO which corresponds to the order Q^3. The explicit expressions for $\mathcal{A}(q_2)$ and $\mathcal{B}(q_2)$ up to N^{4}LO, i.e., up to order Q^5, can be found in Ref. [50]. In the Δ-full framework, the leading contributions are shifted from N^{2}LO to NLO, i.e., to order ϵ^2. These leading Δ contributions have the form

$$\mathcal{A}_\Delta^{(2)}(q_2) = -\frac{g_A^2 h_A^2}{18\,\Delta\,F_\pi^4}\left(2M_\pi^2 + q_2^2\right), \qquad \mathcal{B}_\Delta^{(2)}(q_2) = \frac{g_A^2 h_A^2}{36\,\Delta\,F_\pi^4}, \tag{5.3}$$

and are known to provide the dominant long-range mechanism of the 3*N*F [52]. There are no contributions of the Δ to $\mathcal{A}(q_2)$ and $\mathcal{B}(q_2)$ at N^{2}LO [59], i.e., at order ϵ^3, except for the shift of the LEC h_A as discussed in Sec. IV; see Eq. (4.1). At N^{3}LO (ϵ^4) one has to take into account the contributions emerging from the diagrams shown in Fig. 8. These graphs are analogous to the Δ-less ones shown in Fig. 2 of Ref. [40] but involve at least one intermediate Δ excitation. Notice that in contrast to that work, we do not show in Fig. 8 certain diagrams which yield vanishing results for the sake of compactness. This concerns, for example, one-loop graphs leading to integrals involving an odd power of the loop momentum to be integrated over.

The last three diagrams in Fig. 8 contribute to renormalization of the pion field and the lowest-order pion-nucleon and pion-nucleon-Δ vertices and also give rise to the corresponding Goldberger-Treiman discrepancy relations. These contributions are automatically taken into account by expressing the 3*N*F in terms of physical quantities and using the effective values of the LECs g_A and h_A which account for the Goldberger-Treiman discrepancy; see the discussion in the previous section. We are therefore left with one-loop diagrams constructed out of the lowest-order and tree-order graphs which involve a single insertion of the $1/m_N$ vertices which give rise to the leading relativistic corrections. We remind the reader that the power counting scheme used to derive the nuclear forces and currents in Refs. [32,35,37,40,41,45,46,50,51,90–93] makes the assignment $Q/m_N \sim Q^2/\Lambda_\chi^2$ for the nucleon mass; see Ref. [94] for more details. This implies that $1/m_N$ corrections to the nuclear forces and currents are shifted to higher orders compared to the corresponding static contributions.[2] In particular, the leading relativistic corrections appear at the same order with the leading one-loop diagrams.

It is important to keep in mind that, in order to derive the genuine 3*N*F contributions, one needs to separate the irreducible parts in the corresponding amplitudes in order to avoid double counting when iterating the potentials in the scattering equation. While this can be achieved in different ways (see Ref. [95] for more details), we employ here the method of unitary transformation which was first applied in the context of chiral EFT in Ref. [96]. A comprehensive discussion of this approach can be found in Ref. [97]. The same method was used in our earlier work on the derivation of the three- [40,41,50,51] and four-nucleon forces [45,46] and electroweak nuclear current operators [91–93]. We remind the reader that in this approach one first applies the canonical formalism to the effective chiral Lagrangian expressed in terms of renormalized fields to derive the Hamilton density in the pion-nucleon sector. In the second step, one decouples the purely nucleonic subspace of the Fock space from the rest via a suitably chosen unitary transformation. The determination of the unitary operator and the resulting nuclear potentials is carried out perturbatively within the EFT expansion. Clearly, there is always certain ambiguity in the choice of the unitary operator. However, as was found in Refs. [45,46], most of the choices of the unitary operator lead to nuclear potentials which cannot be renormalized, i.e., the corresponding matrix elements involve ultraviolet-divergent integrals even after expressing all LECs in terms of their physical values. While this is, of course, not a fundamental problem since nuclear potentials do not correspond to observable quantities, it is desirable to have a well-defined and finite nuclear Hamiltonian. Enforcing renormalizability at the level of the Hamiltonian strongly restricts the unitary ambiguity mentioned above. In particular, the renormalizability requirement was found to lead to an unambiguous result for the static parts of the three- [40,41,50,51] and four-nucleon potentials [45,46], while the leading relativistic corrections still depend on two arbitrary constants, which parametrize the unitary ambiguity at this order in the chiral expansion [41]. Explicit expressions for the nuclear Hamiltonian in the operator form after fixing the unitary ambiguity up to N^{4}LO in the Δ-less approach can be found in Refs. [41,46,50].

To employ the method of unitary transformation within the small-scale expansion one can follow the lines of Ref. [46]. The

[2] Notice that the same power counting is employed to determine the LECs from pion-nucleon scattering in Ref. [50] and in this work.

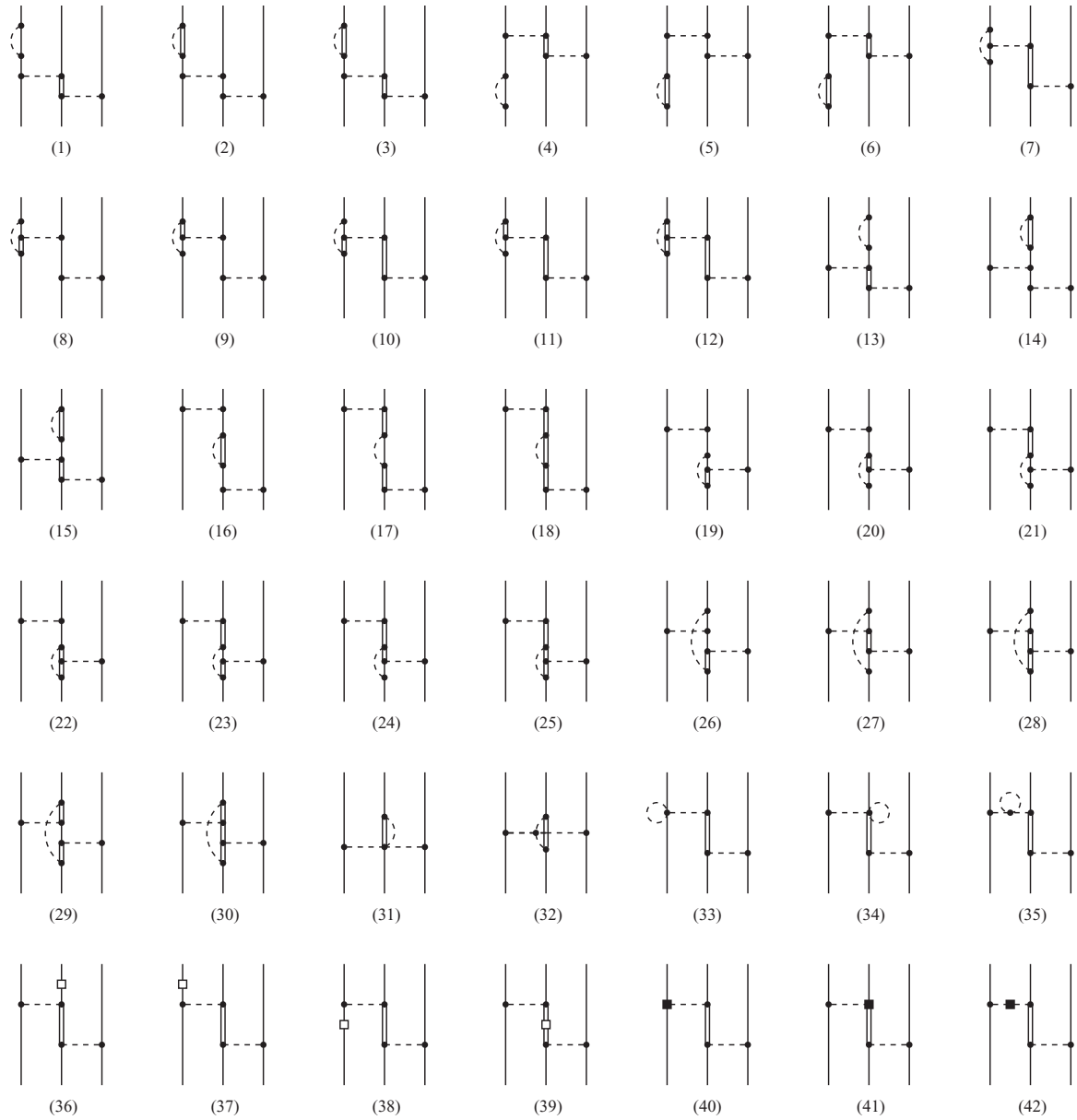

FIG. 8. Two-pion exchange $3N$ diagrams involving intermediate Δ excitations at N^{3}LO. Solid dots and filled rectangles denote vertices from $\mathcal{L}^{(1)}_{\pi N} + \mathcal{L}^{(1)}_{\pi N\Delta} + \mathcal{L}^{(1)}_{\pi\Delta\Delta}$ and $\mathcal{L}^{(3)}_{\pi N} + \mathcal{L}^{(3)}_{\pi N\Delta}$, respectively. Open rectangles refer to $1/m$ vertices from $\mathcal{L}^{(2)}_{\pi N} + \mathcal{L}^{(2)}_{\pi N\Delta}$. Diagrams which result from the interchange of the nucleon lines and/or application of the time-reversal operation are not shown. Also not shown are diagrams which lead to vanishing contributions to the $3N$F. For the remaining notation, see Fig. 2.

crucial difference is that one now needs to decouple not only pions but also the Δ degrees of freedom. As discussed in that work, it is convenient to start with the minimal parametrization of the unitary operator using the ansatz proposed by Okubo [98]; see Eq. (2.12) of Ref. [46]. Using this parametrization, the unitary operator can be calculated via a perturbative solution of the decoupling equation (2.13) of Ref. [46] within the small-scale expansion. The resulting rather lengthy expressions for the Δ contributions to the nuclear force in the operator form are not listed in this work but can be made available as a MATHEMATICA notebook upon request from the authors. Notice further that the resulting nuclear Hamiltonian is defined unambiguously within this ansatz but is not renormalizable as explained before. Following the lines of Ref. [46], we exploit the unitary ambiguity to ensure renormalizability of the nuclear potentials. This is achieved by applying all possible additional unitary transformations acting on the nucleonic subspace of the Fock space which can be constructed at a given order in the SSE; see Ref. [46] for more details. The corresponding transformation angles are to be chosen in such a way that the resulting Hamiltonian is finite. In the Δ-less approach, we had to introduce six such additional unitary transformations (plus two more transformations involving $1/m_N$ corrections) whose generators are given in Ref. [46] (Ref. [92]). The inclusion of the Δ excitations in the intermediate states allows for much more flexibility in the construction of the additional

unitary transformations. In particular, we were able to write 50 anti-Hermitian generators S_i^Δ, which are listed in Eq. (A4). The corresponding unitary transformations generate additional contributions to the nuclear Hamiltonian which depend on 50 real parameters α_i^Δ. In order to derive nuclear potentials, one has to evaluate the corresponding matrix elements of the nuclear Hamilton operator written in second-quantized form. Calculating the $3N$F contributions, expressing them in terms of physical parameter, and requiring that there are no ultraviolet divergencies lead to constraints on α_i^Δ, which are given in Eq. (A5). In particular, we find that 23 specific linear combinations of the α_i^Δ's have to vanish. While these constraints obviously do not allow for a unique determination of these parameters, we find that they lead to an unambiguous result for the $3N$F, which does not depend on any of the undetermined linear combinations of α_i^Δ's.

We now turn to the results for the $3N$F and consider first the static terms. We obtain the following contributions of the Δ isobar to the functions $\mathcal{A}_\Delta(q_2)$ and $\mathcal{B}_\Delta(q_2)$ at leading one-loop order:

$$
\begin{aligned}
\mathcal{A}_\Delta^{(4)}(q_2) = &-\frac{g_A^2 h_A^2}{139968\pi^2\Delta^3 F_\pi^6}\big(81 g_A^2\big(40\Delta^4+34M_\pi^4-\pi\Delta M_\pi^3-13\Delta^2 M_\pi^2\big)\big(2M_\pi^2+q_2^2\big)\\
&-450 g_A g_1\big(8\Delta^4+2M_\pi^4-\pi\Delta M_\pi^3-5\Delta^2 M_\pi^2\big)\big(2M_\pi^2+q_2^2\big)+36\Delta\big(20\pi h_A^2 M_\pi^3\big(2M_\pi^2+q_2^2\big)\\
&-27\big(2\Delta M_\pi^2-\Delta^3\big)\big(M_\pi^2+2q_2^2\big)\big)+25 g_1^2\big(40\Delta^4+34M_\pi^4-17\pi\Delta M_\pi^3-13\Delta^2 M_\pi^2\big)\big(2M_\pi^2+q_2^2\big)\big)\\
&+\frac{g_A^2 h_A^2}{144\pi^2 F_\pi^6}\Delta\, D(q_2)\big(M_\pi^2+2q_2^2\big)\big(-2\Delta^2+2M_\pi^2+q_2^2\big)-\frac{g_A^2 h_A^2}{144\pi^2 F_\pi^6}\Delta\, L(q_2)\big(M_\pi^2+2q_2^2\big)\\
&+\frac{g_A^2 h_A^2}{139968\pi^2\Delta^3 F_\pi^6}H(0)\big(81 g_A^2\big(40\Delta^4+34M_\pi^4-47\Delta^2 M_\pi^2\big)\big(2M_\pi^2+q_2^2\big)\\
&-450 g_A g_1\big(8\Delta^4+2M_\pi^4-7\Delta^2 M_\pi^2\big)\big(2M_\pi^2+q_2^2\big)+25 g_1^2\big(40\Delta^4+34M_\pi^4-47\Delta^2 M_\pi^2\big)\big(2M_\pi^2+q_2^2\big)\\
&-1944\Delta^2\,\big(M_\pi^2-\Delta^2\big)\big(M_\pi^2+2q_2^2\big)\big)+\frac{g_A^2 h_A^2}{34992\pi^2 F_\pi^6}\Delta\,\log\left(\frac{2\Delta}{M_\pi}\right)\big(M_\pi^2\big(1620 g_A^2-1800 g_A g_1+500 g_1^2+729\big)\\
&+2q_2^2\big(405 g_A^2-450 g_A g_1+125 g_1^2+729\big)\big),\\
\mathcal{B}_\Delta^{(4)}(q_2) = &\frac{g_A^2 h_A^2}{279936\pi^2\Delta^3 F_\pi^6}\big(81 g_A^2\big(58\Delta^4+34M_\pi^4-\pi\Delta M_\pi^3+50\Delta^2 M_\pi^2\big)\\
&-450 g_A g_1\big(10\Delta^4+10M_\pi^4-5\pi\Delta M_\pi^3+2\Delta^2 M_\pi^2\big)-144 h_A^2\big(-16\Delta^4+8M_\pi^4-9\pi\Delta M_\pi^3+16\Delta^2 M_\pi^2\big)\\
&+250\Delta^4 g_1^2+850 g_1^2 M_\pi^4-425\pi\Delta g_1^2 M_\pi^3+50\Delta^2 g_1^2 M_\pi^2-972\Delta^2 M_\pi^2\big)\\
&-\frac{g_A^2 h_A^2}{576\pi^2 F_\pi^6}\Delta\, D(q_2)\big(-4\Delta^2+4M_\pi^2+q_2^2\big)+\frac{g_A^2 h_A^2}{288\pi^2 F_\pi^6}\Delta\, L(q_2)\\
&-\frac{g_A^2 h_A^2}{139968\pi^2\Delta^3 F_\pi^6}H(0)\big(486\Delta^4+81 g_A^2\big(29\Delta^4+17M_\pi^4+8\Delta^2 M_\pi^2\big)-450 g_A g_1\big(5\Delta^4+5M_\pi^4-4\Delta^2 M_\pi^2\big)\\
&-576 h_A^2\big(-2\Delta^4+M_\pi^4+\Delta^2 M_\pi^2\big)+125\Delta^4 g_1^2+425 g_1^2 M_\pi^4-400\Delta^2 g_1^2 M_\pi^2-486\Delta^2 M_\pi^2\big)\\
&-\frac{g_A^2 h_A^2}{139968\pi^2 F_\pi^6}\Delta\,\log\left(\frac{2\Delta}{M_\pi}\right)\big(2349 g_A^2-2250 g_A g_1+1152 h_A^2+125 g_1^2+972\big),
\end{aligned}
\tag{5.4}
$$

where we use the notation for the various loop functions introduced in Ref. [57] which, in the case of dimensional regularization, reads

$$
\begin{aligned}
L(q) &= \frac{\sqrt{q^2+4M_\pi^2}}{q}\ln\frac{\sqrt{q^2+4M_\pi^2}+q}{2M_\pi},\\
D(q) &= \frac{1}{\Delta}\int_{2M_\pi}^\infty \frac{d\mu}{q^2+\mu^2}\arctan\frac{\sqrt{\mu^2-4M_\pi^2}}{2\Delta},\\
H(q) &= \frac{4M_\pi^2+2q^2-4\Delta^2}{4M_\pi^2+q^2-4\Delta^2}\big[L(q)-L\big(2\sqrt{\Delta^2-M_\pi^2}\big)\big].
\end{aligned}
\tag{5.5}
$$

The expressions for the loop functions resulting in the framework of spectral function regularization introduced in Ref. [99] can be found in Ref. [58]. $1/\Delta$ expansion of the loop functions is given by

$$D(q) = \frac{-L(q)+\log\left(\frac{2\Delta}{M_\pi}\right)+1}{2\Delta^2} + \frac{-3L(q)\left(4M_\pi^2+q^2\right)+3\left(6M_\pi^2+q^2\right)\log\left(\frac{2\Delta}{M_\pi}\right)+3M_\pi^2+q^2}{72\Delta^4}$$
$$+\frac{-10L(q)\left(4M_\pi^2+q^2\right)^2-15M_\pi^4+10M_\pi^2q^2+10\left(30M_\pi^4+10M_\pi^2q^2+q^4\right)\log\left(\frac{2\Delta}{M_\pi}\right)+2q^4}{1600\Delta^6}+\mathcal{O}(1/\Delta^8), \tag{5.6}$$
$$H(0) = 1-\log\left(\frac{2\Delta}{M_\pi}\right)+\frac{2M_\pi^2-4\,M_\pi^2\log\left(\frac{2\Delta}{M_\pi}\right)}{8\Delta^2}+\frac{7M_\pi^4-12M_\pi^4\log\left(\frac{2\Delta}{M_\pi}\right)}{32\Delta^4}+\frac{74M_\pi^6-120M_\pi^6\log\left(\frac{2\Delta}{M_\pi}\right)}{384\Delta^6}+\mathcal{O}(1/\Delta^8).$$

These expressions indicate that the $\log(\frac{2\Delta}{M_\pi})$ terms in $\mathcal{A}_\Delta^{(4)}(q_2)$ and $\mathcal{B}_\Delta^{(4)}(q_2)$ are essential for vanishing of $\mathcal{A}_\Delta^{(4)}(q_2)$ and $\mathcal{B}_\Delta^{(4)}(q_2)$ in the $\Delta\to\infty$ limit as required by the decoupling theorem. Notice further that the two-pion exchange diagrams shown in Fig. 8 also induce shorter-range contributions, which will be discussed in a separate publication.

The static contributions discussed above depend only on the momentum transfers $\vec{q}_i$ and are therefore local. It is thus natural to switch to the coordinate space representation of these $3N$F terms. The Fourier transform of a local potential is given by

$$\tilde{V}_{3N}(\vec{r}_{12},\vec{r}_{32}) = \int\frac{d^3q_1}{(2\pi)^3}\frac{d^3q_3}{(2\pi)^3}\,e^{i\vec{q}_1\cdot\vec{r}_{12}}\,e^{i\vec{q}_3\cdot\vec{r}_{32}}\,V_{3N}(\vec{q}_1,\vec{q}_3), \tag{5.7}$$

where $\vec{r}_{ij}\equiv\vec{r}_i-r_j$ is the distance between the nucleons i and j. For the two-pion-exchange contribution, we obtain from Eq. (5.1)

$$\tilde{V}_{2\pi}(\vec{r}_{12},\vec{r}_{32}) = -\vec{\sigma}_1\cdot\vec{\nabla}_{12}\,\vec{\sigma}_3\cdot\vec{\nabla}_{32}[\boldsymbol{\tau}_1\cdot\boldsymbol{\tau}_3\,\tilde{A}(\vec{r}_{12},\vec{r}_{32})-\boldsymbol{\tau}_1\times\boldsymbol{\tau}_3\cdot\boldsymbol{\tau}_2\,\vec{\nabla}_{12}\times\vec{\nabla}_{32}\cdot\vec{\sigma}_2\,\tilde{B}(\vec{r}_{12},\vec{r}_{32})]. \tag{5.8}$$

Here and in what follows, the differential operators $\vec{\nabla}_{ij}$ are defined in terms of dimensionless variables $\vec{x}_{ij}=\vec{r}_{ij}M_\pi$ while the functions $\tilde{A}$ and $\tilde{B}$ are defined via

$$\tilde{A}(\vec{r}_{12},\vec{r}_{32}) = \int\frac{d^3q_1}{(2\pi)^3}\frac{d^3q_3}{(2\pi)^3}\,e^{i\vec{q}_1\cdot\vec{r}_{12}}\,e^{i\vec{q}_3\cdot\vec{r}_{32}}\,\frac{1}{q_1^2+M_\pi^2}\frac{1}{q_3^2+M_\pi^2}\,\mathcal{A}(q_2),$$
$$\tilde{B}(\vec{r}_{12},\vec{r}_{32}) = \int\frac{d^3q_1}{(2\pi)^3}\frac{d^3q_3}{(2\pi)^3}\,e^{i\vec{q}_1\cdot\vec{r}_{12}}\,e^{i\vec{q}_3\cdot\vec{r}_{32}}\,\frac{1}{q_1^2+M_\pi^2}\frac{1}{q_3^2+M_\pi^2}\,\mathcal{B}(q_2). \tag{5.9}$$

To perform the integrations, we employ the spectral-function representation of the functions $\mathcal{A}$ and $\mathcal{B}$. The only nonpolynomial in q_2 terms in Eq. (5.4) emerge from the scalar loop functions $L(q_2)$ and $D(q_2)$. Their spectral-function representation is given by

$$L(q_2) = 1+q_2^2\int_{2\,M_\pi}^\infty d\mu\,\frac{\rho_L(\mu)}{q_2^2+\mu^2},\quad \rho_L(\mu)=\frac{\sqrt{\mu^2-4\,M_\pi^2}}{\mu^2},$$
$$D(q_2) = \int_{2\,M_\pi}^\infty d\mu\,\frac{\rho_D(\mu)}{q_2^2+\mu^2},\quad \rho_D(\mu)=\frac{1}{\Delta}\arctan\left(\frac{\sqrt{\mu^2-4\,M_\pi^2}}{2\,\Delta}\right). \tag{5.10}$$

Therefore, the Fourier transform of the $3N$F terms involving these functions can be written as

$$\int\frac{d^3q_1}{(2\pi)^3}\frac{d^3q_3}{(2\pi)^3}\,e^{i\vec{q}_1\cdot\vec{r}_{12}}\,e^{i\vec{q}_3\cdot\vec{r}_{32}}\,\frac{1}{q_1^2+M_\pi^2}\frac{1}{q_3^2+M_\pi^2}L(q_2) = \frac{M_\pi^2}{(4\pi)^2}U_1(x_{12})U_1(x_{32})$$
$$-\frac{M_\pi}{(4\pi)^3}(\vec{\nabla}_{12}+\vec{\nabla}_{32})^2\int d^3x\,U_1(|\vec{x}_{12}+\vec{x}|)U_1(|\vec{x}_{32}+\vec{x}|)V_1(x),$$
$$\int\frac{d^3q_1}{(2\pi)^3}\frac{d^3q_3}{(2\pi)^3}\,e^{i\vec{q}_1\cdot\vec{r}_{12}}\,e^{i\vec{q}_3\cdot\vec{r}_{32}}\,\frac{1}{q_1^2+M_\pi^2}\frac{1}{q_3^2+M_\pi^2}D(q_2) = \frac{1}{(4\pi)^3}\int d^3x\,U_1(|\vec{x}_{12}+\vec{x}|)U_1(|\vec{x}_{32}+\vec{x}|)Q_1(x), \tag{5.11}$$

where the profile functions are given by

$$U_1(x) = \frac{4\pi}{M_\pi}\int\frac{d^3q}{(2\pi)^3}\frac{e^{i\vec{q}\cdot\vec{x}/M_\pi}}{q^2+M_\pi^2} = \frac{e^{-x}}{x},$$
$$V_1(x) = \frac{4\pi}{M_\pi}\int\frac{d^3q}{(2\pi)^3}\,e^{i\vec{q}\cdot\vec{x}/M_\pi}\int_{2M_\pi}^\infty d\mu\,\frac{1}{\mu^2+q^2}\frac{1}{\mu^2}\sqrt{\mu^2-4M_\pi^2} = \frac{1}{x}\int_2^\infty d\mu\,\frac{e^{-x\,\mu}}{\mu^2}\sqrt{\mu^2-4}, \tag{5.12}$$
$$Q_1(x) = \int_2^\infty d\mu\,\frac{e^{-\mu x}}{x}\frac{M_\pi}{\Delta}\arctan\left(\frac{M_\pi}{\Delta}\frac{\sqrt{\mu^2-4}}{2}\right).$$

We are interested here only in the long-range terms and therefore restrict ourselves to the case $x_{ij} \neq 0$. All terms involving positive powers of momenta $\vec{q}_1$ and $\vec{q}_3$ can be expressed through gradients $-iM_\pi\vec{\nabla}_{12}$ and $-iM_\pi\vec{\nabla}_{32}$ which can be taken out of the integrals.

For the NLO delta contributions to $3N$F, we obtain the following coordinate-space expressions:

$$\tilde{\mathcal{A}}_\Delta^{(2)}(\vec{r}_{12},\vec{r}_{32}) = \frac{g_A^2h_A^2}{288\pi^2\Delta F_\pi^4}M_\pi^6[(\vec{\nabla}_{12}+\vec{\nabla}_{32})^2-2]U_1(x_{12})U_1(x_{32}),$$
$$\tilde{\mathcal{B}}_\Delta^{(2)}(\vec{r}_{12},\vec{r}_{32}) = \frac{g_A^2h_A^2}{576\pi^2\Delta F_\pi^4}M_\pi^6U_1(x_{12})U_1(x_{32}). \tag{5.13}$$

The N^{3}LO Δ contributions have the form

$$\begin{aligned}
\tilde{\mathcal{A}}_\Delta^{(4)}(\vec{r}_{12},\vec{r}_{32}) = {}& \frac{g_A^2h_A^2}{2239488\pi^5\Delta^3F_\pi^6}M_\pi^4\Big(243\Delta^4[2(\vec{\nabla}_{12}+\vec{\nabla}_{32})^2-1]\big\{2\Delta^2+M_\pi^2[(\vec{\nabla}_{12}+\vec{\nabla}_{32})^2-2]\big\}\mathcal{Q}_1(\vec{x}_{12},\vec{x}_{32})\\
&+\pi M_\pi^2\Big(-25g_1^2[(\vec{\nabla}_{12}+\vec{\nabla}_{32})^2-2]\big(40\Delta^4[H(0)-1]+34[H(0)-1]M_\pi^4\\
&+\Delta^2[13-47H(0)]M_\pi^2+17\pi\Delta M_\pi^3\big)+1944\Delta^2[H(0)-1][2(\vec{\nabla}_{12}+\vec{\nabla}_{32})^2-1]\big(M_\pi^2-\Delta^2\big)\\
&+4\Delta^4\big\{729[1-2(\vec{\nabla}_{12}+\vec{\nabla}_{32})^2]-250g_1^2[(\vec{\nabla}_{12}+\vec{\nabla}_{32})^2-2]\big\}\log\left(\frac{2\Delta}{M_\pi}\right)\Big)U_1(x_{12})U_1(x_{32})\Big)\\
&+\frac{g_A^2h_A^2}{9216\pi^5F_\pi^6}\Delta M_\pi^6(\vec{\nabla}_{12}+\vec{\nabla}_{32})^2[1-2(\vec{\nabla}_{12}+\vec{\nabla}_{32})^2]\mathcal{V}_1(\vec{x}_{12},\vec{x}_{32})\\
&-\frac{g_A^4h_A^2}{27648\pi^4\Delta^3F_\pi^6}M_\pi^6[(\vec{\nabla}_{12}+\vec{\nabla}_{32})^2-2]U_1(x_{12})U_1(x_{32})\Big(40\Delta^4[H(0)-1]+34[H(0)-1]M_\pi^4\\
&+\Delta^2[13-47H(0)]M_\pi^2+\pi\Delta M_\pi^3+40\Delta^4\log\left(\frac{2\Delta}{M_\pi}\right)\Big)\\
&+\frac{25g_A^3h_A^2g_1}{124416\pi^4\Delta^3F_\pi^6}M_\pi^6[(\vec{\nabla}_{12}+\vec{\nabla}_{32})^2-2]U_1(x_{12})U_1(x_{32})\Big(8\Delta^4[H(0)-1]+2[H(0)-1]M_\pi^4\\
&+\Delta^2[5-7H(0)]M_\pi^2+\pi\Delta M_\pi^3+8\Delta^4\log\left(\frac{2\Delta}{M_\pi}\right)\Big)\\
&+\frac{5g_A^2h_A^4}{15552\pi^3\Delta^2F_\pi^6}M_\pi^9[(\vec{\nabla}_{12}+\vec{\nabla}_{32})^2-2]U_1(x_{12})U_1(x_{32}),\\
\tilde{B}_\Delta^{(4)}(\vec{r}_{12},\vec{r}_{32}) = {}& -\frac{g_A^2h_A^2}{18432\pi^5F_\pi^6}\Delta M_\pi^6(\vec{\nabla}_{12}+\vec{\nabla}_{32})^2\mathcal{V}_1(x_{12},x_{32})+\frac{g_A^2h_A^2}{36864\pi^5F_\pi^6}\Delta M_\pi^4\big\{4\Delta^2+M_\pi^2[(\vec{\nabla}_{12}+\vec{\nabla}_{32})^2-4]\big\}\mathcal{Q}_1(x_{12},x_{32})\\
&-\frac{g_A^4h_A^2}{55296\pi^4\Delta^3F_\pi^6}M_\pi^6U_1(x_{12})U_1(x_{32})\big\{58\Delta^4[H(0)-1]+34[H(0)-1]M_\pi^4\\
&+2\Delta^2[8H(0)-25]M_\pi^2+\pi\Delta M_\pi^3\big\}-\frac{29g_A^4h_A^2}{27648\pi^4F_\pi^6}\Delta M_\pi^6U_1(x_{12})U_1(x_{32})\log\left(\frac{2\Delta}{M_\pi}\right)\\
&+\frac{25g_A^3h_A^2g_1}{248832\pi^4\Delta^3F_\pi^6}M_\pi^6U_1(x_{12})U_1(x_{32})\big\{10\Delta^4[H(0)-1]+10[H(0)-1]M_\pi^4\\
&-2\Delta^2[4H(0)+1]M_\pi^2+5\pi\Delta M_\pi^3\big\}+\frac{125g_A^3h_A^2g_1}{124416\pi^4F_\pi^6}\Delta M_\pi^6U_1(x_{12})U_1(x_{32})\log\left(\frac{2\Delta}{M_\pi}\right)\\
&+\frac{g_A^2h_A^4}{31104\pi^4\Delta^3F_\pi^6}M_\pi^6U_1(x_{12})U_1(x_{32})\big\{-16\Delta^4[H(0)-1]+8[H(0)-1]M_\pi^4\\
&+8\Delta^2[H(0)-2]M_\pi^2+9\pi\Delta M_\pi^3\big\}-\frac{25g_A^2h_A^2}{4478976\pi^4\Delta^3F_\pi^6}g_1^2M_\pi^6U_1(x_{12})U_1(x_{32})\big(10\Delta^4[H(0)-1]\\
&+34[H(0)-1]M_\pi^4-2\Delta^2[16H(0)+1]M_\pi^2+17\pi\Delta M_\pi^3\big)
\end{aligned}$$

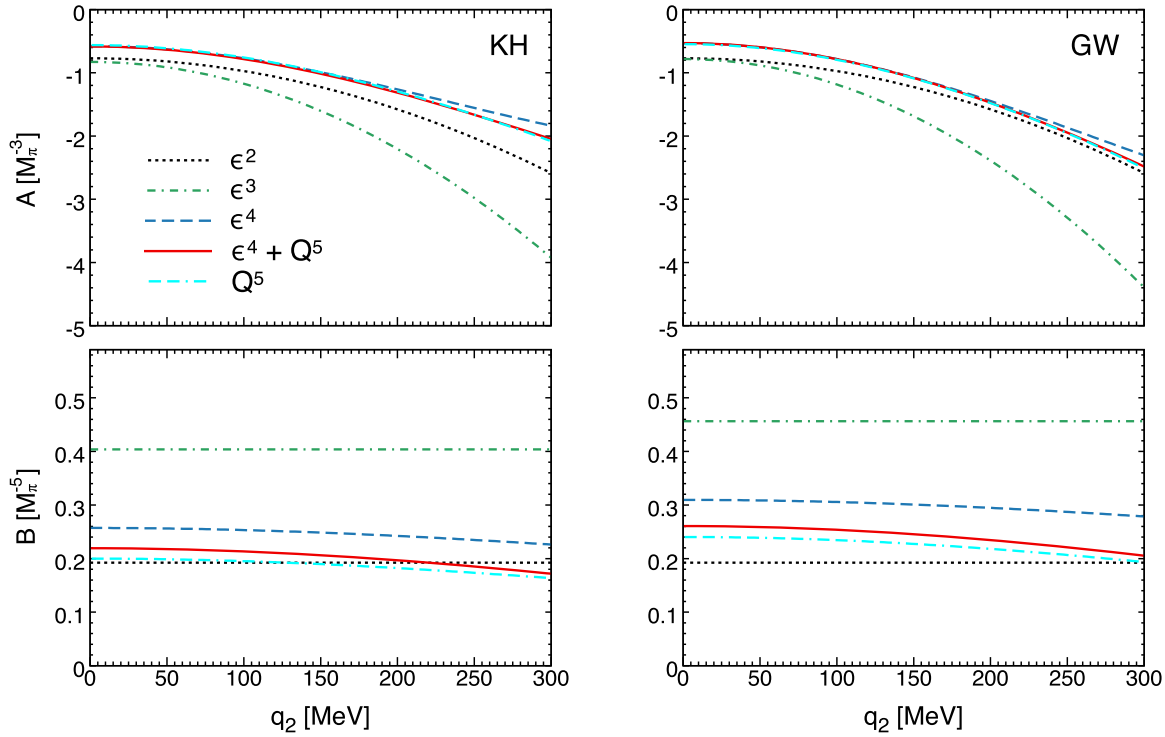

FIG. 9. Chiral expansion of the functions $\mathcal{A}(q_2)$ and $\mathcal{B}(q_2)$ entering the two-pion exchange $3N$F in Eq. (5.1) in the Δ-full and Δ-less theories. Left (right) panel shows the results obtained with the LECs determined from the fit to the KH [80] (GW [79]) partial-wave analysis of pion-nucleon scattering as explained in the text.

$$+\frac{g_A^2h_A^2}{4608\pi^4\Delta F_\pi^6}M_\pi^6\big(M_\pi^2-\Delta^2\big)[H(0)-1]U_1(x_{12})U_1(x_{32})-\frac{g_A^2h_A^4}{1944\pi^4F_\pi^6}\Delta M_\pi^6U_1(x_{12})U_1(x_{32})\log\left(\frac{2\Delta}{M_\pi}\right)$$
$$-\frac{125g_A^2h_A^2g_1^2}{2239488\pi^4F_\pi^6}\Delta M_\pi^6U_1(x_{12})U_1(x_{32})\log\left(\frac{2\Delta}{M_\pi}\right)-\frac{g_A^2h_A^2}{2304\pi^4F_\pi^6}\Delta M_\pi^6U_1(x_{12})U_1(x_{32})\log\left(\frac{2\Delta}{M_\pi}\right), \tag{5.14}$$

where the scalar integrals $\mathcal{Q}_1(\vec{x}_{12},\vec{x}_{32})$ and $\mathcal{V}_1(\vec{x}_{12},\vec{x}_{32})$ are defined as

$$\mathcal{Q}_1(\vec{x}_{12},\vec{x}_{32})=\int d^3x\,U_1(|\vec{x}_{12}+\vec{x}|)U_1(|\vec{x}_{32}+\vec{x}|)Q_1(x),$$
$$\mathcal{V}_1(\vec{x}_{12},\vec{x}_{32})=\int d^3x\,U_1(|\vec{x}_{12}+\vec{x}|)U_1(|\vec{x}_{32}+\vec{x}|)V_1(x). \tag{5.15}$$

At N^{3}LO one also has to take into account relativistic corrections. Nucleonic contributions are already discussed in Ref. [50]. Here we give only the corresponding Δ contributions from the diagrams (36)–(39) of Fig. 8 proportional to $1/m_N$:

$$V_{2\pi,1/m_N}=\frac{\vec{q}_1\cdot\vec{\sigma}_1\vec{q}_3\cdot\vec{\sigma}_3}{\big[q_1^2+M_\pi^2\big]\big[q_3^2+M_\pi^2\big]}\frac{{g_A}^2{h_A}^2}{72\Delta^2F_\pi^4m_N}\{\boldsymbol{\tau}_1\cdot\boldsymbol{\tau}_3[-4(\vec{q}_1\cdot\vec{q}_3)^2+i(2\vec{k}_1\cdot\vec{q}_1-\vec{k}_1\cdot\vec{q}_3+\vec{k}_3\cdot\vec{q}_1-2\vec{k}_3\cdot\vec{q}_3)\vec{q}_1\cdot\vec{q}_3\times\vec{\sigma}_2]$$
$$-i\vec{q}_1\cdot\vec{q}_3\boldsymbol{\tau}_1\cdot\boldsymbol{\tau}_2\times\boldsymbol{\tau}_3(2\vec{k}_1\cdot\vec{q}_1-\vec{k}_1\cdot\vec{q}_3+\vec{k}_3\cdot\vec{q}_1-2\vec{k}_3\cdot\vec{q}_3-i\vec{q}_1\cdot\vec{q}_3\times\vec{\sigma}_2)\}. \tag{5.16}$$

At this stage several comments are in order:

(1) There are no contributions from $1/m_N$ corrections to pion-nucleon and pion-nucleon-Δ vertices since both of them are proportional to zeroth components of momenta and for this reason vanish in the kinematics relevant for nuclear forces. This argument is, however, only applicable to irreducible topologies since the corresponding $3N$F contributions can be calculated using Feynman rules. All diagrams with intermediate Δ excitations involving $1/m_N$ corrections to pion-nucleon or pion-nucleon-Δ vertices are indeed irreducible. The situation is different in the case of nucleonic contributions, where we used the unitary transformation technique to extract the corresponding irreducible pieces; see Ref. [41] for more details.

(2) Since the Fujita-Miyazawa $3N$F corresponds to an irreducible diagram, we cannot construct additional unitary transformations which would affect relativistic corrections to it. For this reason, the expression in Eq. (5.16) is unambiguous.

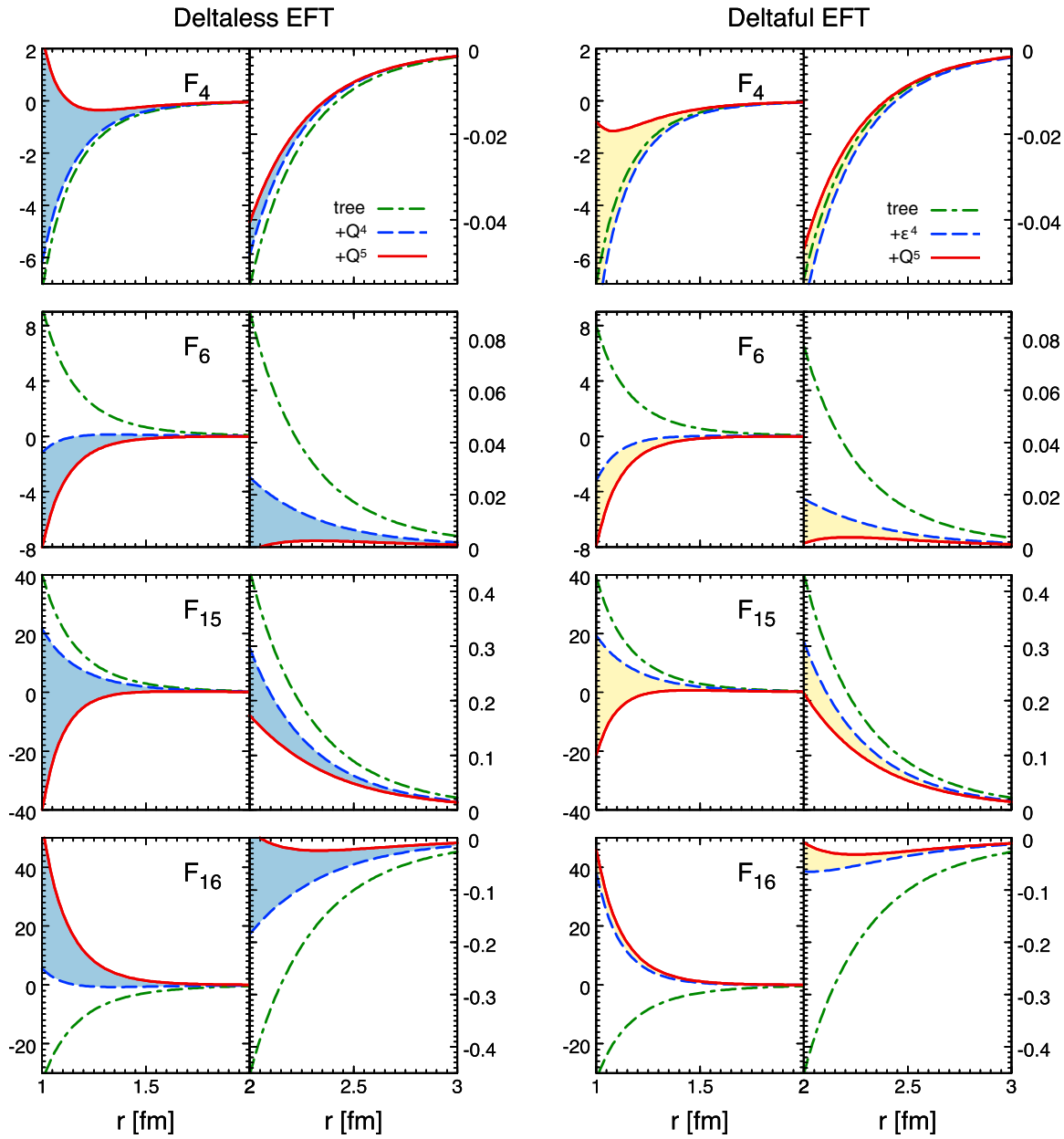

FIG. 10. Profile functions $\mathcal{F}_4(r)$, $\mathcal{F}_6(r)$, $\mathcal{F}_{15}(r)$, and $\mathcal{F}_{16}(r)$ in units of MeV generated by the two-pion exchange $3N$F topology in the Δ-less approach of Ref. [50] (left panel) and in the Δ-full approach of the current work (right panel). The dash-dotted, dashed, and solid lines are the results of the calculation at order $Q^3(\epsilon^3)$, $Q^4(\epsilon^4)$, and $Q^5(\epsilon^4+Q^5)$, respectively. The bands indicate the purely nucleonic contribution at order Q^5.

This is, again, different for nucleonic contributions, where additional unitary transformations can be employed and the corresponding relativistic corrections do depend on arbitrary parameters $\bar{\beta}_8$ and $\bar{\beta}_9$ [41].

(3) Finally, we emphasize that Eq. (5.16) is consistent with the resonance saturation of the nucleonic N^{5}LO two-pion-exchange tree-level diagram with one of the vertices taken from the order-Q^3 πN-Lagrangian proportional to d_i. Indeed, if we replace the d_i constants of this diagram with their resonance saturation values given in Eq. (4.14), we reproduce the result of Eq. (5.16).

In coordinate space, the corresponding relativistic corrections are given by

$$\begin{aligned}\tilde{V}_{2\pi,1/m_N} = {} & \frac{{g_A}^2 {h_A}^2 M_\pi^7}{1152\pi^2\Delta^2 F_\pi^4 m_N}\vec{\nabla}_{12}\cdot\vec{\sigma}_1\vec{\nabla}_{32}\cdot\vec{\sigma}_3(\vec{\nabla}_{12}\cdot\vec{\nabla}_{32}\boldsymbol{\tau}_1\cdot\boldsymbol{\tau}_2\times\boldsymbol{\tau}_3(-2\vec{k}_1\cdot\vec{\nabla}_{12}+\vec{k}_1\cdot\vec{\nabla}_{32}-\vec{k}_3\cdot\vec{\nabla}_{12}\\ & +2\vec{k}_3\cdot\vec{\nabla}_{32}+M_\pi\vec{\nabla}_{12}\cdot\vec{\nabla}_{32}\times\vec{\sigma}_2)+\boldsymbol{\tau}_1\cdot\boldsymbol{\tau}_3(2\vec{k}_1\cdot\vec{\nabla}_{12}-\vec{k}_1\cdot\vec{\nabla}_{32}+\vec{k}_3\cdot\vec{\nabla}_{12}-2\vec{k}_3\cdot\vec{\nabla}_{32})\vec{\nabla}_{12}\cdot\vec{\nabla}_{32}\times\vec{\sigma}_2\\ & +4M_\pi(\vec{\nabla}_{12}\cdot\vec{\nabla}_{32})^2\boldsymbol{\tau}_1\cdot\boldsymbol{\tau}_3)U_1(x_{12})U_1(x_{32}).\end{aligned} \tag{5.17}$$

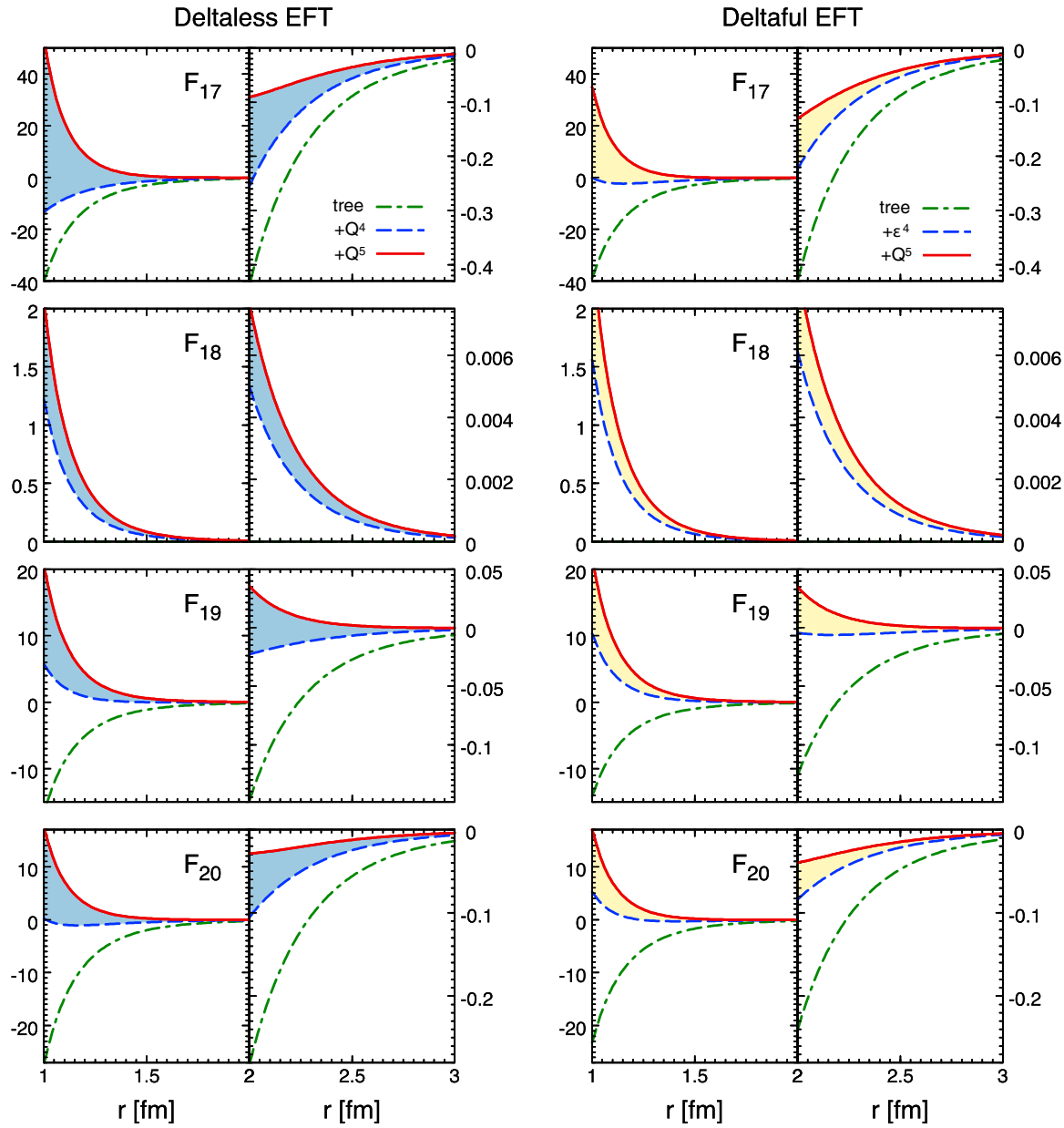

FIG. 11. Profile functions $\mathcal{F}_{17}(r)$, $\mathcal{F}_{18}(r)$, $\mathcal{F}_{19}(r)$, $\mathcal{F}_{20}(r)$ in units of MeV generated by the two-pion exchange $3N$F topology in the Δ-less approach of Ref. [50] (left panel) and in the Δ-full approach of the current work (right panel). The dash-dotted, dashed, and solid lines are the results of the calculation at order $Q^3(\epsilon^3)$, $Q^4(\epsilon^4)$, and $Q^5(\epsilon^4 + Q^5)$, respectively. The bands indicate the purely nucleonic contribution at order Q^5.

VI. DISCUSSION

Having constructed explicitly the two-pion-exchange Δ-full three-nucleon force and having determined all the relevant low-energy constants, we are now in the position to analyze the convergence of chiral expansion for the long-range part of the $3N$F. In Fig. 9, we show the results for the functions $\mathcal{A}(q_2)$ and $\mathcal{B}(q_2)$ for small values of the momentum transfer q_2, $q_2 < 300$ MeV at various orders in the small-scale expansion. In addition to the ϵ^2, ϵ^3, and ϵ^4 results, we show also the results, where the purely nucleonic contributions of order Q^5 are added to the ϵ^4 result in order to compare it with the Δ-less N^{4}LO calculation from Ref. [50] (double-dash-dotted lines in Fig. 9). One should, however, keep in mind that this is not a complete ϵ^5 result. We use here at all orders the low-energy constants c_i, $\bar{d}_i$, and $\bar{e}_i$ determined from the order-$\epsilon^3 + Q^4$ fit to the KH and GW partial wave analyses as described in Sec. IV and listed in Table I. We also adopt the same conventions regarding the LECs as in the case of pion-nucleon scattering; see Eqs. (4.9) and (4.11). Notice that although some of the $\bar{e}_i$ constants ($\bar{e}_{15,16,18}$) are rather sensitive to a particular choice of the partial wave analysis in pion-nucleon scattering (see Table I), the functions $\mathcal{A}$ and $\mathcal{B}$ depend only on the LECs $\bar{e}_{14,17}$, which are quite stable.

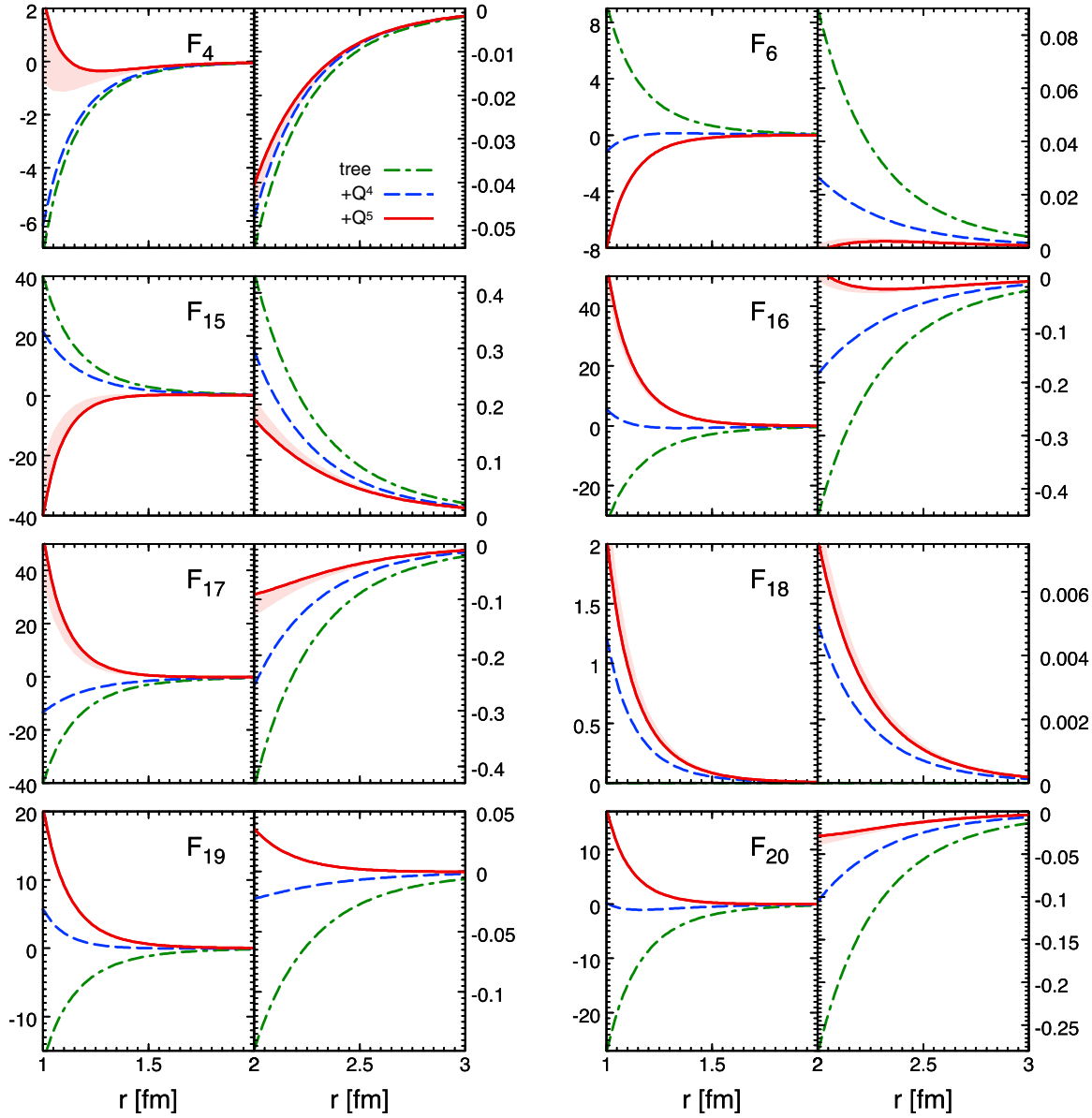

FIG. 12. Profile functions $\mathcal{F}_i(r)$ in units of MeV generated by the two-pion exchange $3N$F topology in the Δ-less approach of Ref. [50]. The dash-dotted, dashed, and solid lines are the results of the calculation at orders Q^3, Q^4, and Q^5, respectively. The bands indicate the difference between the Δ-less-Q^5 result and the Δ-full result at order $\epsilon^4 + Q^5$.

One observes a fairly slow convergence for the functions $\mathcal{A}(q_2)$ and $\mathcal{B}(q_2)$ when going from order ϵ^2 to ϵ^4. On the other hand, the difference between the results at orders ϵ^4 and $\epsilon^4 + Q^5$ is small for the function $\mathcal{B}(q_2)$ and almost negligible for the function $\mathcal{A}(q_2)$, which may indicate that convergence is reached at this order. Making a more definite statement about the convergence would, however, require performing a complete ϵ^5 derivation of the $3N$F.

It is also comforting to see that the results at order $\epsilon^4 + Q^5$ are very close to the Δ-less calculation at order Q^5. This indicates that the contributions of the Δ-isobar to the two-pion exchange $3N$F topology can be well represented in terms of resonance saturation of the LECs c_i, $\bar{d}_i$, and $\bar{e}_i$ at N^{4}LO in the Δ-less approach. This also indicates that nucleonic terms at order Q^6 and higher saturated by the double- and triple-Δ excitations are small.

Another instructive way to quantitatively analyze the obtained three-nucleon forces is to look at the structure functions $\mathcal{F}_i(r_{12},r_{23},r_{31})$ for the equilateral triangle configuration of the nucleons given by the condition $r_{12} = r_{23} = r_{31} = r$ [51]. Structure functions $\mathcal{F}_i(r_{12},r_{23},r_{31})$ are the coefficients in the expansion of a general local three-nucleon force in the basis of 20 operators $\tilde{\mathcal{G}}_i$ (for their explicit form, see Ref. [100]):

$$V_{3\mathrm{N}}^{\mathrm{full}} = \sum_{i=1}^{20} \tilde{\mathcal{G}}_i \mathcal{F}_i(r_{12},r_{23},r_{31}) + 5\,\text{permutations}. \qquad (6.1)$$

Only 8 out of 20 structure functions do not vanish for the two-pion-exchange topology, namely $\mathcal{F}_4$, $\mathcal{F}_6$, $\mathcal{F}_{15}$, $\mathcal{F}_{16}$, $\mathcal{F}_{17}$, $\mathcal{F}_{18}$, $\mathcal{F}_{19}$, and $\mathcal{F}_{20}$. Our results for these structure functions are visualized in Figs. 10–12.

We first comment on the convergence pattern of the chiral expansion for the Δ-less (Δ-full) scheme (see Figs. 10 and 11) by looking at the tree-level results and at the results at orders Q^4 (ϵ^4) and Q^5 ($\epsilon^4 + Q^5$). We observe a better convergence of the Δ-full approach, which is reflected in significantly smaller bands on the right panels of Figs. 10 and 11, which indicate the size of the purely nucleonic contributions at order Q^5. This means that the large loop contributions at order Q^5 in the Δ-less theory reported in Refs. [50,100] are, to a considerable extent, saturated by the lower order (ϵ^4) contributions in the Δ-full scheme. As the distance increases to $r \sim 2.5$–3.0 fm, the results at all orders get closer together for both the Δ-less and Δ-full approaches, fully in line with the general expectation that the chiral expansion converges most rapidly at large distances.

It is also instructive to compare with each other the results within the Δ-less and Δ-full approaches at the highest considered orders Q^5 and $\epsilon^4 + Q^5$, respectively. As shown in Fig. 12, the Δ-isobar contributions to the structure functions $\mathcal{F}_6$, $\mathcal{F}_{16}$, $\mathcal{F}_{18}$, $\mathcal{F}_{19}$, and $\mathcal{F}_{20}$ are almost completely given by the resonance saturation of the corresponding LECs. Indeed, the bands indicating the difference between the order-Q^5 Δ-less and order-$(\epsilon^4 + Q^5)$ Δ-full results are almost invisible in those cases even at relatively short distances of $r \sim 1.0$–1.5 fm. For the functions $\mathcal{F}_{15}$ and $\mathcal{F}_{17}$, the saturation at this chiral order explains only a part of the Δ contributions. For the $\mathcal{F}_4$ function, the Δ-less and Δ-full results turn out to be of a different sign at short distances. Notice, however, that the corresponding structure function is rather small in magnitude as compared to other ones. For larger distances of $r \sim 2.5$–3.0 fm, the saturation pattern improves and holds true for all structure functions. This means that Δ-resonance saturation of the Δ-less contributions at orders beyond Q^5, emerging from the considered diagrams at order $\epsilon^4 + Q^5$, leads to small effects for the two-pion exchange $3N$F topology. This may be considered as yet another indication of the convergence of the theory at orders Q^5 and $\epsilon^4 + Q^5$.

VII. SUMMARY AND CONCLUSIONS

In this paper, we have analyzed the longest-range contribution to the three-nucleon force at N^{3}LO utilizing the heavy-baryon formulation of chiral EFT with pions, nucleons, and Δs as the only explicit degrees of freedom. The pertinent results of our study can be summarized as follows:

(1) We worked out in detail renormalization of the lowest-order effective chiral Lagrangian at the one-loop level.
(2) Employing renormalization conditions which maintain the explicit decoupling of the Δ isobar, we derived the Δ contributions to those LECs c_i, $\bar{d}_i$, and $\bar{e}_i$ from the effective Lagrangians $\mathcal{L}^{(2)}_{\pi N}$, $\mathcal{L}^{(3)}_{\pi N}$, and $\mathcal{L}^{(4)}_{\pi N}$ which contribute to pion-nucleon scattering at the considered order.
(3) In order to determine the LECs c_i, $\bar{d}_i$ and $\bar{e}_i$ contributing to the 2π-exchange $3N$F, we reanalyzed pion-nucleon scattering at order $\epsilon^3 + Q^4$ employing the same power counting scheme as in the derivation of the nuclear forces and using the same fitting protocol as in the Δ-less analysis of Ref. [50]. We used the available partial-wave analyses of the pion-nucleon scattering data to determine all relevant LECs. The resulting values turn out to be rather stable and consistent with our Δ-less analysis reported in Ref. [50].
(4) We worked out the N^{3}LO Δ contributions to the 2π-exchange $3N$F. The unitary ambiguity of the Hamilton operator is parametrized by 50 additional unitary transformations. After imposing the renormalizability constraint, i.e., the requirement that the resulting $3N$F matrix elements are finite, the expressions for the $3N$F appear to be defined unambiguously. These findings pave the way for the derivation of the remaining $3N$F contributions at the same order, which are not considered in this paper.
(5) The obtained results for the 2π-exchange $3N$F at N^{3}LO of the SSE are in good agreement with the N^{4}LO calculations of Ref. [50] within the Δ-less approach. The agreement becomes even better when adding the nucleonic contributions at order N^{4}LO to the expressions at N^{3}LO of the SSE. This indicates that the effects of the Δ isobar for this particular topology are well represented by resonance saturation of the LECs c_i, $\bar{d}_i$, and $\bar{e}_i$ at N^{4}LO in the Δ-less approach.

The presented calculations should be extended to the intermediate-range topologies, where we do expect significant contributions of the Δ to be still missing in the N^{4}LO analysis of Ref. [51] within the Δ-less framework, as well as to short-range contributions. Work along these lines is in progress.

ACKNOWLEDGMENTS

We are grateful to Ulf-G. Meißner for sharing his insights into the considered topics and useful discussions. This work was supported by BMBF (Contract No. 05P2015, NUSTAR R&D) and by Deutsche Forschungsgemeinschaft through funds provided to the Sino-German CRC 110 "Symmetries and the Emergence of Structure in QCD" (Grant No. TRR110).

APPENDIX A: UNITARY AMBIGUITY OF THE $3N$F AND CONSTRAINTS IMPOSED BY THE RENORMALIZABILITY REQUIREMENT

To derive the effective potential, we use the method of unitary transformation. A detailed discussion of this approach including the explicit form of the unitary operator at low orders in the chiral expansion can be found in Ref. [46]. As explained in Sec. V, this method can be straightforwardly extended to carry out calculations within the Δ-full chiral EFT approach. In this appendix, we discuss the restrictions on the choice of the unitary transformation imposed by the condition that the resulting nuclear Hamiltonian is renormalizable.

We first specify our notation. The indices in the interaction vertices $H^{(\kappa)}_{a,b,c,d,e}$ have the following meaning:

$$\begin{aligned} a &= \text{Number of pion fields} \\ b &= \text{Number of outgoing nucleons} \\ c &= \text{Number of outgoing } \Delta\text{s} \\ d &= \text{Number of incoming nucleons} \\ e &= \text{Number of incoming } \Delta\text{s} \\ \kappa &= d + \tfrac{3}{2}(b+c+d+e) + a - 4, \end{aligned} \tag{A1}$$

where d is the number of derivatives at a given vertex. We also introduce the projection operators η and λ onto the purely nucleonic and the remaining parts of the Fock space, respectively. These operators satisfy the usual relations $\eta^2 = \eta$, $\lambda^2 = \lambda$, $\eta\lambda = \lambda\eta = 0$, and $\lambda + \eta = \mathbf{1}$. We also need to differentiate the states from the λ subspace by introducing the operators $\lambda^{a,b}$, where a and b refer to the number of pions and Δs in the corresponding intermediate state, respectively. The total energy of the pions and Δs in the corresponding state will be denoted by $E_{\pi\Delta} = \mathcal{O}(\epsilon)$.

As pointed out in Sec. V, renormalizability of the nuclear Hamiltonian is achieved by performing all possible η-space unitary transformations after decoupling of pions and deltas by means of the (minimal) Okubo-type unitary transformation. Such additional unitary operators have a general form

$$U = e^S, \tag{A2}$$

where S is an anti-Hermitian operator ($S^\dagger = -S$) acting on the η space. We parametrize the operator S as

$$S = \sum_i \alpha_i S_i + \sum_i \alpha_i^\Delta S_i^\Delta, \tag{A3}$$

where α_i and α_i^Δ are real numbers. The operators S_i include only nucleon degrees of freedom and have already been discussed earlier [46,50]. We now give 50 operators S_i^Δ which include Δ contribution:

$$S_1^\Delta = \eta H^{(1)}_{1,1,0,0,1} \frac{\lambda^{1,1}}{E^2_{\pi\Delta}} H^{(1)}_{1,1,0,1,0} \frac{\lambda^{0,1}}{E_{\pi\Delta}} H^{(1)}_{1,1,0,1,0} \frac{\lambda^{1,1}}{E_{\pi\Delta}} \times H^{(1)}_{1,0,1,1,0}\eta - hc,$$

$$S_2^\Delta = \eta H^{(1)}_{1,1,0,0,1} \frac{\lambda^{1,1}}{E^2_{\pi\Delta}} H^{(1)}_{1,1,0,1,0} \frac{\lambda^{2,1}}{E_{\pi\Delta}} H^{(1)}_{1,1,0,1,0} \frac{\lambda^{1,1}}{E_{\pi\Delta}} \times H^{(1)}_{1,0,1,1,0}\eta - hc,$$

$$S_3^\Delta = \eta H^{(1)}_{1,1,0,1,0} \frac{\lambda^{1,0}}{E^2_{\pi\Delta}} H^{(1)}_{1,1,0,0,1} \frac{\lambda^{0,1}}{E_{\pi\Delta}} H^{(1)}_{1,0,1,1,0} \frac{\lambda^{1,0}}{E_{\pi\Delta}} \times H^{(1)}_{1,1,0,1,0}\eta - hc,$$

$$S_4^\Delta = \eta H^{(1)}_{1,1,0,1,0} \frac{\lambda^{1,0}}{E^2_{\pi\Delta}} H^{(1)}_{1,1,0,0,1} \frac{\lambda^{2,1}}{E_{\pi\Delta}} H^{(1)}_{1,0,1,1,0} \frac{\lambda^{1,0}}{E_{\pi\Delta}} \times H^{(1)}_{1,1,0,1,0}\eta - hc,$$

$$S_5^\Delta = \eta H^{(1)}_{1,1,0,0,1} \frac{\lambda^{1,1}}{E^2_{\pi\Delta}} H^{(1)}_{1,1,0,1,0} \frac{\lambda^{0,1}}{E_{\pi\Delta}} H^{(1)}_{1,0,1,1,0} \frac{\lambda^{1,0}}{E_{\pi\Delta}} \times H^{(1)}_{1,1,0,1,0}\eta - hc,$$

$$S_6^\Delta = \eta H^{(1)}_{1,1,0,0,1} \frac{\lambda^{1,1}}{E_{\pi\Delta}} H^{(1)}_{1,1,0,1,0} \frac{\lambda^{0,1}}{E^2_{\pi\Delta}} H^{(1)}_{1,0,1,1,0} \frac{\lambda^{1,0}}{E_{\pi\Delta}} \times H^{(1)}_{1,1,0,1,0}\eta - hc,$$

$$S_7^\Delta = \eta H^{(1)}_{1,1,0,0,1} \frac{\lambda^{1,1}}{E_{\pi\Delta}} H^{(1)}_{1,1,0,1,0} \frac{\lambda^{0,1}}{E_{\pi\Delta}} H^{(1)}_{1,0,1,1,0} \frac{\lambda^{1,0}}{E^2_{\pi\Delta}} \times H^{(1)}_{1,1,0,1,0}\eta - hc,$$

$$S_8^\Delta = \eta H^{(1)}_{1,1,0,0,1} \frac{\lambda^{1,1}}{E^2_{\pi\Delta}} H^{(1)}_{1,1,0,1,0} \frac{\lambda^{2,1}}{E_{\pi\Delta}} H^{(1)}_{1,0,1,1,0} \frac{\lambda^{1,0}}{E_{\pi\Delta}} \times H^{(1)}_{1,1,0,1,0}\eta - hc,$$

$$S_9^\Delta = \eta H^{(1)}_{1,1,0,0,1} \frac{\lambda^{1,1}}{E_{\pi\Delta}} H^{(1)}_{1,1,0,1,0} \frac{\lambda^{2,1}}{E^2_{\pi\Delta}} H^{(1)}_{1,0,1,1,0} \frac{\lambda^{1,0}}{E_{\pi\Delta}} \times H^{(1)}_{1,1,0,1,0}\eta - hc,$$

$$S_{10}^\Delta = \eta H^{(1)}_{1,1,0,0,1} \frac{\lambda^{1,1}}{E_{\pi\Delta}} H^{(1)}_{1,1,0,1,0} \frac{\lambda^{2,1}}{E_{\pi\Delta}} H^{(1)}_{1,0,1,1,0} \frac{\lambda^{1,0}}{E^2_{\pi\Delta}} \times H^{(1)}_{1,1,0,1,0}\eta - hc,$$

$$S_{11}^\Delta = \eta H^{(1)}_{1,1,0,0,1} \frac{\lambda^{1,1}}{E^2_{\pi\Delta}} H^{(1)}_{1,0,1,1,0} \frac{\lambda^{2,0}}{E_{\pi\Delta}} H^{(1)}_{1,1,0,1,0} \frac{\lambda^{1,0}}{E_{\pi\Delta}} \times H^{(1)}_{1,1,0,1,0}\eta - hc,$$

$$S_{12}^\Delta = \eta H^{(1)}_{1,1,0,0,1} \frac{\lambda^{1,1}}{E_{\pi\Delta}} H^{(1)}_{1,0,1,1,0} \frac{\lambda^{2,0}}{E^2_{\pi\Delta}} H^{(1)}_{1,1,0,1,0} \frac{\lambda^{1,0}}{E_{\pi\Delta}} \times H^{(1)}_{1,1,0,1,0}\eta - hc,$$

$$S_{13}^\Delta = \eta H^{(1)}_{1,1,0,0,1} \frac{\lambda^{1,1}}{E_{\pi\Delta}} H^{(1)}_{1,0,1,1,0} \frac{\lambda^{2,0}}{E_{\pi\Delta}} H^{(1)}_{1,1,0,1,0} \frac{\lambda^{1,0}}{E^2_{\pi\Delta}} \times H^{(1)}_{1,1,0,1,0}\eta - hc,$$

$$S_{14}^\Delta = \eta H^{(1)}_{1,1,0,0,1} \frac{\lambda^{1,1}}{E^2_{\pi\Delta}} H^{(1)}_{1,0,1,0,1} \frac{\lambda^{0,1}}{E_{\pi\Delta}} H^{(1)}_{1,1,0,1,0} \frac{\lambda^{1,1}}{E_{\pi\Delta}} \times H^{(1)}_{1,0,1,1,0}\eta - hc,$$

$$S_{15}^\Delta = \eta H^{(1)}_{1,1,0,0,1} \frac{\lambda^{1,1}}{E^2_{\pi\Delta}} H^{(1)}_{1,1,0,1,0} \frac{\lambda^{0,1}}{E_{\pi\Delta}} H^{(1)}_{1,0,1,0,1} \frac{\lambda^{1,1}}{E_{\pi\Delta}} \times H^{(1)}_{1,0,1,1,0}\eta - hc,$$

$$S_{16}^\Delta = \eta H^{(1)}_{1,1,0,0,1} \frac{\lambda^{1,1}}{E^2_{\pi\Delta}} H^{(1)}_{1,0,1,0,1} \frac{\lambda^{0,1}}{E_{\pi\Delta}} H^{(1)}_{1,0,1,0,1} \frac{\lambda^{1,1}}{E_{\pi\Delta}} \times H^{(1)}_{1,0,1,1,0}\eta - hc,$$

$$S_{17}^\Delta = \eta H^{(1)}_{1,1,0,0,1} \frac{\lambda^{1,1}}{E^2_{\pi\Delta}} H^{(1)}_{1,0,1,0,1} \frac{\lambda^{0,1}}{E^2_{\pi\Delta}} H^{(1)}_{1,1,0,1,0} \frac{\lambda^{1,1}}{E_{\pi\Delta}} \times H^{(1)}_{1,0,1,1,0}\eta - hc,$$

$$S_{18}^\Delta = \eta H^{(1)}_{1,1,0,0,1} \frac{\lambda^{1,1}}{E^2_{\pi\Delta}} H^{(1)}_{1,0,1,0,1} \frac{\lambda^{2,1}}{E_{\pi\Delta}} H^{(1)}_{1,1,0,1,0} \frac{\lambda^{1,1}}{E_{\pi\Delta}} \times H^{(1)}_{1,0,1,1,0}\eta - hc,$$

$$S_{19}^{\Delta} = \eta H_{1,1,0,0,1}^{(1)} \frac{\lambda^{1,1}}{E_{\pi\Delta}^2} H_{1,1,0,1,0}^{(1)} \frac{\lambda^{2,1}}{E_{\pi\Delta}} H_{1,0,1,0,1}^{(1)} \frac{\lambda^{1,1}}{E_{\pi\Delta}} \times H_{1,0,1,1,0}^{(1)} \eta - hc,$$

$$S_{20}^{\Delta} = \eta H_{1,1,0,0,1}^{(1)} \frac{\lambda^{1,1}}{E_{\pi\Delta}^2} H_{1,0,1,0,1}^{(1)} \frac{\lambda^{2,1}}{E_{\pi\Delta}} H_{1,0,1,0,1}^{(1)} \frac{\lambda^{1,1}}{E_{\pi\Delta}} \times H_{1,0,1,1,0}^{(1)} \eta - hc,$$

$$S_{21}^{\Delta} = \eta H_{1,1,0,0,1}^{(1)} \frac{\lambda^{1,1}}{E_{\pi\Delta}} H_{1,0,1,0,1}^{(1)} \frac{\lambda^{2,1}}{E_{\pi\Delta}^2} H_{1,1,0,1,0}^{(1)} \frac{\lambda^{1,1}}{E_{\pi\Delta}} \times H_{1,0,1,1,0}^{(1)} \eta - hc,$$

$$S_{22}^{\Delta} = \eta H_{1,1,0,0,1}^{(1)} \frac{\lambda^{1,1}}{E_{\pi\Delta}^2} H_{1,0,1,0,1}^{(1)} \frac{\lambda^{0,1}}{E_{\pi\Delta}} H_{1,0,1,1,0}^{(1)} \frac{\lambda^{1,0}}{E_{\pi\Delta}} \times H_{1,1,0,1,0}^{(1)} \eta - hc,$$

$$S_{23}^{\Delta} = \eta H_{1,1,0,0,1}^{(1)} \frac{\lambda^{1,1}}{E_{\pi\Delta}} H_{1,0,1,0,1}^{(1)} \frac{\lambda^{0,1}}{E_{\pi\Delta}^2} H_{1,0,1,1,0}^{(1)} \frac{\lambda^{1,0}}{E_{\pi\Delta}} \times H_{1,1,0,1,0}^{(1)} \eta - hc,$$

$$S_{24}^{\Delta} = \eta H_{1,1,0,0,1}^{(1)} \frac{\lambda^{1,1}}{E_{\pi\Delta}} H_{1,0,1,0,1}^{(1)} \frac{\lambda^{0,1}}{E_{\pi\Delta}} H_{1,0,1,1,0}^{(1)} \frac{\lambda^{1,0}}{E_{\pi\Delta}^2} \times H_{1,1,0,1,0}^{(1)} \eta - hc,$$

$$S_{25}^{\Delta} = \eta H_{1,1,0,0,1}^{(1)} \frac{\lambda^{1,1}}{E_{\pi\Delta}^2} H_{1,0,1,0,1}^{(1)} \frac{\lambda^{2,1}}{E_{\pi\Delta}} H_{1,0,1,1,0}^{(1)} \frac{\lambda^{1,0}}{E_{\pi\Delta}} \times H_{1,1,0,1,0}^{(1)} \eta - hc,$$

$$S_{26}^{\Delta} = \eta H_{1,1,0,0,1}^{(1)} \frac{\lambda^{1,1}}{E_{\pi\Delta}} H_{1,0,1,0,1}^{(1)} \frac{\lambda^{2,1}}{E_{\pi\Delta}^2} H_{1,0,1,1,0}^{(1)} \frac{\lambda^{1,0}}{E_{\pi\Delta}} \times H_{1,1,0,1,0}^{(1)} \eta - hc,$$

$$S_{27}^{\Delta} = \eta H_{1,1,0,0,1}^{(1)} \frac{\lambda^{1,1}}{E_{\pi\Delta}} H_{1,0,1,0,1}^{(1)} \frac{\lambda^{2,1}}{E_{\pi\Delta}} H_{1,0,1,1,0}^{(1)} \frac{\lambda^{1,0}}{E_{\pi\Delta}^2} \times H_{1,1,0,1,0}^{(1)} \eta - hc,$$

$$S_{28}^{\Delta} = \eta H_{1,1,0,0,1}^{(1)} \frac{\lambda^{1,1}}{E_{\pi\Delta}^3} H_{1,0,1,1,0}^{(1)} \eta H_{1,1,0,1,0}^{(1)} \frac{\lambda^{1,0}}{E_{\pi\Delta}} \times H_{1,1,0,1,0}^{(1)} \eta - hc,$$

$$S_{29}^{\Delta} = \eta H_{1,1,0,0,1}^{(1)} \frac{\lambda^{1,1}}{E_{\pi\Delta}^2} H_{1,0,1,1,0}^{(1)} \eta H_{1,1,0,1,0}^{(1)} \frac{\lambda^{1,0}}{E_{\pi\Delta}^2} \times H_{1,1,0,1,0}^{(1)} \eta - hc,$$

$$S_{30}^{\Delta} = \eta H_{1,1,0,0,1}^{(1)} \frac{\lambda^{1,1}}{E_{\pi\Delta}} H_{1,0,1,1,0}^{(1)} \eta H_{1,1,0,1,0}^{(1)} \frac{\lambda^{1,0}}{E_{\pi\Delta}^3} \times H_{1,1,0,1,0}^{(1)} \eta - hc,$$

$$S_{31}^{\Delta} = \eta H_{1,1,0,0,1}^{(1)} \frac{\lambda^{1,1}}{E_{\pi\Delta}^3} H_{1,0,1,1,0}^{(1)} \eta H_{1,1,0,0,1}^{(1)} \frac{\lambda^{1,1}}{E_{\pi\Delta}} \times H_{1,0,1,1,0}^{(1)} \eta - hc,$$

$$S_{32}^{\Delta} = \eta H_{2,1,0,1,0}^{(2)} \frac{\lambda^{2,0}}{E_{\pi\Delta}^2} H_{1,1,0,0,1}^{(1)} \frac{\lambda^{1,1}}{E_{\pi\Delta}} H_{1,0,1,1,0}^{(1)} \eta - hc,$$

$$S_{33}^{\Delta} = \eta H_{2,1,0,1,0}^{(2)} \frac{\lambda^{2,0}}{E_{\pi\Delta}} H_{1,1,0,0,1}^{(1)} \frac{\lambda^{1,1}}{E_{\pi\Delta}^2} H_{1,0,1,1,0}^{(1)} \eta - hc,$$

$$S_{34}^{\Delta} = \eta H_{1,1,0,0,1}^{(1)} \frac{\lambda^{1,1}}{E_{\pi\Delta}^2} H_{2,1,0,1,0}^{(2)} \frac{\lambda^{1,1}}{E_{\pi\Delta}} H_{1,0,1,1,0}^{(1)} \eta - hc,$$

$$S_{35}^{\Delta} = \eta H_{2,1,0,0,1}^{(2)} \frac{\lambda^{2,1}}{E_{\pi\Delta}^2} H_{1,0,1,1,0}^{(1)} \frac{\lambda^{1,0}}{E_{\pi\Delta}} H_{1,1,0,1,0}^{(1)} \eta - hc,$$

$$S_{36}^{\Delta} = \eta H_{2,1,0,0,1}^{(2)} \frac{\lambda^{2,1}}{E_{\pi\Delta}} H_{1,0,1,1,0}^{(1)} \frac{\lambda^{1,0}}{E_{\pi\Delta}^2} H_{1,1,0,1,0}^{(1)} \eta - hc,$$

$$S_{37}^{\Delta} = \eta H_{2,1,0,0,1}^{(2)} \frac{\lambda^{2,1}}{E_{\pi\Delta}^2} H_{1,1,0,1,0}^{(1)} \frac{\lambda^{1,1}}{E_{\pi\Delta}} H_{1,0,1,1,0}^{(1)} \eta - hc,$$

$$S_{38}^{\Delta} = \eta H_{2,1,0,0,1}^{(2)} \frac{\lambda^{2,1}}{E_{\pi\Delta}} H_{1,1,0,1,0}^{(1)} \frac{\lambda^{1,1}}{E_{\pi\Delta}^2} H_{1,0,1,1,0}^{(1)} \eta - hc,$$

$$S_{39}^{\Delta} = \eta H_{2,1,0,0,1}^{(2)} \frac{\lambda^{2,1}}{E_{\pi\Delta}^2} H_{1,0,1,0,1}^{(1)} \frac{\lambda^{1,1}}{E_{\pi\Delta}} H_{1,0,1,1,0}^{(1)} \eta - hc,$$

$$S_{40}^{\Delta} = \eta H_{2,1,0,0,1}^{(2)} \frac{\lambda^{2,1}}{E_{\pi\Delta}} H_{1,0,1,0,1}^{(1)} \frac{\lambda^{1,1}}{E_{\pi\Delta}^2} H_{1,0,1,1,0}^{(1)} \eta - hc,$$

$$S_{41}^{\Delta} = \eta H_{1,1,0,1,0}^{(1)} \frac{\lambda^{1,0}}{E_{\pi\Delta}^2} H_{2,1,0,0,1}^{(2)} \frac{\lambda^{1,1}}{E_{\pi\Delta}} H_{1,0,1,1,0}^{(1)} \eta - hc,$$

$$S_{42}^{\Delta} = \eta H_{1,1,0,1,0}^{(1)} \frac{\lambda^{1,0}}{E_{\pi\Delta}} H_{2,1,0,0,1}^{(2)} \frac{\lambda^{1,1}}{E_{\pi\Delta}^2} H_{1,0,1,1,0}^{(1)} \eta - hc,$$

$$S_{43}^{\Delta} = \eta H_{1,1,0,0,1}^{(1)} \frac{\lambda^{1,1}}{E_{\pi\Delta}^2} H_{2,0,1,0,1}^{(2)} \frac{\lambda^{1,1}}{E_{\pi\Delta}} H_{1,0,1,1,0}^{(1)} \eta - hc,$$

$$S_{44}^{\Delta} = \eta H_{1,1,0,0,1}^{(1)} \frac{\lambda^{1,1}}{E_{\pi\Delta}^2} H_{1,1,0,0,1}^{(1)} \frac{\lambda^{2,2}}{E_{\pi\Delta}} H_{1,0,1,1,0}^{(1)} \frac{\lambda^{1,1}}{E_{\pi\Delta}} \times H_{1,0,1,1,0}^{(1)} \eta - hc,$$

$$S_{45}^{\Delta} = \eta H_{1,1,0,0,1}^{(1)} \frac{\lambda^{1,1}}{E_{\pi\Delta}^2} H_{1,1,0,0,1}^{(1)} \frac{\lambda^{0,2}}{E_{\pi\Delta}} H_{1,0,1,1,0}^{(1)} \frac{\lambda^{1,1}}{E_{\pi\Delta}} \times H_{1,0,1,1,0}^{(1)} \eta - hc,$$

$$S_{46}^{\Delta} = \eta H_{1,1,0,0,1}^{(1)} \frac{\lambda^{1,1}}{E_{\pi\Delta}^2} H_{1,0,1,1,0}^{(1)} \frac{\lambda^{2,0}}{E_{\pi\Delta}} H_{1,1,0,0,1}^{(1)} \frac{\lambda^{1,1}}{E_{\pi\Delta}} \times H_{1,0,1,1,0}^{(1)} \eta - hc,$$

$$S_{47}^{\Delta} = \eta H_{0,2,0,0,2}^{(2)} \frac{\lambda^{0,2}}{E_{\pi\Delta}^2} H_{1,0,1,1,0}^{(1)} \frac{\lambda^{1,1}}{E_{\pi\Delta}} H_{1,0,1,1,0}^{(1)} \eta - hc,$$

$$S_{48}^{\Delta} = \eta H_{0,2,0,0,2}^{(2)} \frac{\lambda^{0,2}}{E_{\pi\Delta}} H_{1,0,1,1,0}^{(1)} \frac{\lambda^{1,1}}{E_{\pi\Delta}^2} H_{1,0,1,1,0}^{(1)} \eta - hc,$$

$$S_{49}^{\Delta} = \eta H_{0,2,0,2,0}^{(2)} \eta H_{1,1,0,0,1}^{(1)} \lambda^{1,1} \frac{1}{E_{\pi\Delta}^3} H_{1,0,1,1,0}^{(1)} \eta - hc,$$

$$S_{50}^{\Delta} = \eta H_{1,1,0,0,1}^{(1)} \frac{\lambda^{1,1}}{E_{\pi\Delta}^2} H_{0,1,1,1,1}^{(2)} \frac{\lambda^{1,1}}{E_{\pi\Delta}} H_{1,0,1,1,0}^{(1)} \eta - hc. \tag{A4}$$

The requirement that the Δ contributions to the $3N$F are renormalizable leads to the following constraints on the coefficients α_i^Δ:

$$\begin{aligned}
\alpha_7^\Delta - \alpha_{13}^\Delta &= 0,\\
-\alpha_{13}^\Delta + \alpha_8^\Delta + \tfrac{1}{2} &= 0,\\
\alpha_9^\Delta &= 0,\\
\alpha_{10}^\Delta - \alpha_{13}^\Delta &= 0,\\
\alpha_{13}^\Delta + 2\alpha_{29}^\Delta - \tfrac{1}{4} &= 0,\\
\alpha_{18}^\Delta - \alpha_{25}^\Delta &= 0,\\
\alpha_{21}^\Delta - \alpha_{26}^\Delta &= 0,\\
\alpha_{19}^\Delta + \alpha_{26}^\Delta - \alpha_{27}^\Delta + \tfrac{1}{2} &= 0,\\
\alpha_{15}^\Delta - \alpha_{25}^\Delta &= 0,\\
\alpha_{17}^\Delta + \alpha_{25}^\Delta - \alpha_{27}^\Delta + \tfrac{1}{2} &= 0,\\
\alpha_{14}^\Delta + \alpha_{26}^\Delta - \alpha_{27}^\Delta + \tfrac{1}{2} &= 0,\\
\alpha_{24}^\Delta - \alpha_{27}^\Delta &= 0,\\
\alpha_1^\Delta - \alpha_2^\Delta &= 0,\\
-\alpha_{11}^\Delta + \alpha_2^\Delta + 2\alpha_{29}^\Delta + \alpha_5^\Delta + \tfrac{1}{4} &= 0,\\
-2\alpha_{29}^\Delta + \alpha_3^\Delta + \tfrac{1}{4} &= 0,\\
-2\alpha_{29}^\Delta + \alpha_4^\Delta + \tfrac{1}{4} &= 0,\\
\alpha_5^\Delta - \alpha_{11}^\Delta &= 0,\\
-\alpha_{11}^\Delta - 2\alpha_{29}^\Delta + \alpha_6^\Delta - \tfrac{1}{4} &= 0,\\
\alpha_{12}^\Delta + 4\alpha_{29}^\Delta &= 0,\\
\alpha_{35}^\Delta - \alpha_{37}^\Delta &= 0,\\
\alpha_{36}^\Delta - \alpha_{37}^\Delta + \alpha_{38}^\Delta + \tfrac{1}{2} &= 0,\\
\alpha_{37}^\Delta - \alpha_{38}^\Delta + \alpha_{41}^\Delta - \tfrac{1}{2} &= 0,\\
\alpha_{30}^\Delta - \tfrac{1}{2} &= 0.
\end{aligned} \tag{A5}$$

APPENDIX B: Δ-ISOBAR CONTRIBUTIONS TO THE INVARIANT πN AMPLITUDES $g^\pm(\omega,t)$ AND $h^\pm(\omega,t)$

In this Appendix, we present the explicit expressions for the invariant amplitudes $g^\pm(\omega,t)$ and $h^\pm(\omega,t)$ which parametrize the pion-nucleon scattering matrix at first three orders in ϵ expansion (for an earlier calculation, see Ref. [101]). We give only contributions due to intermediate Δ excitations, which have to be added to the nucleonic terms calculated within the Δ-less theory and listed in Ref. [50].

Contributions at order ϵ^1:

$$\begin{aligned}
g^+ &= \frac{4\Delta h_A^2\left(-2M_\pi^2 + t + 2\omega^2\right)}{9F_\pi^2(\Delta-\omega)(\Delta+\omega)},\\
g^- &= -\frac{2h_A^2\omega\left(-2M_\pi^2 + t + 2\omega^2\right)}{9F_\pi^2(\Delta-\omega)(\Delta+\omega)},\\
h^+ &= \frac{4h_A^2\omega}{9F_\pi^2(\omega^2-\Delta^2)},\\
h^- &= \frac{2\Delta h_A^2}{9F_\pi^2(\Delta^2-\omega^2)}.
\end{aligned} \tag{B1}$$

Contributions at order ϵ^2:

$$g^+ = 0, \quad g^- = 0, \quad h^+ = 0, \quad h^- = 0. \tag{B2}$$

Contributions at order ϵ^3:

$$g^\pm = g^\pm_{\rm SL} + g^\pm_{1/m_N}, \quad h^\pm = h^\pm_{\rm SL} + h^+_{1/m_N}, \tag{B3}$$

with static limit contributions given by

$$\begin{aligned}
g^+_{\rm SL} = {}& \frac{h_A^2}{486F_\pi^4\omega^2}\bar{J}_0(-\Delta)\left(\left(81g_A^2 - 50g_Ag_1 + 25g_1^2\right)\left(M_\pi^2-\Delta^2\right)\left(-2M_\pi^2 + t + 2\omega^2\right) - 108\omega^2\left(M_\pi^2 - 2t\right)\right)\\
&+ \frac{h_A^2}{4374F_\pi^4\omega^2(\Delta-\omega)^2}\bar{J}_0(\omega-\Delta)\left(M_\pi^2 - (\Delta-\omega)^2\right)\left(2M_\pi^2 - t - 2\omega^2\right)\left(9\Delta^2\left(81g_A^2 - 50g_Ag_1 + 25g_1^2\right)\right.\\
&\left. - 10\omega(\Delta-\omega)(9g_A - 5g_1)^2\right) + \frac{h_A^2}{36\pi^2F_\pi^4}D(\sqrt{-t})\Delta\left(M_\pi^2 - 2t\right)\left(-2\Delta^2 + 2M_\pi^2 - t\right)\\
&+ \frac{8h_A^2}{243F_\pi^4(\Delta^2-\omega^2)^2}\bar{J}_0(\omega)\left(\omega^2 - M_\pi^2\right)\left(-2M_\pi^2 + t + 2\omega^2\right)\left(9g_A^2(\Delta^2-\omega^2) + h_A^2(5\Delta^2 + 4\omega^2)\right)\\
&+ \frac{h_A^2}{34992\pi^2F_\pi^4(\Delta^2-\omega^2)^2}\left(\left(2M_\pi^2 - t - 2\omega^2\right)\left(\left(81g_A^2 - 50g_Ag_1 + 25g_1^2\right)\left(9\Delta(\Delta^2-\omega^2)^2\right.\right.\right.\\
&+ \left.\left.\left.\pi M_\pi^3\left(17\Delta^2 + \omega^2\right) + 9\Delta M_\pi^2(\omega^2-\Delta^2)\right) + 400\pi g_Ag_1M_\pi^3(\Delta^2-\omega^2)\right) - 486\Delta(\Delta^2-\omega^2)^2\left(M_\pi^2 - 2t\right)\right)\\
&+ \frac{\Delta h_A^2\log\left(\frac{2\Delta}{M_\pi}\right)\left(10(9g_A - 5g_1)^2\left(2M_\pi^2 - t - 2\omega^2\right) + 729\left(M_\pi^2 - 2t\right)\right)}{8748\pi^2F_\pi^4} + \frac{2\Delta h_A^2\bar{I}_{20}(t)\left(M_\pi^2 - 2t\right)}{9F_\pi^4} + (\omega \to -\omega),
\end{aligned} \tag{B4}$$

$$\begin{aligned}
g^-_{\rm SL} = {}& \frac{h_A^2}{69984F_\pi^4\pi^2\Delta\omega(\Delta^2-\omega^2)^2}\left(\left(2M_\pi^2 - 2\omega^2 - t\right)\left(-81\left(2\pi(12\Delta^4 - 35\omega^2\Delta^2 + 20\omega^4)M_\pi^3\right.\right.\right.\\
&\left.\left.\left. - 3(6\Delta^5 - 13\omega^2\Delta^3 + 7\omega^4\Delta)M_\pi^2 + 9\Delta(\Delta^2-\omega^2)^2(4\Delta^2 + 3\omega^2)\right)g_A^2\right.\right.
\end{aligned}$$

$$
\begin{aligned}
&+\ 150g_1\Delta\big(6\pi\Delta\omega^2M_\pi^3-3(2\Delta^4-3\omega^2\Delta^2+\omega^4)M_\pi^2+(\Delta^2-\omega^2)^2(12\Delta^2+13\omega^2)\big)g_A\\
&+\ 25g_1^2\big(-23\Delta\omega^6+\big(8\pi M_\pi^3-3\Delta M_\pi^2+34\Delta^3\big)\omega^4+\Delta^2\big(-26\pi M_\pi^3-3\Delta M_\pi^2+\Delta^3\big)\omega^2+6\Delta^5\big(M_\pi^2-2\Delta^2\big)\big)\big)\\
&-18\Delta\omega^2(\Delta^2-\omega^2)\big(4h_A^2\big(2M_\pi^2-2\omega^2-t\big)\big(3M_\pi^2-4\Delta^2-2\omega^2\big)-3\big(24M_\pi^2-72\Delta^2-19t\big)(\Delta^2-\omega^2)\big)\big)\\
&+\frac{\Delta^2\big(-2M_\pi^2+2\Delta^2+t\big)\omega D(\sqrt{-t})h_A^2}{18F_\pi^4\pi^2}+\frac{\big(8M_\pi^2-12\Delta^2-5t\big)\omega\bar{I}_{20}(t)h_A^2}{27F_\pi^4}\\
&+\frac{h_A^2}{4374F_\pi^4\Delta\omega(\Delta^2-\omega^2)^2}\big(\big(2M_\pi^2-2\omega^2-t\big)\big(36h_A^2\big(4\Delta^4-10\omega^2\Delta^2+M_\pi^2(5\Delta^2+\omega^2)\big)\omega^2\\
&+\ (\Delta^2-\omega^2)\big(81\big(-19\Delta^4+15\omega^2\Delta^2+M_\pi^2(12\omega^2-8\Delta^2)\big)g_A^2+1350g_1\Delta^2(\Delta^2-\omega^2)g_A\\
&+\ 25g_1^2\big(4M_\pi^2-13\Delta^2\big)(\Delta^2-\omega^2)\big)\big)-972\Delta^2\omega^2(\Delta^2-\omega^2)^2\big)\bar{J}_0(-\Delta)\\
&-\frac{2\big(2M_\pi^2-2\omega^2-t\big)\big(\omega^2-M_\pi^2\big)(2h_A^2\omega(\Delta^2-12\omega\Delta+2\omega^2)-9g_A^2(3\Delta-\omega)(\Delta^2-\omega^2))\bar{J}_0(\omega)h_A^2}{243F_\pi^4\omega(\Delta^2-\omega^2)^2}\\
&+\frac{h_A^2}{8748F_\pi^4(\Delta-\omega)^2\omega^2}\big(M_\pi^2-(\Delta-\omega)^2\big)\big(6\big(243g_A^2-150g_1g_A+25g_1^2\big)\Delta^2\\
&-5(9g_A-5g_1)^2(4\Delta-\omega)\omega\big)\big(2M_\pi^2-2\omega^2-t\big)\bar{J}_0(\omega-\Delta)\\
&+\frac{\omega\big(\big(243g_A^2+450g_1g_A-288h_A^2-125g_1^2\big)\big(2M_\pi^2-2\omega^2-t\big)-810t\big)\log\big(\frac{2\Delta}{M_\pi}\big)h_A^2}{34992F_\pi^4\pi^2}-(\omega\to-\omega),
\end{aligned}
\tag{B5}
$$

$$
\begin{aligned}
h_{\rm SL}^+=&-\frac{h_A^2}{4374F_\pi^4\omega^2(\Delta-\omega)^2}\bar{J}_0(\omega-\Delta)\big(M_\pi^2-(\Delta-\omega)^2\big)\big(6\Delta^2\big(243g_A^2-150g_Ag_1+25g_1^2\big)+(5\omega^2-20\Delta\omega)(9g_A-5g_1)^2\big)\\
&+\frac{h_A^2}{2187\Delta F_\pi^4\omega(\Delta^2-\omega^2)^2}\bar{J}_0(-\Delta)\big((\Delta^2-\omega^2)\big(81g_A^2\big(19\Delta^4-3\omega^2\big(5\Delta^2+4M_\pi^2\big)+8\Delta^2M_\pi^2\big)\\
&-\ 1350\Delta^2g_Ag_1(\Delta^2-\omega^2)-25g_1^2(\Delta^2-\omega^2)\big(4M_\pi^2-13\Delta^2\big)\big)-36h_A^2\omega^2\big(4\Delta^4-10\Delta^2\omega^2+M_\pi^2(5\Delta^2+\omega^2)\big)\big)\\
&-\frac{4h_A^2\bar{J}_0(\omega)\big(M_\pi^2-\omega^2\big)\big(2h_A^2\omega(\Delta^2-12\Delta\omega+2\omega^2)-9g_A^2(\Delta-\omega)(3\Delta-\omega)(\Delta+\omega)\big)}{243F_\pi^4\omega(\Delta^2-\omega^2)^2}\\
&+\frac{h_A^2}{34992\pi^2\Delta F_\pi^4\omega(\Delta^2-\omega^2)^2}\big((\Delta^2-\omega^2)\big(\Delta(\Delta^2-\omega^2)\big(729g_A^2(4\Delta^2+3\omega^2)-150g_Ag_1(12\Delta^2+13\omega^2)\\
&+\ 25g_1^2(12\Delta^2+23\omega^2)\big)-72\Delta h_A^2\omega^2\big(4\Delta^2-3M_\pi^2+2\omega^2\big)\big)+81g_A^2\big(2\pi M_\pi^3(12\Delta^4-35\Delta^2\omega^2+20\omega^4)\\
&-\ 3M_\pi^2(6\Delta^5-13\Delta^3\omega^2+7\Delta\omega^4)\big)-150\Delta g_Ag_1\big(6\pi\Delta M_\pi^3\omega^2-3M_\pi^2(2\Delta^4-3\Delta^2\omega^2+\omega^4)\big)\\
&+\ 25g_1^2\big(\pi M_\pi^3(26\Delta^2\omega^2-8\omega^4)+3\Delta M_\pi^2(-2\Delta^4+\Delta^2\omega^2+\omega^4)\big)\big)\\
&+\frac{h_A^2\omega\big(-243g_A^2-450g_Ag_1+288h_A^2+125g_1^2\big)\log\big(\frac{2\Delta}{M_\pi}\big)}{17496\pi^2F_\pi^4}-(\omega\to-\omega),
\end{aligned}
\tag{B6}
$$

$$
\begin{aligned}
h_{\rm SL}^-=&\frac{\Delta h_A^2D(\sqrt{-t})\big(4\Delta^2-4M_\pi^2+t\big)}{144\pi^2F_\pi^4}-\frac{\Delta h_A^2\bar{I}_{20}(t)}{9F_\pi^4}\\
&+\frac{h_A^2}{4374F_\pi^4\omega^2(\Delta^2-\omega^2)^2}\bar{J}_0(-\Delta)\big(10(\Delta^2-\omega^2)^2\big(81g_A^2-90g_Ag_1+5g_1^2\big)\big(M_\pi^2-\Delta^2\big)\\
&+648\Delta^2g_A^2(\Delta^2-\omega^2)\big(M_\pi^2-\Delta^2\big)+9\omega^2\big(27(\Delta^2-\omega^2)^2+32h_A^2\big(2\Delta^2(\Delta^2-2\omega^2)+M_\pi^2(\Delta^2+\omega^2)\big)\big)\big)\\
&-\frac{4h_A^2\bar{J}_0(\omega)\big(M_\pi^2-\omega^2\big)\big(h_A^2\omega(9\Delta^2-8\Delta\omega+8\omega^2)-9g_A^2(\Delta-2\omega)(\Delta^2-\omega^2)\big)}{243F_\pi^4\omega(\Delta^2-\omega^2)^2}\\
&+\frac{h_A^2}{69984\pi^2F_\pi^4(\Delta^2-\omega^2)^2}\big(\Delta(\Delta^2-\omega^2)\big(M_\pi^2\big(81g_A^2-450g_Ag_1-576h_A^2+225g_1^2\big)+1152\Delta^2h_A^2\big)\\
&+\Delta(\Delta^2-\omega^2)^2\big(-7047g_A^2+3150g_Ag_1+25g_1^2\big)+\pi M_\pi^3(5g_1-9g_A)(\Delta^2(297g_A-85g_1)-\omega^2(279g_A+5g_1))\big)
\end{aligned}
$$

$$
\begin{aligned}
&- \frac{\Delta h_A^2\left(2349 g_A^2 - 2250 g_A g_1 + 1152 h_A^2 + 125 g_1^2 + 972\right)\log\left(\frac{2\Delta}{M_\pi}\right)}{34992\pi^2 F_\pi^4} \\
&- \frac{h_A^2(9g_A - 5g_1)\bar{J}_0(\omega-\Delta)\left(M_\pi^2 - (\Delta-\omega)^2\right)(-360\Delta\omega g_A + 4\Delta^2(81 g_A - 5 g_1) + 5\omega^2(9 g_A - 5 g_1))}{8748 F_\pi^4 \omega^2(\Delta-\omega)^2} + (\omega \to -\omega),
\end{aligned}
\tag{B7}
$$

and $1/m_N$ corrections given by

$$
\begin{aligned}
g^+_{1/m_N} &= -\frac{h_A^2}{9F_\pi^2 m_N(\Delta^2-\omega^2)^2}\left\{16\Delta^4\omega^2 - 4\Delta^3\omega\left(-4M_\pi^2 + t + 4\omega^2\right)\right. \\
&\quad + \Delta^2\left(4M_\pi^4 - 4M_\pi^2(t+6\omega^2) + t^2 + 8t\omega^2 - 12\omega^4\right) - 2\Delta\omega\left(8M_\pi^4 - 2M_\pi^2(3t+4\omega^2) + t(t+4\omega^2)\right) \\
&\quad \left. + \omega^2\left(4M_\pi^4 - 4M_\pi^2(t-2\omega^2) + t^2 + 4\omega^4\right)\right\} + \frac{16\, h_A^2\,\omega^2}{9F_\pi^2 m_N}, \\
g^-_{1/m_N} &= -\frac{h_A^2}{18F_\pi^2 m_N(\Delta^2-\omega^2)^2}\left\{-4\Delta^3\omega\left(-4M_\pi^2 + t + 4\omega^2\right) + \Delta^2\left(8M_\pi^4 - 2M_\pi^2(3t+16\omega^2) + t^2 + 10t\omega^2 + 24\omega^4\right)\right. \\
&\quad - 2\Delta\omega\left(4M_\pi^4 - 4M_\pi^2 t + t^2 + 2t\omega^2 - 4\omega^4\right) + \omega^2\left(8M_\pi^4 - 6M_\pi^2 t + t^2 + 2t\omega^2 - 8\omega^4\right)\Big\} \\
&\quad - \frac{h_A^2}{9F_\pi^2 m_N \Delta}\omega\left(t + 8\left(\omega^2 - M_\pi^2\right)\right), \\
h^+_{1/m_N} &= \frac{h_A^2\left[4\Delta^3\omega + \Delta^2\left(4M_\pi^2 - t - 8\omega^2\right) + 2\Delta\omega\left(t - 2M_\pi^2\right) + \omega^2\left(4M_\pi^2 - t\right)\right]}{9F_\pi^2 m_N(\Delta^2-\omega^2)^2} - \frac{4\, h_A^2\,\omega}{9F_\pi^2 m_N \Delta}, \\
h^-_{1/m_N} &= \frac{h_A^2\left(4\Delta^3\omega + \Delta^2\left(2M_\pi^2 - t - 6\omega^2\right) + 2\Delta\omega\left(-4M_\pi^2 + t + 2\omega^2\right) + \omega^2\left(2M_\pi^2 - t + 2\omega^2\right)\right)}{18F_\pi^2 m_N(\Delta^2-\omega^2)^2}.
\end{aligned}
\tag{B8}
$$

The loop functions are defined via

$$
\begin{aligned}
2M_\pi^2\lambda_\pi &= \mu^{4-d}\int\frac{d^d l}{(2\pi)^d}\frac{i}{l^2 - M_\pi^2 + i\epsilon}, \\
\bar{J}_0(\omega) &= \begin{cases} \frac{\omega}{8\pi^2} + \frac{\sqrt{\omega^2 - M_\pi^2}}{4\pi^2}\,\mathrm{arccosh}\left(-\frac{\omega}{M_\pi}\right) & \text{for} \quad \omega < -M_\pi \\ \frac{\omega}{8\pi^2} - \frac{\sqrt{\omega^2 - M_\pi^2}}{4\pi^2}\left(\mathrm{arccosh}\left(\frac{\omega}{M_\pi}\right) - i\,\pi\right) & \text{for} \quad \omega > M_\pi \\ \frac{\omega}{8\pi^2} - \frac{\sqrt{M_\pi^2 - \omega^2}}{4\pi^2}\,\arccos\left(-\frac{\omega}{M_\pi}\right) & \text{for} \quad |\omega| < M_\pi \end{cases}, \\
D(x) &= \frac{1}{\Delta}\int_{2M_\pi}^{\infty}\frac{d\mu}{\mu^2 + x^2}\arctan\frac{\sqrt{\mu^2 - 4M_\pi^2}}{2\Delta}, \\
\bar{I}_{20}(t) &= \frac{1}{16\pi^2} - \frac{\sqrt{1 - 4M_\pi^2/t}}{16\pi^2}\log\frac{\sqrt{1 - 4M_\pi^2/t} + 1}{\sqrt{1 - 4M_\pi^2/t} - 1}.
\end{aligned}
\tag{B9}
$$

[1] E. Stephan, S. Kistryn, R. Sworst, A. Biegun, K. Bodek, I. Ciepal, A. Deltuva, E. Epelbaum, A. C. Fonseca, J. Golak *et al.*, Phys. Rev. C **82**, 014003 (2010).

[2] I. Ciepal, S. Kistryn, E. Stephan, A. Biegun, K. Bodek, A. Deltuva, E. Epelbaum, M. Eslami-Kalantari *et al.*, Phys. Rev. C **85**, 017001 (2012).

[3] M. Viviani, L. Girlanda, A. Kievsky, L. E. Marcucci, and S. Rosati, EPJ Web Conf. **3**, 05011 (2010).

[4] H. Witala, J. Golak, R. Skibinski, and K. Topolnicki, J. Phys. G **41**, 094011 (2014).

[5] P. Navratil, V. G. Gueorguiev, J. P. Vary, W. E. Ormand, and A. Nogga, Phys. Rev. Lett. **99**, 042501 (2007).

[6] D. Gazit, S. Quaglioni, and P. Navratil, Phys. Rev. Lett. **103**, 102502 (2009).

[7] R. Roth, J. Langhammer, A. Calci, S. Binder, and P. Navratil, Phys. Rev. Lett. **107**, 072501 (2011).

[8] K. Hebeler, J. M. Lattimer, C. J. Pethick, and A. Schwenk, Phys. Rev. Lett. **105**, 161102 (2010).

[9] G. Hagen, M. Hjorth-Jensen, G. R. Jansen, R. Machleidt, and T. Papenbrock, Phys. Rev. Lett. **108**, 242501 (2012).

[10] J. D. Holt, J. Menendez, and A. Schwenk, Phys. Rev. Lett. **110**, 022502 (2013).

[11] I. Tews, T. Krüger, K. Hebeler, and A. Schwenk, Phys. Rev. Lett. **110**, 032504 (2013).

[12] R. Skibinski *et al.*, Few Body Syst. **54**, 1315 (2013).
[13] A. Ekström, G. R. Jansen, K. A. Wendt, G. Hagen, T. Papenbrock, S. Bacca, B. Carlsson, and D. Gazit, Phys. Rev. Lett. **113**, 262504 (2014).
[14] J. Golak *et al.*, Eur. Phys. J. A **50**, 177 (2014).
[15] K. Hebeler, H. Krebs, E. Epelbaum, J. Golak, and R. Skibinski, Phys. Rev. C **91**, 044001 (2015).
[16] S. Binder, A. Calci, E. Epelbaum, R. J. Furnstahl, J. Golak, K. Hebeler, H. Kamada, H. Krebs, J. Langhammer, S. Liebig *et al.* (LENPIC Collaboration), Phys. Rev. C **93**, 044002 (2016).
[17] A. Ekström, G. R. Jansen, K. A. Wendt, G. Hagen, T. Papenbrock, B. D. Carlsson, C. Forssen, M. Hjorth-Jensen, P. Navratil, and W. Nazarewicz, Phys. Rev. C **91**, 051301 (2015).
[18] J. E. Lynn, I. Tews, J. Carlson, S. Gandolfi, A. Gezerlis, K. E. Schmidt, and A. Schwenk, Phys. Rev. Lett. **116**, 062501 (2016).
[19] H. Witała *et al.*, Few Body Syst. **57**, 1213 (2016).
[20] C. Drischler, T. Krüger, K. Hebeler, and A. Schwenk, Phys. Rev. C **95**, 024302 (2017).
[21] A. Ekström, G. Hagen, T. D. Morris, T. Papenbrock, and P. D. Schwartz, Phys. Rev. C **97**, 024332 (2018).
[22] C. Drischler, K. Hebeler, and A. Schwenk, arXiv:1710.08220 [nucl-th].
[23] M. Piarulli, A. Baroni, L. Girlanda, A. Kievsky, A. Lovato, E. Lusk, L. E. Marcucci, S. C. Pieper, R. Schiavilla, M. Viviani, and R. B. Wiringa, Phys. Rev. Lett. **120**, 052503 (2018).
[24] I. Tews, J. Carlson, S. Gandolfi, and S. Reddy, Astrophys. J. **860**, 149 (2018).
[25] S. Binder *et al.*, arXiv:1802.08584 [nucl-th].
[26] N. Kalantar-Nayestanaki, E. Epelbaum, J. G. Messchendorp, and A. Nogga, Rept. Prog. Phys. **75**, 016301 (2012).
[27] H. W. Hammer, A. Nogga, and A. Schwenk, Rev. Mod. Phys. **85**, 197 (2013).
[28] E. Epelbaum, H.-W. Hammer, and U.-G. Meißner, Rev. Mod. Phys. **81**, 1773 (2009).
[29] R. Machleidt and D. R. Entem, Phys. Rept. **503**, 1 (2011).
[30] S. Weinberg, Phys. Lett. B **251**, 288 (1990).
[31] C. Ordonez, L. Ray, and U. van Kolck, Phys. Rev. Lett. **72**, 1982 (1994).
[32] E. Epelbaum, W. Glöckle, and U.-G. Meißner, Nucl. Phys. A **747**, 362 (2005).
[33] D. R. Entem and R. Machleidt, Phys. Rev. C **68**, 041001 (2003).
[34] D. R. Entem, N. Kaiser, R. Machleidt, and Y. Nosyk, Phys. Rev. C **91**, 014002 (2015).
[35] E. Epelbaum, H. Krebs, and U.-G. Meißner, Phys. Rev. Lett. **115**, 122301 (2015).
[36] D. R. Entem, R. Machleidt, and Y. Nosyk, Phys. Rev. C **96**, 024004 (2017).
[37] P. Reinert, H. Krebs, and E. Epelbaum, arXiv:1711.08821 [nucl-th].
[38] U. van Kolck, Phys. Rev. C **49**, 2932 (1994).
[39] E. Epelbaum, A. Nogga, W. Glöckle, H. Kamada, Ulf-G. Meißner, and H. Witała, Phys. Rev. C **66**, 064001 (2002).
[40] V. Bernard, E. Epelbaum, H. Krebs, and Ulf-G. Meißner, Phys. Rev. C **77**, 064004 (2008).
[41] V. Bernard, E. Epelbaum, H. Krebs, and Ulf-G. Meißner, Phys. Rev. C **84**, 054001 (2011).
[42] S. Ishikawa and M. R. Robilotta, Phys. Rev. C **76**, 014006 (2007).
[43] J. Golak, D. Rozpedzik, R. Skibinski, K. Topolnicki, H. Witała, W. Glöckle, A. Nogga, E. Epelbaum *et al.*, Eur. Phys. J. A **43**, 241 (2010).
[44] R. Skibinski, J. Golak, K. Topolnicki, H. Witała, E. Epelbaum, W. Glöckle, H. Krebs, and A. Nogga, and H. Kamada, Phys. Rev. C **84**, 054005 (2011).
[45] E. Epelbaum, Phys. Lett. B **639**, 456 (2006).
[46] E. Epelbaum, Eur. Phys. J. A **34**, 197 (2007).
[47] D. Rozpedzik, J. Golak, R. Skibinski, H. Witala, W. Glöckle, E. Epelbaum, A. Nogga, and H. Kamada, Acta Phys. Polon. B **37**, 2889 (2006).
[48] A. Nogga *et al.*, EPJ Web Conf. **3**, 05006 (2010).
[49] N. Kaiser and R. Milkus, Eur. Phys. J. A **52**, 4 (2016).
[50] H. Krebs, A. Gasparyan, and E. Epelbaum, Phys. Rev. C **85**, 054006 (2012).
[51] H. Krebs, A. Gasparyan, and E. Epelbaum, Phys. Rev. C **87**, 054007 (2013).
[52] J. Fujita and H. Miyazawa, Prog. Theor. Phys. **17**, 360 (1957).
[53] S. C. Pieper, V. R. Pandharipande, R. B. Wiringa, and J. Carlson, Phys. Rev. C **64**, 014001 (2001).
[54] A. Deltuva, K. Chmielewski, and P. U. Sauer, Phys. Rev. C **67**, 034001 (2003).
[55] T. R. Hemmert, B. R. Holstein, and J. Kambor, J. Phys. G **24**, 1831 (1998).
[56] C. Ordonez, L. Ray, and U. van Kolck, Phys. Rev. C **53**, 2086 (1996).
[57] N. Kaiser, S. Gerstendorfer, and W. Weise, Nucl. Phys. A **637**, 395 (1998).
[58] H. Krebs, E. Epelbaum, and U.-G. Meißner, Eur. Phys. J. A **32**, 127 (2007).
[59] E. Epelbaum, H. Krebs, and U.-G. Meißner, Nucl. Phys. A **806**, 65 (2008).
[60] E. Epelbaum, H. Krebs, and Ulf-G. Meißner, Phys. Rev. C **77**, 034006 (2008).
[61] V. Bernard, T. R. Hemmert, and U.-G. Meißner, Phys. Lett. B **565**, 137 (2003).
[62] V. Bernard, T. R. Hemmert, and U.-G. Meißner, Phys. Lett. B **622**, 141 (2005).
[63] T. Ledwig, J. Martin-Camalich, V. Pascalutsa, and M. Vanderhaeghen, Phys. Rev. D **85**, 034013 (2012).
[64] V. Bernard, E. Epelbaum, H. Krebs, and Ulf-G. Meißner, Phys. Rev. D **87**, 054032 (2013).
[65] D. Siemens, V. Bernard, E. Epelbaum, H. Krebs, and Ulf-G. Meißner, Phys. Rev. C **89**, 065211 (2014).
[66] H. B. Tang and P. J. Ellis, Phys. Lett. B **387**, 9 (1996).
[67] V. Pascalutsa, Phys. Lett. B **503**, 85 (2001).
[68] H. Krebs, E. Epelbaum, and U.-G. Meißner, Phys. Lett. B **683**, 222 (2010).
[69] J. Gasser and H. Leutwyler, Ann. Phys. **158**, 142 (1984).
[70] T. Appelquist and J. Carazzone, Phys. Rev. D **11**, 2856 (1975).
[71] E. Epelbaum, U.-G. Meißner, and W. Glöckle, Nucl. Phys. A **714**, 535 (2003).
[72] V. Bernard, H. W. Fearing, T. R. Hemmert and U.-G. Meißner, Nucl. Phys. A **635**, 121 (1998); **642**, 563(E) (1998).
[73] N. Fettes and U.-G. Meißner, Nucl. Phys. A **676**, 311 (2000).
[74] R. G. E. Timmermans, T. A. Rijken, and J. J. de Swart, Phys. Rev. Lett. **67**, 1074 (1991).
[75] V. Baru, C. Hanhart, M. Hoferichter, B. Kubis, A. Nogga, and D. R. Phillips, Phys. Lett. B **694**, 473 (2011).
[76] R. Dashen, E. Jenkins, and A. V. Manohar, Phys. Rev. D **49**, 4713 (1994); **51**, 2489(E) (1995).

[77] R. F. Dashen and A. V. Manohar, Phys. Lett. B **315**, 425 (1993).
[78] D. Siemens, J. Ruiz de Elvira, E. Epelbaum, M. Hoferichter, H. Krebs, B. Kubis, and U.-G. Meißner, Phys. Lett. B **770**, 27 (2017).
[79] R. A. Arndt, W. J. Briscoe, I. I. Strakovsky, and R. L. Workman, Phys. Rev. C **74**, 045205 (2006).
[80] R. Koch, Nucl. Phys. A **448**, 707 (1986).
[81] J. M. Alarcon, J. M. Camalich, J. A. Oller, and L. Alvarez-Ruso, Phys. Rev. C **83**, 055205 (2011); **87**, 059901(E) (2013).
[82] D. Siemens, V. Bernard, E. Epelbaum, A. Gasparyan, H. Krebs, and Ulf-G. Meißner, Phys. Rev. C **94**, 014620 (2016).
[83] D. L. Yao, D. Siemens, V. Bernard, E. Epelbaum, A. M. Gasparyan, J. Gegelia, H. Krebs, and U.-G. Meißner, J. High Energy Phys. 05 (2016) 038.
[84] D. Siemens, V. Bernard, E. Epelbaum, A. M. Gasparyan, H. Krebs, and Ulf-G. Meißner, Phys. Rev. C **96**, 055205 (2017).
[85] M. Hoferichter, J. Ruiz de Elvira, B. Kubis, and U.-G. Meißner, Phys. Rept. **625**, 1 (2016).
[86] K. A. Wendt, B. D. Carlsson, and A. Ekström, arXiv:1410.0646 [nucl-th].
[87] B. D. Carlsson, A. Ekström, C. Forssén, D. Fahlin Strömberg, G. R. Jansen, O. Lilja, M. Lindby, B. A. Mattsson, and K. A. Wendt, Phys. Rev. X **6**, 011019 (2016).
[88] N. Fettes, U.-G. Meißner, and S. Steininger, Nucl. Phys. A **640**, 199 (1998).
[89] V. Bernard, N. Kaiser, and U.-G. Meißner, Nucl. Phys. A **615**, 483 (1997).
[90] E. Epelbaum, H. Krebs, and U.-G. Meißner, Eur. Phys. J. A **51**, 53 (2015).
[91] S. Kolling, E. Epelbaum, H. Krebs, and U.-G. Meißner, Phys. Rev. C **80**, 045502 (2009).
[92] S. Kolling, E. Epelbaum, H. Krebs, and U.-G. Meißner, Phys. Rev. C **84**, 054008 (2011).
[93] H. Krebs, E. Epelbaum, and U.-G. Meißner, Ann. Phys. **378**, 317 (2017).
[94] S. Weinberg, Nucl. Phys. B **363**, 3 (1991).
[95] E. Epelbaum, Prog. Part. Nucl. Phys. **57**, 654 (2006).
[96] E. Epelbaum, W. Glöckle, and U.-G. Meißner, Nucl. Phys. A **637**, 107 (1998).
[97] E. Epelbaum, arXiv:1001.3229 [nucl-th].
[98] S. Okubo, Prog. Theor. Phys. **12**, 603 (1954).
[99] E. Epelbaum, W. Glöckle, and U.-G. Meißner, Eur. Phys. J. A **19**, 125 (2004).
[100] E. Epelbaum, A. M. Gasparyan, H. Krebs, and C. Schat, Eur. Phys. J. A **51**, 26 (2015).
[101] N. Fettes and U.-G. Meißner, Nucl. Phys. A **679**, 629 (2001).